

**Classification of main irrigated crop types towards sustainable
development using Landsat and Sentinel data by GIS and remote
sensing techniques in a semi-arid area in Tashkent Province,
Uzbekistan**

**Dissertation
for the award of the degree
"Doctor rerum naturalium" (Dr.rer.nat.)
of the Georg-August-Universität Göttingen**

**within the doctoral program Geography
of the Georg-August University School of Science (GAUSS)**

submitted by
ELBEK ERDANAEV
Göttingen, December 2022

Thesis Committee

Prof. Dr. Martin Kappas

(Department of Cartography, GIS and Remote Sensing / (Georg-August Universität Göttingen))

Prof. Dr. Daniela Sauer

(Department of Physical Geography / Georg-August Universität Göttingen)

Prof. Dr. Elisabeth Dietze

(Department of Physical Geography / Georg-August Universität Göttingen)

Prof. i.R. Dr. Gerhard Gerold

(Department of Physical Geography / Georg-August Universität Göttingen)

Dr. Daniel Wyss

(Department of Cartography, GIS and Remote Sensing / (Georg-August Universität Göttingen))

Dr. Michael Klinge

(Department of Physical Geography / Georg-August Universität Göttingen)

Dr. Birgitta Putzenlechner

(Department of Cartography, GIS and Remote Sensing / (Georg-August Universität Göttingen))

Members of the Examination Board

Reviewer 1: Prof. Dr. Martin Kappas

(Department of Cartography, GIS and Remote Sensing / (Georg-August Universität Göttingen))

Reviewer 2: Prof. i.R. Dr. Gerhard Gerold

(Department of Physical Geography / Georg-August Universität Göttingen)

Date of the oral examination: **February 07, 2023**

**To my father Erdanaev Shodmon, mother Erdanaeva Mekhri, and my wife Urakova
Umida**

CONTENT OF DISSERTATION

This doctoral dissertation consists of a general introduction and the following published articles. The papers will be referred to by their Roman numbers (Papers I-III). The published papers are reprinted with permission from the respective copyright holders.

- I. Erdanaev, E.; Kappas, M.; Pulatov, A.; Klinge, M. (2015): Short Review of Climate and Land Use change Impact on Land Degradation in Tashkent Province. *International Journal of Geoinformatics*, 11(4), 39–48.
- II. Erdanaev, E., Kappas, M., & Wyss, D. (2022). The Identification of Irrigated Crop Types Using Support Vector Machine, Random Forest and Maximum Likelihood Classification Methods with Sentinel-2 Data in 2018: Tashkent Province, Uzbekistan. *International Journal of Geoinformatics*, 18(2), 37–53. <https://doi.org/10.52939/ijg.v18i2.2151>.
- III. Erdanaev, E., Kappas, M., & Wyss, D. (2022). Irrigated crop types mapping in Tashkent Province of Uzbekistan with remote sensing-based classification methods. *Sensors* **2022**, 22(15), 5683; <https://doi.org/10.3390/s22155683>.

Table of Contents

Content of dissertation	IV
Table of Contents.....	V
List of Figures	IX
List of Tables.....	XIV
List of Abbreviations.....	XV
ABSTRACT	1
1 Introduction	5
1.1 Research objectives	7
1.2 Research Questions.....	8
1.3 Overview of the thesis	8
1.4 Irrigated lands contribution to the total yield	11
1.5 The role of irrigated agricultural land in the economy	14
1.6 Cotton and wheat are major crops	16
1.7 Climate change impact on agricultural production and irrigation....	17
1.8 Indices used for major irrigated crop types classification	18
1.9 Classification methods.....	20
1.10 Accuracy Assessment	20
1.11 Accuracy Assessment Formulas	21
1.12 Actuality and major outcomes of this research	24
2 Overview of the study area	25
2.1 Location of the study area	25
2.2 The population of the region	26
2.3 Annual agricultural crops area changes in Tashkent Province.....	28
2.4 Water resources of the study area.....	30
2.5 Soils of the study area and their quality	32
3 Short Review of Climate and Land Use Change Impact on Land Degradation in Tashkent Province	35
3.1 Abstract.....	35
3.2 Introduction	36
3.3 Land Degradation in CA.....	37
3.4 Climate Change in CA.....	40

3.5	Climate Change Analysis in Tashkent Province	42
3.6	Land Use Change Analysis in Tashkent Province	48
3.7	Conclusions	51
4	The Identification of Irrigated Crop Types Using Support Vector Machine, Random Forest and Maximum Likelihood Classification Methods with Sentinel-2 Data in 2018: Tashkent Province, Uzbekistan.....	53
4.1	Abstract	53
4.2	Introduction	54
4.3	Materials and Methods	58
4.3.1	Study area.....	58
4.3.2	Data Collection and Pre-Processing.....	59
4.3.3	Methodology	61
4.3.4	Training and Ground Truth data	63
4.3.5	Classification Methods.....	65
4.3.6	Cropping Calendar	67
4.4	Results	68
4.4.1	Accuracy Assessment of Image Classification	72
4.4.2	Comparison Sentinel Derived Cropland Products with National Statistical Data.....	73
4.5	Discussion	75
4.6	Conclusions	78
5	Irrigated crop types mapping in Tashkent Province of Uzbekistan with remote sensing-based classification methods	81
5.1	Abstract	81
5.2	Introduction	82
5.3	Materials and methods	86
5.3.1	Study area.....	86
5.3.2	Data	89
5.3.3	Methodology	93
5.3.3.1	Data Preprocessing	93
5.3.3.2	Indexes	93
5.3.3.3	ML Algorithms	95
5.3.3.4	Accuracy of RS Classification.....	98
5.4	Results	99
5.4.1	Results from land use classification.....	99
5.4.2	Results for classification accuracy	108
5.5	Discussion	110
5.5.1	Performance of ML Classifiers	110
5.5.2	Using Different Indices and Their Performance	111
5.5.3	Comparing Derived Main Crop Types Area with OSS Data.....	113

5.5.4 Theoretical and Practical Implications of the Research	114
5.5.5 Limitations and Recommendations	115
5.6 Conclusions	115
6 General conclusions, limitations, and recommendations.....	117
6.1 Summary findings.....	117
6.2 Limitations.....	120
6.3 Recommendations	121
References	123

List of Figures

Chapter 1

Figure 1.1. The framework of the research.....	10
Figure 1.2. Countries by irrigated land area in 2012. Countries/territories shown with the irrigated land area as '0' are shaded with the '<100' color (lightest green); those with no data are shaded with the 'N/A' color (grey). Source: CIA World Factbook, 2016.....	11
Figure 1.3. Cotton production of the world by country. Source: PSD Online http://www.fas.usda.gov/psdonline by (Malik and Ahsan 2016).....	12
Figure 1.4. Wheat production of the world by country. Source: FAOSTAT.	13
Figure 1.5. Increase of global agriculture value-added. Source: FAO, 2021.	14
Figure 1.6. Share of agriculture in global GDP. Source: FAO, 2021.....	14
Figure 1.7. Value-added of agriculture, forestry, and fishing by regions. Source: FAOSTAT.....	14
Figure 1.8. Share of agriculture, forestry, and fishing value-added in total GDP by region (US\$ 2015 prices). Source: FAOSTAT.....	14
Figure 1.9. Sector's contribution to the country's GDP in 2020. Source: State Statistics, 2021.....	15

Figure 1.10. Growth in agricultural GDP. Source: State Statistics, 2021..... 15

Figure 1.11. Sown crops in Uzbekistan. Source: State Statistics, 2020..... 16

Chapter 2

Figure 2.1. Administrative map of Uzbekistan and the location of the study area (Nations Project, 2022)..... 25

Figure. 2.2. Population growth in Uzbekistan..... 27

Figure 2.3. The population growth rate in Uzbekistan..... 27

Figure 2.4. Population growth Tashkent Province..... 28

Figure 2.5. Agricultural cropland area changes in Tashkent Province..... 329

Figure 2.6. Cotton and winter-wheat area changes in Tashkent Province... 29

Figure 2.7. Available water basins in Tashkent Province derived from Advanced Spaceborne Thermal Emission and Reflection Radiometer (ASTER) Global Digital Elevation Model (GDEM) data (Tachikawa et al., 2011)..... 31

Figure 2.8. The soil type of Tashkent province (Khurshidbek Makhmudov 2015)..... 33

Chapter 3

Figure 3.1. 30 m grid Digital Elevation Model (DEM) of Tashkent Province retrieved from Advanced Spaceborne Thermal Emission and Reflection Radiometer (ASTER) Global Digital Elevation Model (GDEM) (Tachikawa et al., 2011)..... 43

Figure 3.2. Average monthly surface precipitation over Tashkent Province interpolated by Kriging using CFSR weather data between 1979-2013..... 44

Figure 3.3. Average monthly surface temperature over Tashkent Province interpolated by Kriging using CFSR weather data from 1979 to 2013..... 46

Figure 3.4. Annual average temperature change diagrams of croplands and grasslands in Tashkent Province..... 47

Figure 3.5. Annual precipitation changes diagrams of croplands and grasslands in Tashkent Province.....	47
Figure 3.6. Changes in irrigated agricultural cropland between 1999 and 2010 in Tashkent Province.....	48
Figure 3.7. Population growth between 1991 and 2013 in Tashkent Province.....	49
Figure 3.8. Changes in agricultural cropland area in Tashkent Province...	50

Chapter 4

Figure 4. 1. Location of the study area and the administrative districts.....	58
Figure 4. 2. Outline of irrigated cropland area.....	61
Figure 4. 3. Flowchart of the study methods.....	62
Figure 4. 4. Idealized cropping calendar of the main crop types grown in the study area based on the guidance of regional agricultural land management authority and local experts.....	64
Figure 4. 5. Monthly NDVI profiles during the vegetation period in 2018 at the field level were retrieved from multitemporal Sentinel-2 data. Mean NDVI and its standard deviation error bars are also shown.....	69
Figure 4. 6. Supervised classification methods output and the subset of Agricultural LU maps in 2018: SVM classification; RF classification; and MLC classification.....	70 71
Figure 4. 7. LU map subsets from different classification methods.....	74
Figure 4. 8. Comparison of Sentinel 2 -derived cropland product with national statistical data.....	75
Figure 4. 9. OA and KA value of classifiers.....	76

Chapter 5

Figure 5.1. Location of the study region.....	88
--	----

Figure 5.2. Location of training and ground-truthing samples.....	92
Figure 5.3. Methodology applied for this research.....	95
Figure 5.4. Linear SVM example adapted from (Burges, 1998).....	96
Figure 5.5. RF concept adapted from (Denisko & Hoffman, 2018).....	97
Figure 5.6. Comparison of classified crop types area with OSS data for RF classifier with S2 sensor.....	99
Figure 5.7. Comparison of classified crop types area with OSS data for SVM classifier with S2 sensor.....	100
Figure 5.8. Comparison of classified crop types area with OSS data for SVM classifier with L8 sensor.....	100
Figure 5.9. Comparison of classified crop types area with OSS data for RF classifier with L8 sensor	101
Figure 5.10. Subsets of land use maps derived from different indices using the SVM classification method for both S2 (left) and L8 (right).....	104
Figure 5.11. Subsets of LU maps derived from different indices using the RF classification method for both S2 (left) and L8 (right).....	105
Figure 5.12. Classification result of S2-SVM-EVI-NDVI (highest OA 88% for SVM).....	106
Figure 5.13. Classification result of L8-RF-EVI (highest OA 90% for RF).....	107

Figure 5.14. OA of SVM and RF classifiers on different indices and satellites	111
Figure 5.15. KA of SVM and RF classifiers on different indices and satellites	112
Figure 5.16. Difference between the total area of OSS data and classified area by sensors, classifiers, and indices	114

List of Tables

Chapter 1

Table 1.1. Interpretation of the agreement for Kappa coefficient (Landis and Koch 1977).....	23
---	----

Chapter 4

Table 4.1. Band parameter of each spectral band of Sentinel – 2.....	60
Table 4.2. Sentinel-2 data used for image classification.....	60
Table 4.3. Training and Ground Truthing Samples.....	63
Table 4.4. Confusion matrices and classification methods accuracy based on ground-truthing data.....	72

Chapter 5

Table 5.1. Sentinel-2 and Landsat-8 tiles were downloaded for the classification.....	89
Table 5.2. Specifications of spectral bands for Sentinel-2 MS (ESA, 2021) and Landsat 8-OLI (USGS, 2020b).....	90
Table 5.3. Numerical information on training and validation data	92
Table 5.4. Differences between classification results and OSS (1000 ha).	102
Table 5.5. Accuracy assessment (in %) results of SVM classifier	108
Table 5.6. Accuracy assessment (in %) results of RF classifier.....	108
Table 5.7. Deviation (in %) between the total mapped crop areas and OSS data (280.4 thousand ha).....	114

List of Abbreviations

AD	anno domini
AI	Artificial Intelligence
AM	Arithmetic Average
ASTER	Advanced Spaceborne Thermal Emission and Reflection Radiometer
AVHRR	The Advanced Very High-Resolution Radiometer
BETHY/DLR	Biosphere Energy Transfer Hydrology Model
CA	Central Asia
CFSR	Climate Forecast System Reanalysis
CIA	Central Intelligence Agency
CO₂	Carbon Dioxide
DEM	Digital Elevation Model
DOS	Dark Object Subtraction
ESA	European Space Agency
ET	Evapotranspiration
EU	European Union
EVI	Enhanced Vegetation Index
FAO	Food and Agriculture Organization
FB	Field Based
GDEM	Global Digital Elevation Model
GDP	Gross Domestic Product

GE	Google Earth
GIS	Geographic Information System
IPCC	The Intergovernmental Panel on Climate Change
KA	Kappa Accuracy
L8	Landsat - 8
LIDAR	Light Detection and Ranging
LSR	Land Surface Reflectance
LU	Land Use
LULC	Land Use Land Cover
MLA	Machine Learning Algorithm
MLC	Maximum Likelihood Classification
MODIS	Moderate Resolution Imaging Spectroradiometer
MS	Multi-Spectral
NASA	The National Aeronautics and Space Administration
NCEP	National Centers of Environmental Prediction
NDVI	Normalized Difference Vegetation Index
NDWI	Normalized Difference Water Index
NIR	Near-Infrared
NOAA	National Oceanic and Atmospheric Administration
NPP	Net Primary Productivity
OA	Overall Accuracy
OLI	Operational Land Imager
PA	Producer's Accuracy

PB	Pixel Based
QGIS	Quantum GIS
R, G, B	Red, Green, Blue
RE	Red Edge
RF	Random Forest
RSI	Remote Sensing Imagery
RVI	Ratio Vegetation Index
S2	Sentinel - 2
SAVI	Soil Adjusted Vegetation Index
SFDI	Spring Frost Damage Index
SOLAW	The State of the world's land and water resources for food and agriculture
SOM	Soil Organic Matter
SSR	The Soviet Socialist Republic
SVM	Support-Vector Machine
SWIR	Shortwave infrared
TOA	Top of Atmosphere
TVI	Triangle Vegetation Index
UA	User's Accuracy
UAV	Unmanned Aerial Vehicles
UNCCD	The United Nations Convention to Combat Desertification
USGS	United States Geological Survey
VI	Vegetation Index

VIIRS The Visible Infrared Imaging Radiometer Suite

WA Weighted Average

Acknowledgment

This Ph.D. study was supported by the ERASMUS MUNDUS Action 2 TIMUR (Training of Individuals through Mobility to EU from the Uzbek Republic) project of the European Commission.

First and foremost, I am very grateful to my main supervisor Prof. Dr. Martin Kappas for his invaluable advice, continuous support, and patience during my Ph.D. study. His immense plentiful experience and knowledge have encouraged me all the time in my academic research and daily life. I would also like to thank Dr. Daniel Wyss and Dr. Michael Klinge for their valuable advice, and technical support in my study. I would like to thank my friends, colleagues, and research team – Martina Beck, Dr. Daniel Wyss, Timo Pascal Lehmann, Dr. Birgitta Putzenlechner, and Dr. Roland Bauböck, Dr. Holger Vogt, and Dr. Oyudari Vova for a cherished time spent together in the department, and social settings.

My sincere thanks to Dr. Alim Pulatov at Tashkent Institute of Irrigation and Agricultural Mechanization Engineers in Uzbekistan who provided valuable knowledge and experience as well as for his first encouragement to contribute to the exciting field of GIS and remote sensing research.

I would like to express my gratitude to my father Erdanaev Shodmon, my mother Erdanaeva Mekhri, and my children Asilbek Shodmonov, Sofiya Shodmonova, and Elisa Shodmonova who motivated me and guided me to complete my degree successfully. Without their tremendous understanding and encouragement in the past few years during my Ph.D. study, it would be impossible for me to complete my study.

Finally, I would like to thank my wife, best friend, and love Umida Urakova. Thank you for providing inspiration and endless encouragement during the completion of my Ph.D.

ABSTRACT

As the world population increases and cropland expansion occurs, there will be a high need in the food supply soon which will require higher agricultural yields. Crop yield estimation, management, and production assessments at the regional and country-level are very important in Uzbekistan which requires supplemental spatial data that provides timely information on crop type's spatial distribution, condition, and potential yields. Crop-type identification at the local and regional level is very important in agricultural regions in developing countries where it contributes the main share of the country's GDP.

Nowadays the number of satellites and free availability of these data with the integration of multi-sensor images offers coherent time series which gives new opportunities for land cover and crop type classification. Poor or developing countries compile their agricultural statistics in tabular form by their provincial administrative areas, which gives no information about the exact locations where specific crops are cultivated. Such data is poorly suited for early warning and assessment of crop production. 5-Daily Sentinel and 16-Daily Landsat satellites image time series of Tashkent Province, Uzbekistan, acquired in 2018 in combination with reported crop area statistics were used to produce the required crop types map. Three well-known machine learning algorithms Support Vector-Machine, Random Forest, and Maximum Likelihood classifications were used to derive crop types maps and compared for recommended suitable methods. Four indices NDVI, EVI, NDWI1, and NDWI2 were calculated using blue, green, near-infrared, SWIR 1, and SWIR 2 bands and used as input data.

Firstly, based on the literature review it was found that only limited research was carried out to identify irrigated croplands by crop types at the provincial level. Most of the available land use land cover maps have low resolution and classified crop types as croplands or agriculture. Besides, we have not found any research which compares derived crop types area with official state statistics at the provincial level in the study area. Thus, it is very important to recommend an accurate and timely crop types

mapping method for the local land control and management authorities and policy makers.

Preliminary climate change analysis over the 35 years of 1979 through 2013 demonstrated the increasing trend of temperature and decreasing trend of precipitation over the croplands, pasturelands, and grasslands of the study area. Precipitation decrease in the study area may reduce plant productivity and temperature increase may have either positive or negative influence on plant production due to more evaporation than precipitation. Besides, expansion of agricultural irrigated cropland and population increase has a significant influence on land-use intensity.

Secondly, a comparison of three classifiers algorithms SVM, RF, and MLC performance was studied and the result showed SVM and RF classifiers produced a visually pleasant and realistic irrigated cropland map in the research area. Accuracy assessment results showed that SVM yielded the highest OA and KA. KA of classified images for SVM were 0.90 and 0.89 for the RF algorithm. Both performed well and achieved identical close values. But MLC showed a lower result of KA 0.60.

Thirdly, further analysis of testing different indices (NDVI, EVI, NDWI1, and NDWI2) with recommended SVM and RF classifiers using Sentinel-2 and Landsat-8 sensors data were carried out. The results of OA, KA, UA, and PA have shown that RS imagery from both sensors is of comparable quality. But the differences in accuracy results vary higher based on the vegetation indices used than on sensor data. KA values vary between 75% to 88 % in all indices. The lowest KA values were achieved in all indices with the SVM classifier of L8 sensor data. The highest KA values 88% and 87% were achieved with the RF classifier of L8 data when EVI and EVI-NDVI were used respectively. Using NDWI 1 and NDWI 2 which uses SWIR 1 and SWIR 2 bands is not achieved good results in both accuracies point and area comparison and it is not recommended for irrigated crop types mapping.

Fourthly, the difference between remote sensing derived classified maps area and officially recorded statistic crops area was compared. It was found that the smallest absolute weighted average value difference of 0.2 thousand ha was obtained using EVI-NDVI with RF method and NDVI with SVM method of Landsat 8 sensor data. For Sentinel 2 sensor data, the smallest absolute value difference result of 0.1 thousand

ha was obtained using EVI with RF method and 0.4 thousand ha using NDVI with SVM method.

Finally, it can be recommended that using medium 30 m resolution Landsat sensor data is sufficient for mapping irrigated crop types over the study area, and since the launch of this satellite in 1972, historical irrigated cropland mapping is possible for the period up to today. Besides, the recent successful launch of Landsat-9 will successfully continue the Landsat data suite and enable new opportunities in the joint use of Landsat and Sentinel data to capture high temporal resolution during the vegetation growth period which helps to distinguish other minor crop types as well as increase classification accuracy.

Classified irrigated crop types maps can benefit regional land management administration offices to monitor the spatial extent of crops location and its monitoring as well as modeling and predicting crop yields and production by different agroecological models. And also, the use of remote sensing-based irrigated crop types data periodically to monitor and evaluate agricultural land uses which can save time, effort, and capital that are needed for traditional human-based ground surveys.

1 Introduction

The land is the basis for agriculture and other rural land uses, encompassing soils, climate, vegetation, topography, and other natural resources. Globally agriculture uses around 4 750 million ha of land for growing crops and livestock farming. More than 1 500 million ha occupy temporary and permanent crops. And around 3 300 million ha of land are used as permanent meadows and pastures. In general, agricultural land areas change is very small since 2000. However, irrigated croplands and permanent crops have increased, while permanent meadows and pasturelands have significantly declined. Between 2000 and 2019 cropland increased by 4 percent in the world which is about 63 million ha. Besides, the fast growth of urban areas is replacing agricultural lands (SOLAW 2021).

Irrigated croplands use a lot of water resources. Water resources in the world are under pressure nowadays. The water stress level in Central Asia is over 70 percent which indicates medium and high. In the study area, most of the agricultural areas are irrigated croplands and agriculture plays an important role in water stress and it is very high in Uzbekistan because all irrigated croplands compete for the water of river basins.

Irrigation in Central Asian countries began as early as the 6-7th centuries before AD. The region's climate is sharply continental, mostly arid and semi-arid. Average annual precipitation (falling mainly in winter and spring) is about 270 mm, varying between 600-800 mm in the mountains and 80-150 mm in desert areas. Tracing the history of the development of irrigation networks, it can be noted that irrigated agriculture originated in areas adjacent to natural waterways. Factors contributing to the development of irrigation in these areas were the proximity of the location sources of water and relatively flat and large areas and the length of loess-covered terrace surfaces. Soil cover, formed on loess rocks, is characterized by high fertility. Under irrigation conditions on these tracts, it is possible to obtain yields of all crops (FAO).

A discussion of land use issues in Uzbekistan would be incomplete without mentioning the most important problem of water and irrigation. 80% of the territory of Uzbekistan is deserts or semi-desert, and only 4.2 million hectares (out of 20.5 million hectares belonging to the category of agricultural land) are irrigated land. Agriculture accounts for 17.6% of the Uzbek economy and 27.1% of the population are engaged in agriculture. The total land area of the Republic of Uzbekistan is 44410.3 thousand hectares, of which 4212.8 thousand hectares are irrigated lands, 11143.8 hectares are hayfields and pastures, and the remaining 29053.7 hectares are other lands. Irrigated land accounts for 23.8% of total agricultural land. Agriculture consists of two major sectors: agriculture and animal husbandry. Of the arable land, 39.6% is wheat, 35.8% is cotton and the remaining 24.6% is main crops (fruits, vegetables, livestock, and various cereals).

There is a need for an integrated approach to the planning and management of land resources in the country. The land is a limited resource and is increasingly impacted by competition between mutually exclusive uses. Due to the effects of climate change, desertification, erosion, pollution and population increase, pollution, urbanization, and other factors, fertile land in rural regions is becoming increasingly scarce. Government authorities and agricultural organizations need to know which areas of the country's land area are used for which purpose.

Agricultural land use (LU) maps are needed to identify and qualify the agricultural lands as well as the major uses of land occurring there. LU maps contribute to better management of land by helping to control the allocation of land for specific uses. This ensures the availability of resources for future generations. It minimizes the effect of economic activities and development on the environment. Land-use planning can assist in achieving a balance between these competing and occasionally opposing purposes.

Local cadastre office records showing the extent, value, and ownership of lands are not always available in developing or poor countries. The ability to ascribe land ownership is one of the main principles to make land-use planning and management effectiveness. When either cadastre records exist and other forms of digital records are unavailable, remote sensing technologies, i.e. those processing and monitoring an

area's physical characteristics from satellite or aircraft imagery, allow bridging the informational gap.

Therefore, the use of GIS and remote sensing techniques with modern machine learning algorithms and data periodically to monitor and evaluate agricultural croplands can save time, effort, and capital which are needed for traditional human-based ground surveys. And also, it is very important to integrate the gathered human-based statistics with the remote sensing techniques to interpret the capability of derived cropland maps which this research intends to investigate.

1.1 Research objectives

The main goal of this research is to provide explicit recommendations on the application of different supervised classification methods for precise and accurate irrigated croplands extent product of Tashkent Province in Uzbekistan using Sentinel - 2 and Landsat - 8 data in 2018, within the GIS and Remote Sensing software. To achieve this goal, the following specific objectives were developed:

- i. to review scientific articles, local reports, and expert's opinions on land use and climate change, land degradation issues of the study area to clarify future study activities;
- ii. to map and compare the performance of Machine Learning Algorithms (MLA) such as SVM, RF, and MLC methods for main irrigated croplands by crop types with 10 m high-resolution Sentinel – 2 data;
- iii. to map and compare irrigated croplands using both Sentinel - 2 and Landsat- 8 data by utilizing different indices such as NDVI, EVI, NDWI1, and NDWI2 with the best-performed classification algorithm from the previous objective;
- iv. to compare the area of all derived agricultural land use maps with the official data from the State Committee for Statistics of Uzbekistan;

- v. to recommend an accurate and precise irrigated croplands classification method that concerns spatial-temporal resolution, sensor type, and spectral bands.

1.2 Research Questions

Based on these objectives, the following research questions were answered in this dissertation:

1. What kind of research and studies related to the dissertation was carried out in the study area and what should be studied in the future?
2. What is the situation of land use and climate changes in the study area?
3. How do different classifier algorithms perform in irrigated crop type classification using multi-temporal satellite data?
4. What is the performance of classifier algorithms when different indices were used for image classification?
5. Which remote sensing-based derived crop types areas by satellite types and different indices close to the official data?
6. What is the spatial resolution requirement for crop type identification via the supervised image classification methods?

1.3 Overview of the thesis

This section describes an overview content of each thesis chapter. This dissertation consists of six chapters, of which chapters 3, 4, and 5 have been written in the form of scientific manuscripts.

Chapter 1 presents a basic background of the research, general overview, main goal, objectives, and research questions of the study.

Chapter 2 describes the location, climate, demography, agricultural lands, and the soils of the study area.

Chapter 3 present a short literature review of scientific articles, local reports, and expert's opinion on land degradation caused by climate change (in particular temperature and precipitation change) and land-use change in Central Asia (CA) with a special interest in Tashkent Province and aspects of regional water management in CA to clarify future study activities. This chapter also presents the preliminary analysis of climate and land-use changes in Tashkent Province and the author's opinion about the impact of these changes on potential land degradation.

Chapter 4 provides the potential use of multitemporal Sentinel-2 satellite data using different classifier algorithms to derive an up-to-date irrigated crop types classification map of the study area for the growing season in 2018. And also compares the area of derived irrigated cropland area with data from the State Committee for Statistics of Uzbekistan for selected crop types. The best-performed classification algorithm was used to further analysis using different indices and satellite sensors to find spatial resolution requirements for specific crop types mapping as described in Chapter 5.

Chapter 5 presents research to compare and assess the importance of optical remote sensing data in a crop type classification using medium Landsat 8 and high spatial resolution Sentinel-2 RS imagery in 2018. Four indices “Normalized Difference Vegetation Index” (NDVI), “Enhanced Vegetation Index” (EVI), and “Normalized Difference Water Index” (NDWI 1 and NDWI 2) were used and calculated using blue, red, near-infrared, shortwave infrared 1, and shortwave infrared 2 bands. Comparing the area of derived irrigated cropland area with data from the State Committee for Statistics of Uzbekistan for selected crop types was also shown.

Chapter 6 summarizes the main findings and conclusions of this dissertation, states its limitations, and makes suggestions for future research on the topic.

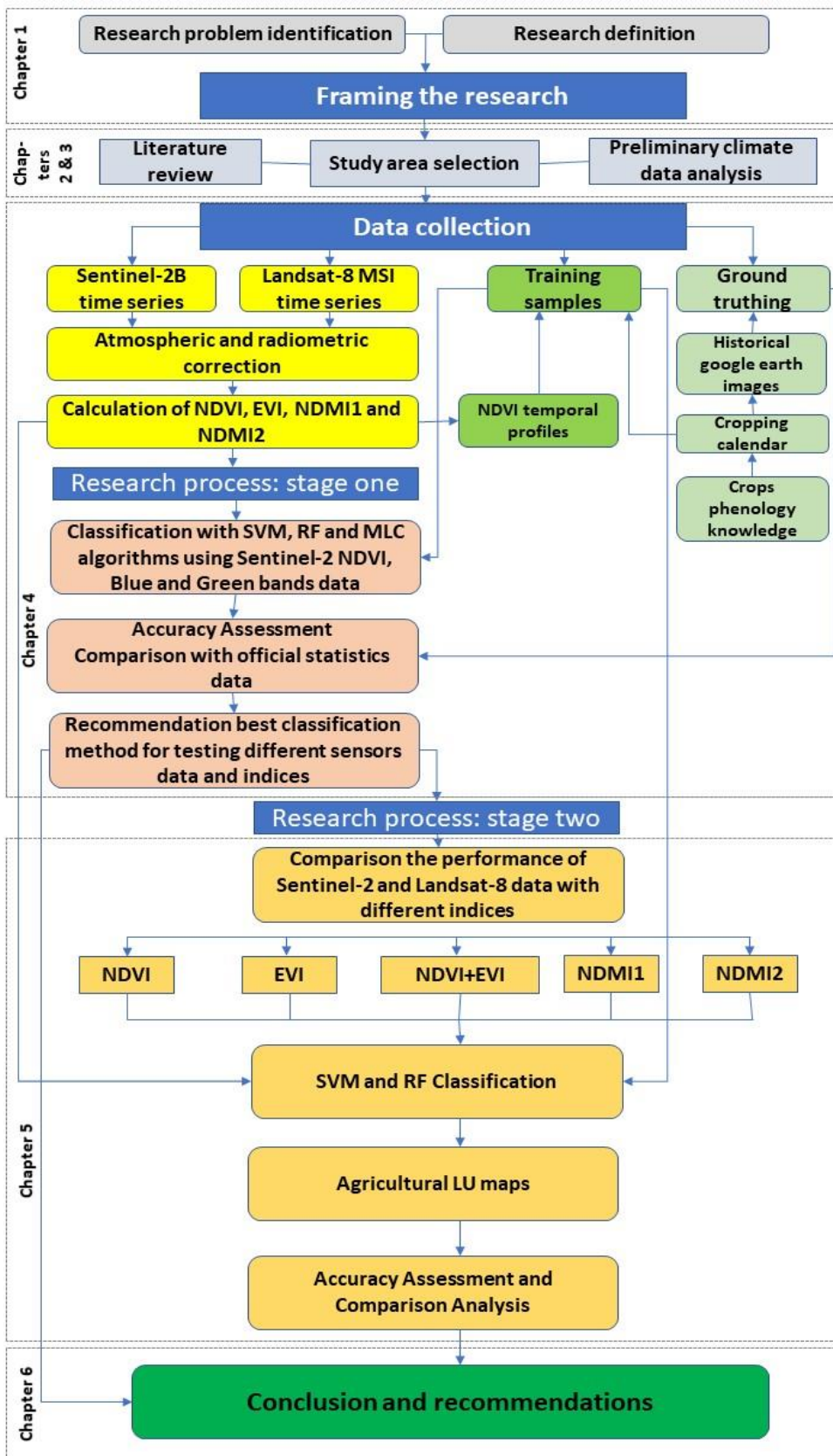


Figure 1.1. The framework of the research.

1.4 Irrigated lands contribution to the total yield

Crop yields and multiple cropping sowing are systematically higher in irrigated lands than in rainfed areas. Worldwide about 20% of the total arable area is irrigated lands but they produce about 40% of all crops and about 60% of cereal production. Therefore, it is expected to increase irrigated lands further. (Jean-Marc Faurès, Jippe Hoogeveen and Jelle Bruinsma, 2016).

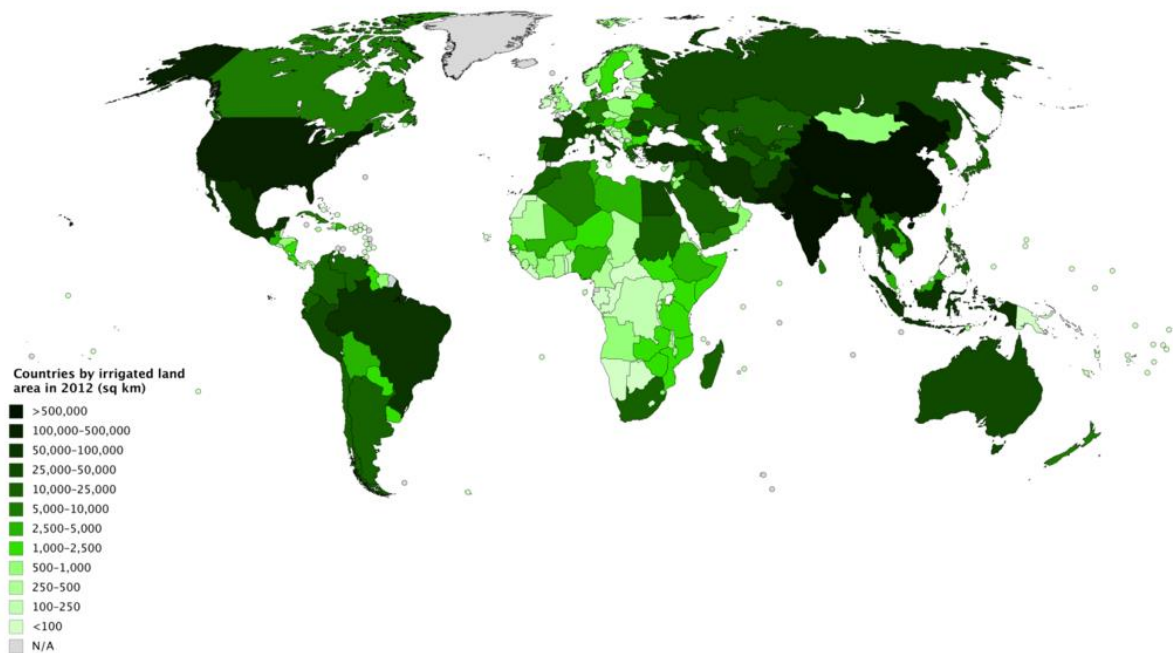


Figure 1.2. Countries by irrigated land area in 2012. Countries/territories shown with the irrigated land area as '0' are shaded with the '<100' color (lightest green); those with no data are shaded with the 'N/A' color (grey). Source: CIA World Factbook, 2016.

China and India are the largest irrigated land area, which makes up 21.3% and 20.6% of worldwide irrigated land area. Uzbekistan ranked 14th place in the world with about 4,2 million ha of irrigated lands in 2012 (Wikipedia 2021).

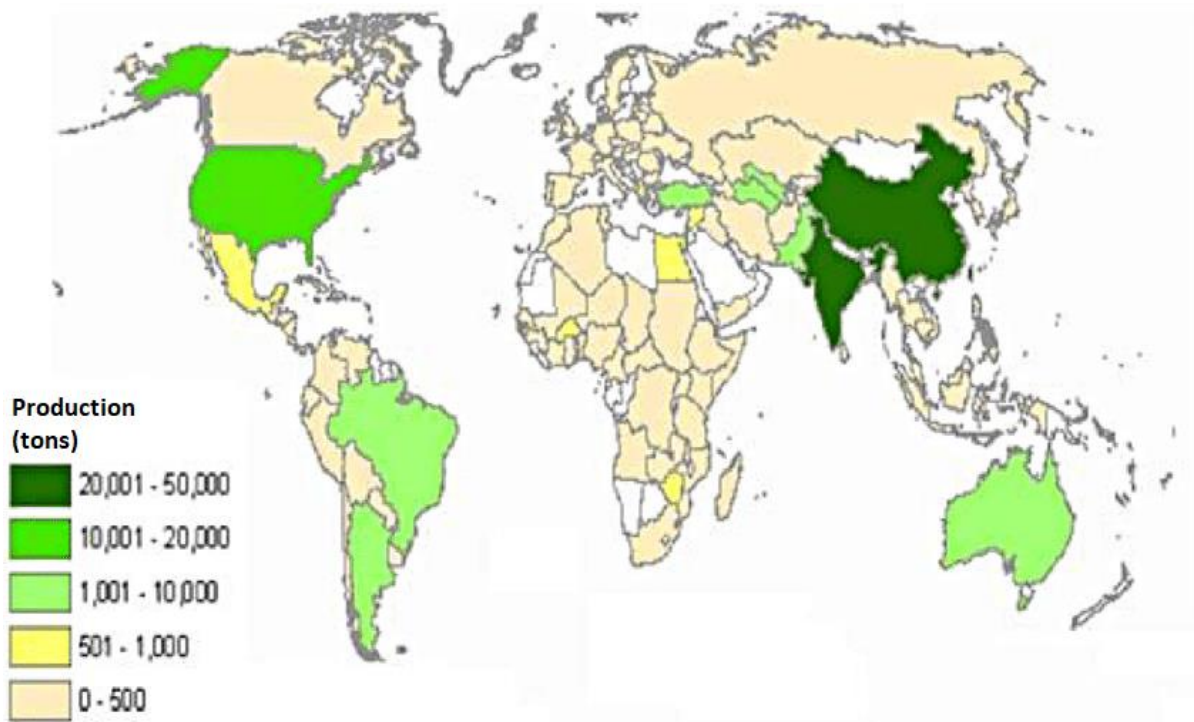


Figure 1.3. Cotton production of the world by country. Source: PSD Online <http://www.fas.usda.gov/psdonline> by (Malik and Ahsan 2016).

One of the world's most important crops is cotton. India is the largest producer of cotton in the world and produces about 6.2 million tons per year. Like Uzbekistan, India's climate is very favorable for cotton growing. China is the world's second-largest cotton producer. China is produced about 6.17 million tons of cotton every year. The United States is the third-largest cotton producer in the world, with a production of 3.6 million tons. Uzbekistan is the world's 6th cotton producer, with a production of about 1.1 million tons. But it ranks second place in production per person 33.9 kg after Australia (FAOSTAT 2020a).

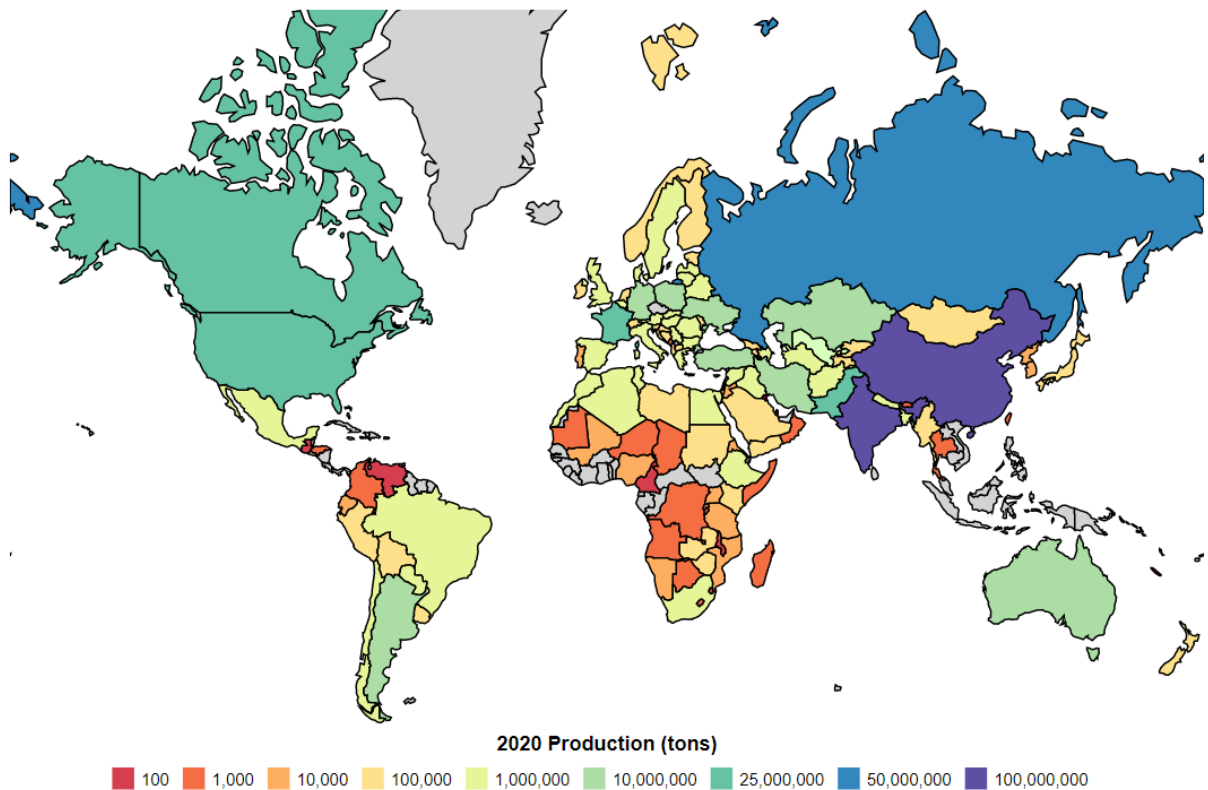


Figure 1.4. Wheat production of the world by country. Source: FAOSTAT.

Wheat is the second-most-produced cereal grain behind maize in the world. The world trade in wheat is greater than all other crops combined. In 2020, the total global production of wheat was 760 million tons. The three largest individual wheat producers in the world are China, India, and Russia which produce about 41% of the world’s total wheat production. Uzbekistan ranked 23rd place in the world with 6.2 million metric tons of wheat production in 2020 (FAOSTAT 2020b).

1.5 The role of irrigated agricultural land in the economy



Figure 1.5. Increase of global agriculture value-added. Source: FAO, 2021.

Figure 1.6. Share of agriculture in global GDP. Source: FAO, 2021.

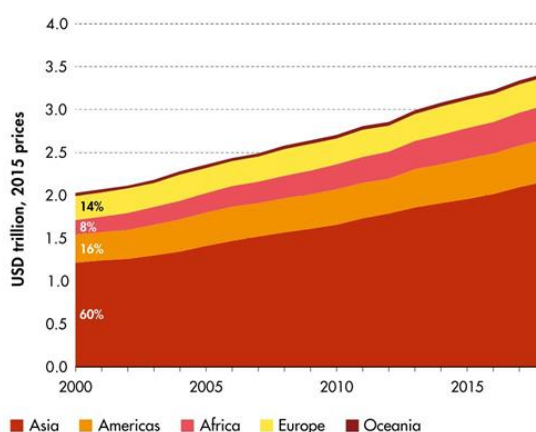


Figure 1.7. Value-added of agriculture, forestry, and fishing by regions. Source: FAOSTAT.

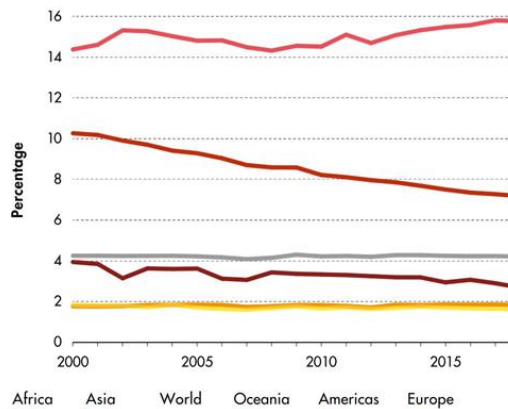


Figure 1.8. Share of agriculture, forestry, and fishing value-added in total GDP by region (US\$ 2015 prices). Source: FAOSTAT.

The global value-added generated by agriculture, forestry, and fishing grew by 73 percent in real terms between 2000 and 2019, reaching USD 3.5 trillion in 2018 compared to USD 1.5 trillion in 2000. Asian countries were the main contributor with

64 percent of the world total in 2019 which is 2.2 USD trillion (FAO Statistical Yearbook, 2021).

Agriculture is an important state-controlled sector of the Uzbek economy, accounting for approximately 28.2% of GDP in 2020 (Figures 1.7. and 1.8.) which is over one-quarter of the Uzbek economy. It employs about 4 million people, which is more than 26.8% of the total employment in the country.

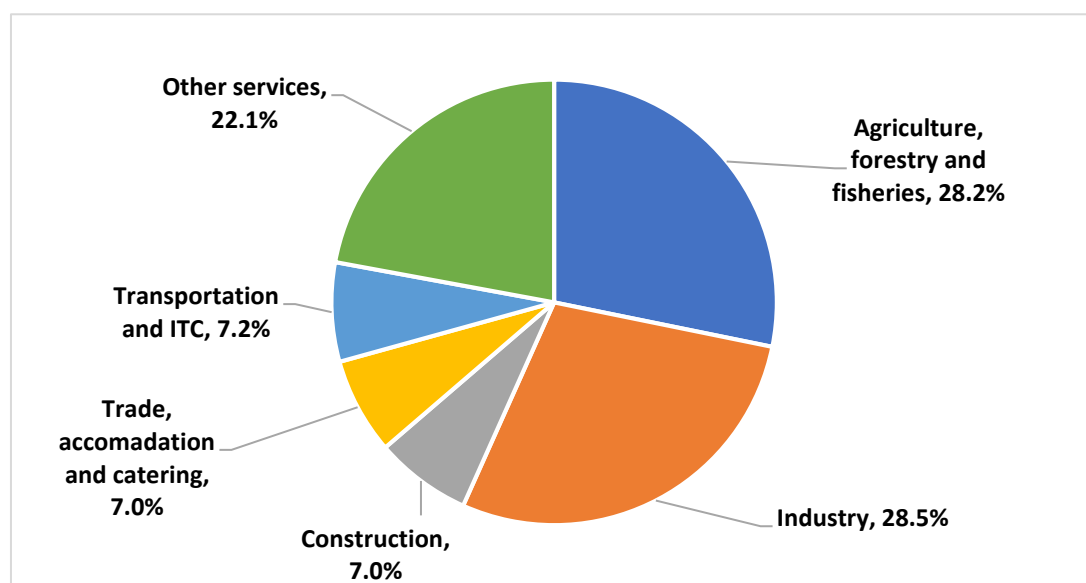


Figure 1.9. Sector's contribution to the country's GDP in 2020. Source: State Statistics, 2021..

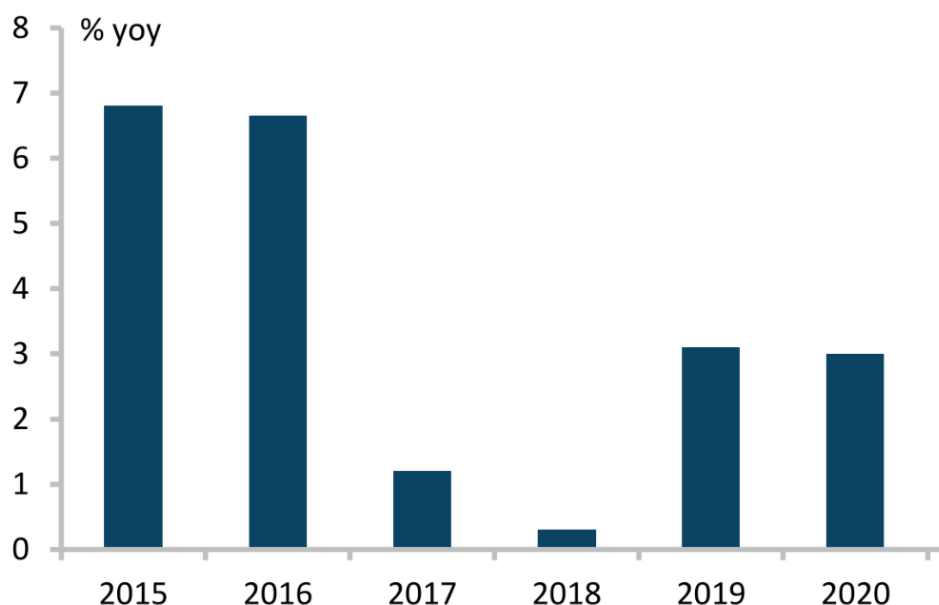


Figure 1.10. Growth in agricultural GDP. Source: State Statistics, 2021.

Growth in agriculture slowed down after 2015 as shown in Figure 1.10. However, it has uncertain about the reliability of earlier statistics. The recent agricultural growth rate is about 3%. Agricultural Development Strategy in Uzbekistan for 2020-2030 calls for annual growth of 3% in 2021, and 5% by 2025. (Stephan von Cramon-Taubadel, Shavkat Hasanov 2021).

1.6 Cotton and wheat are major crops

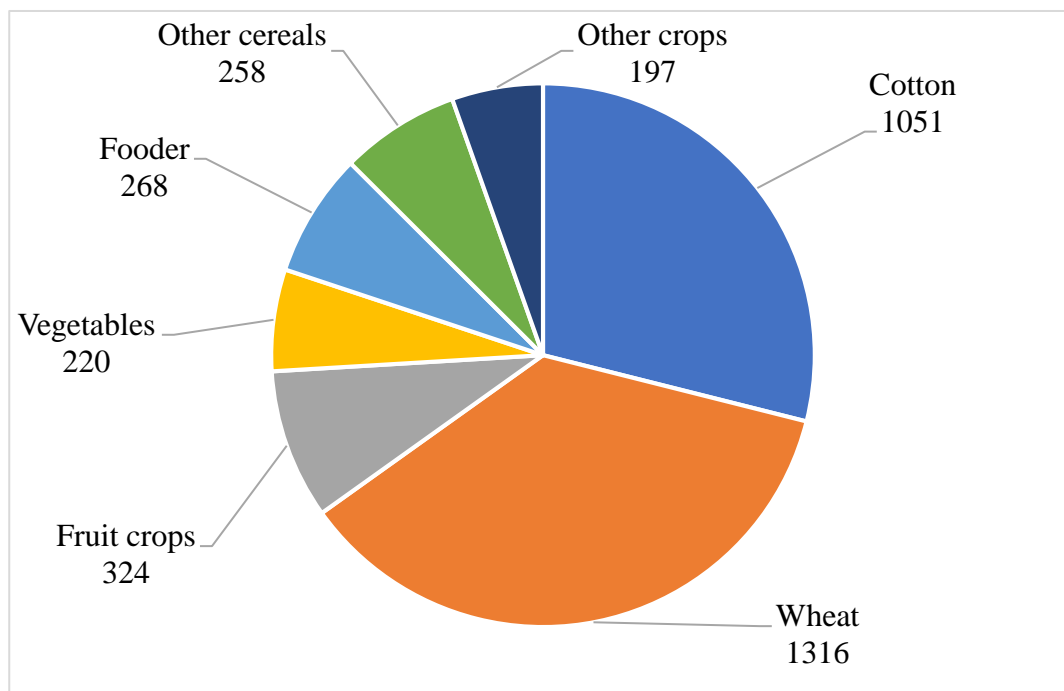


Figure 1.11. Sown crops (thousands ha) in Uzbekistan. Source: State Statistics, 2020.

The crops cotton and wheat dominate the sown area throughout the country. In 2020, almost 65% of the sown area was allocated to these crops. In Tashkent province, cotton and wheat occupied over 61% percent of the total sown area in 2018. In general, cotton and wheat are less sown in Karakalpakstan and Jizzakh, Tashkent, and Khorezm provinces, occupying less than two-thirds of sown land area. In 2016, the average sown area per rural inhabitant is 0.23 ha and it is in relative scarcity in Uzbekistan. The highest density of rural population is in Andijan, Samarkand, Surkhadarya, and Fergana provinces, while the lowest densities are observed in Syrdarya and Jizzakh provinces. But in Tashkent province sown area per rural inhabitant is above average 0.24 ha (Djanibekov 2019).

For the last 60 years, crop-planted areas in Central Asian countries passed three periods: expansion (1960–1990), reduction (1990–2000), and restoration (2000–2016). During this time, the grain yield in Central Asia increased from 0.9 t/ha in 1960 to 1.9 t/ha in 2016. The cotton yield increased from 1.9 to 2.6 t/ha from 1960 to 1990 and has declined significantly since the 1990s. Unfortunately, water consumption per hectare has not changed significantly; the consumption rate for grain is 4326–5417 m³/ha and for cotton 8155–9157 m³/ha. Water consumption of cotton crops is high compared with grain. Under constant sown areas, reducing the proportion of cotton area can reduce the total water consumption of crops (Liu et al. 2020).

The major irrigation practices take place during the vegetation period between April and October, and light irrigation and large-scale maintenance of water infrastructure are carried out during the non-vegetation period between November and February (Djumaboev et al., 2017).

1.7 Climate change impact on agricultural production and irrigation

Central Asian countries face significant difficulties to supply their growing population with food, water, and land resources. Especially, climate change will impact water availability in the region, which is already limited and often used at unsustainable rates. Investigating the effects of global change and exploring appropriate agricultural land use classification under climate change is very important. Climate change not only affects water availability but also the demand for water resources globally. If a region becomes drier and warmer, the decreased water availability will be exacerbated by an increased water resources demand. Irrigation will be mostly influenced by climate change in the water use sector. Nowadays about 67% of the current global water withdrawal belongs to the irrigation sector. The share of irrigated agricultural land in the total cropped area is less than 20% but it produces about 40% of the world's food. Therefore, it is expected that irrigated agriculture will have to be extended in the future to feed the world's growing population. But, it is still not yet known whether

there will be enough water resources available for the necessary extension (Petra Döll, 2002).

For the last 50-60 years, climate change has reduced Central Asia's glaciers by 30%. It is projected that the region's GDP drop by 11 percent due to this glacial decline to result in water availability.

Uzbekistan is one of the Central Asian countries beset by water scarcity, which will be aggravated by climate change, which will lengthen droughts. The entire water deficit in the country has surpassed 3 billion cubic meters, and it is expected to rise to 7 billion cubic meters by 2030 and 15 billion cubic meters by 2050.

Water availability per capita has also decreased during the last 15 years, from 3048 to 1589 cubic meters, while the country's population is growing at a rate of 650-700 thousand people each year.

Uzbekistan's population is expected to reach 39 million by 2030. Water demands will rise by 18-20% as a result of the population increase.

Kazakhstan to the north, Kyrgyzstan and Tajikistan to the east, and Turkmenistan to the south border of Uzbekistan. Droughts and water scarcity are more likely in the desert, which covers 78 percent of the country's total territory (Climate Adaptation Platform 2021).

1.8 Indices used for major irrigated crop types classification

Four spectral vegetation indices, the Normalized Difference Vegetation Index (NDVI) [Tucker 1979], Enhanced Vegetation Index (EVI) [Huete et al. 1997, Huete et al., 2002], Normalized Difference Water Index 1 (NDWI1), and Normalized Difference Water Index 2 (NDWI2) [Gao 1996, Wilson et al 2002], were calculated using the surface reflectance values. These indices were formulated by using the following equations:

$$NDVI = \frac{\rho_{NIR} - \rho_{Red}}{\rho_{NIR} + \rho_{Red}} \quad \text{Equation 1.1}$$

$$EVI = 2.5 * \frac{\rho_{NIR} - \rho_{Red}}{\rho_{NIR} + 6 * \rho_{Red} - 7 * \rho_{Blue} + 1} \quad \text{Equation 1.2}$$

$$NDWI1 = \frac{\rho_{NIR} - \rho_{SWIR1}}{\rho_{NIR} + \rho_{SWIR1}} \quad \text{Equation 1.3}$$

$$NDWI2 = \frac{\rho_{NIR} - \rho_{SWIR2}}{\rho_{NIR} + \rho_{SWIR2}} \quad \text{Equation 1.4}$$

where ρ_{Blue} , ρ_{Red} , ρ_{NIR} , ρ_{SWIR1} , and ρ_{SWIR2} are the surface reflectance values of Band 2 (blue, 0.45–0.51 μm), Band 4 (red, 0.64–0.67 μm), Band 5 (near-infrared, 0.85–0.88 μm), Band 6 (shortwave-infrared 1, 1.57–1.65 μm), and Band 7 (shortwave-infrared 2, 2.11–2.29 μm) in the Landsat-8 LOI and Sentinel -2 images, respectively (Table 5.2).

1.9 Classification methods

There are two kinds of classification procedures available in remote sensing: 1) unsupervised classification and 2) supervised classification. In unsupervised classifications, pixels are assigned to groups based on each pixel's similarity to other pixels (no truth, or observed, data are required) (e.g. forest, agricultural, water, etc). Usually, this after the fact assignment of spectral clusters is difficult or not possible due to these clusters containing assemblages of mixed land cover types. Principally, unsupervised classification is useful for quickly assigning labels to uncomplicated, broad land cover classes such as water, vegetation/non-vegetation, forested/non-forested, etc). Besides, the unsupervised classification may reduce analyst bias. In supervised classifications, the user instructs the image processing software to specify the land cover classes of interest. For each land cover type of interest, the user creates "training sites" - places on the map that are known to be representative of that land cover type. Training data is collected in the field with high accuracy GPS devices or expertly selected on the computer (M. S. Boori, R. Paringer, K. Choudhary, A. Kupriyanov, R. Banda 2018). Many studies have conducted the application of multispectral imagery of Sentinel and Landsat in the classification and mapping of agricultural land uses in particular crops by crop types. Therefore, this study is intended to evaluate SVM, RF, and MLC methods on their performance in mapping main irrigated cropland by crop types. The description of these classification methods is given in *Chapters 4.3.5 and 5.3.3*.

1.10 Accuracy Assessment

Designing and performing an accuracy evaluation is the most reliable approach to assessing the accuracy of a map quantitatively. The findings of an accuracy evaluation usually give us a picture of the map's overall accuracy as well as the accuracy of each class. Any classification should include an estimate of accuracy. Accurately assessing a product made with remotely sensed data can be time-consuming and expensive. This

is the fundamental reason why, in trying to save time or money, this critical stage is sometimes skipped or drastically altered in mapping projects. Accuracy assessment can be done through a comparison of a map produced from remotely-sensed data with another map from some other source. A determination is made of how closely the produced map from the remotely-sensed data matches the reference map (Gary M. Senseman, Calvin F. Bagley, Scott Tweddale 1995).

Error matrixes have been produced for each classified map and only user's accuracy (UA), producer's accuracy (PA), overall accuracy (OA) and Kappa coefficient (KA) values have been taken from all tables of matrices to abridge the thesis.

1.11 Accuracy Assessment Formulas

Overall accuracy

Overall accuracy, ' or the percentage of cases appropriately allocated, is one of the most common. This is a straightforward indicator of the classification's overall correctness. If the focus is on the accuracy of individual classes, the confusion matrix can be used to calculate the percentage of cases correctly allocated by dividing the number of cases correctly allocated by the total number of cases in that class.

$$OA = \frac{\sum_{k=1}^q n_{kk}}{n} \times 100 \quad \text{Equation 1.5}$$

There are two further measures of map accuracies, from two standpoints, which gives rise to the terms user's and producer's accuracy, which as the names suggest, depend on whether the calculations are based upon the matrix's row or column marginals.

User's accuracy

The user's accuracy is derived by dividing the total number of valid classifications for a given class by the total number of rows using data from simple random sampling. A number of fundamental assumptions are made, such as that each case (e.g. pixel) to be

classified belongs entirely to one of the discrete and mutually exclusive classes in an exhaustively defined set.

$$UA = \frac{n_{ii}}{n_{i+}} \quad \text{Equation 1.6}$$

where: n_{ii} - number of correctly classified pixels in row i

n_{i+} - total number of pixels in column i

Producer's accuracy

The producer's accuracy measures a map's correctness from the perspective of the map maker or producer and indicates the likelihood of a given land cover of a region on the ground being categorized as such, or how often genuine characteristics on the ground are correctly depicted on the classified map.

$$PA = \frac{n_{ii}}{n_{+i}} \quad \text{Equation 1.7}$$

where: n_{ii} - number of correctly classified pixels in row i

n_{+i} - total number of pixels in row i

Kappa Accuracy

The kappa statistic, developed by Cohen (Vieira, 2010) is used to control only those instances that may have been correctly classified by chance. Both the observed (total) accuracy and the random accuracy can be used to compute this. It is proposed that it should be accepted as a standard measure to assess map accuracy in specific instances since it has many appealing properties as a classification accuracy index. It compensates for chance agreement in particular, and a variance term for it may be generated, allowing statistical testing of the significance of the difference between two coefficients. This is crucial since there is frequently a desire to compare different classes and so matrices.

$$KA = \frac{n \sum_{k=1}^q n_{kk} - \sum_{k=1}^q n_{k+} n_{+k}}{n^2 - \sum_{k=1}^q n_{k+} n_{+k}} \quad \text{Equation 1.8}$$

where: n – total number of pixels

q – number of classes

$\sum n_{kk}$ – total diagonal elements (sum of correctly classified pixels in all images)

N_{k+} - total number of pixels in row i

n_{+k} - total number of pixels in column i

Table 1.1. Interpretation of the agreement for Kappa coefficient (Landis and Koch 1977).

Value of Kappa	Interpretation of agreement
$0,81 \leq K \leq 1$	almost perfect agreement
$0,61 \leq K \leq 0,80$	substantial agreement
$0,41 \leq K \leq 0,60$	moderate agreement
$0,21 \leq K \leq 0,40$	fair agreement
$0,0 \leq K \leq 0,20$	slight agreement
$K \leq 0,0$	no agreement

1.12 Actuality and major outcomes of this research

The agricultural sector globally is facing many difficulties caused by a range of factors such as rapidly growing populations, depletion of natural resources, environmental pollution, crop diseases, and climate change. Precise methods of agricultural land use are a promising approach to address these issues by improving agricultural land-use practices, for example, by effective water and fertilizer resources, estimating crop yields and biomass, and reducing environmental impact. Constant and accurate monitoring of the growth and condition of agricultural land uses is very important for the effective use of agricultural resources, to manage the potential harvest, and to monitor and control crop types area for better management. Technological advances in remote sensing and GIS technologies have proven valuable for characterizing agricultural arable land at the field to regional and global scales. Over the past four decades, traditional multispectral satellite sensors have been widely used for crop area estimation and seasonal monitoring of land uses. Remote sensing can identify crop types within a field and provide useful information for specific field management practices.

At the same time, the range and degree of utilization and implementation of the above-mentioned technologies in Tashkent province at regional and local levels do not correspond to the economic importance of crop production. Therefore, it is very actual to investigate appropriate crop types classification methods, oriented to the local agricultural crop species during the vegetation period towards sustainable development.

Thus, theoretically, the actuality of this study is determined by the necessity to develop methodological support for monitoring the state and types of irrigated crops in the region. In the practical aspect, the actuality of the work is related to the achievement of a new level of information support for crop type classification, based on the materials of remote sensing of the satellite images and GIS technologies.

2 Overview of the study area

2.1 Location of the study area

Uzbekistan is one of Central West Asia's fastest-growing economies and has sustained rapid economic growth over the past decade. The nation's growth is primarily attributable to Tashkent Province, the nation's most economically advanced region and largest agglomeration. Tashkent Province is located in the northeastern part of the country, between the Syrdarya River and the Tien Shan Mountains. It borders Kyrgyzstan, Tajikistan, Syrdarya Province, and Namangan Province. It covers an area of 15,300 km². The population is around 2.95 mln. (in 2022) about 48% of the population lives in urban areas. The climate is a typically continental climate with mild wet winters and hot dry summers.



Figure 2.1. Administrative map of Uzbekistan and the location of the study area (Nations Project, 2022).

Tashkent Province has a highly developed agricultural industry that is based primarily on irrigation with an increasingly unmet demand for surface water. The main crops are cotton and wheat, but cereals, citrus, fruits, and vegetables are on the rise. It generates about one-quarter of the nation's entire gross domestic product.

Tashkent province has 14 districts and six major cities Akhangaran, Almalyk, Angren, Bekobod, Chirchik, and Yangiyul cities which are regarded as key economic centers. There are three strategically important rivers, Chirchik (north catchment), Akhangaran (central catchment), and Syr Darya (south catchment) serving as the main sources for irrigation and drainage in the province.

2.2 The population of the region

The current population of Uzbekistan is 34,246,664 based on projections of the latest United Nations (UN) data (Figure 2.2.). The UN estimates the July 1, 2022 population at 34,382,084. Uzbekistan's population is currently growing at a steady pace. The current population is 33.47 million people, which is expected to increase over the next few decades until its peaks at 44.4 million people in 2070. By the end of the century, the population is estimated to be about 42.27 million people.

Uzbekistan is currently growing at a rate of 1.5% per year. The population growth rate has decreased from 1.66% in 2016 to 1.48%, a trend that is expected to continue until 2070 when the population growth rate will dip into the negative (Figure 2.3.).

The current fertility rate in Uzbekistan is 2.43 births per woman and the median age is 27.8 years, allowing the population to continue to grow. While the fertility rate is high enough for population replacement now, it is less than half of what it was in 1980 when the fertility rate was 5.46 births per woman. This declining fertility rate trend is expected to continue over time. ("Uzbekistan Population 2022 - World Population Review", 2022).

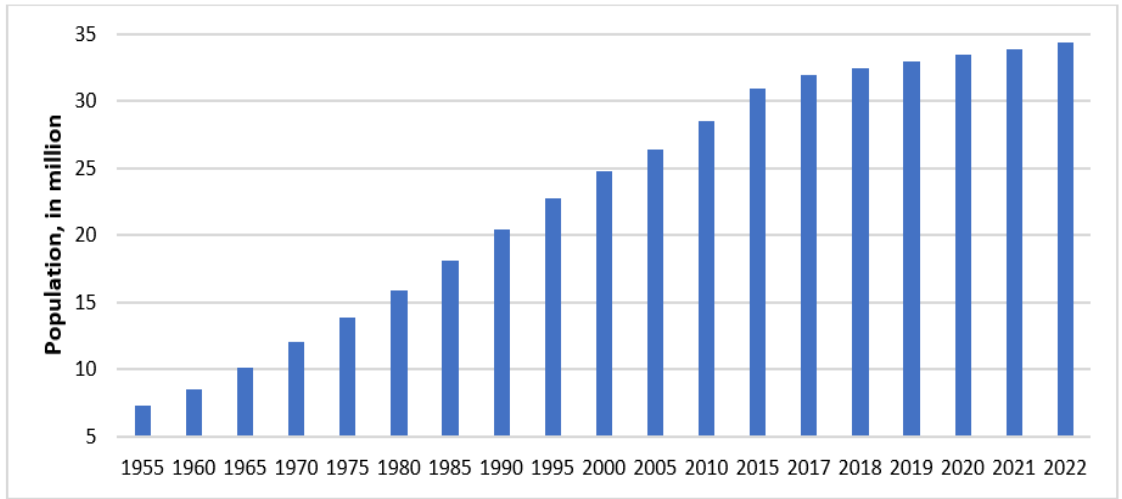


Figure 2.2. Population growth in Uzbekistan.

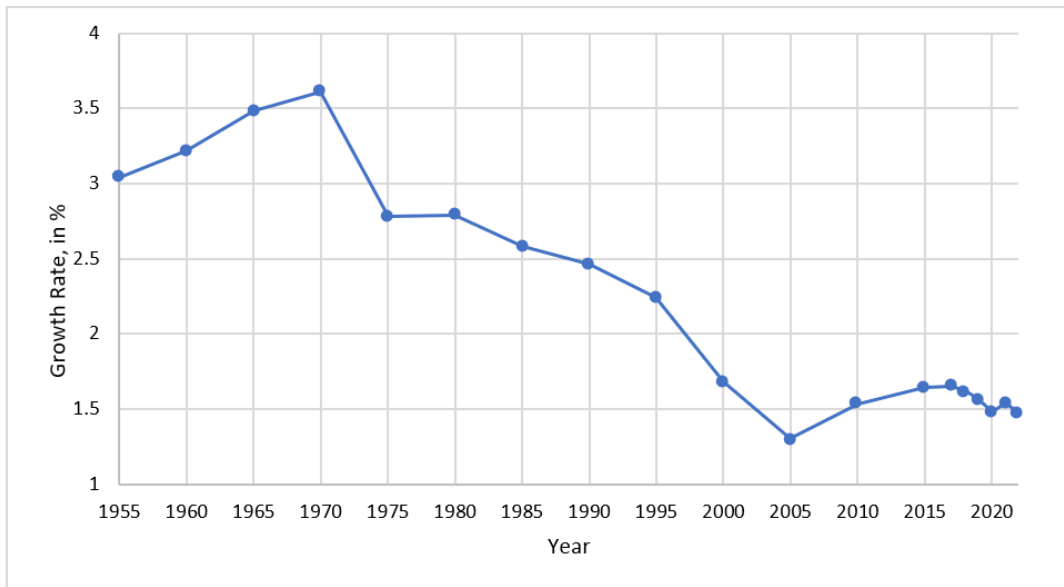


Figure 2.3. The population growth rate in Uzbekistan.

Tashkent Province Statistical data on population growth showed the population of the area is gradually increasing every year with a 1.07 % average annual growth rate since 1991 (Figure 2.4.).

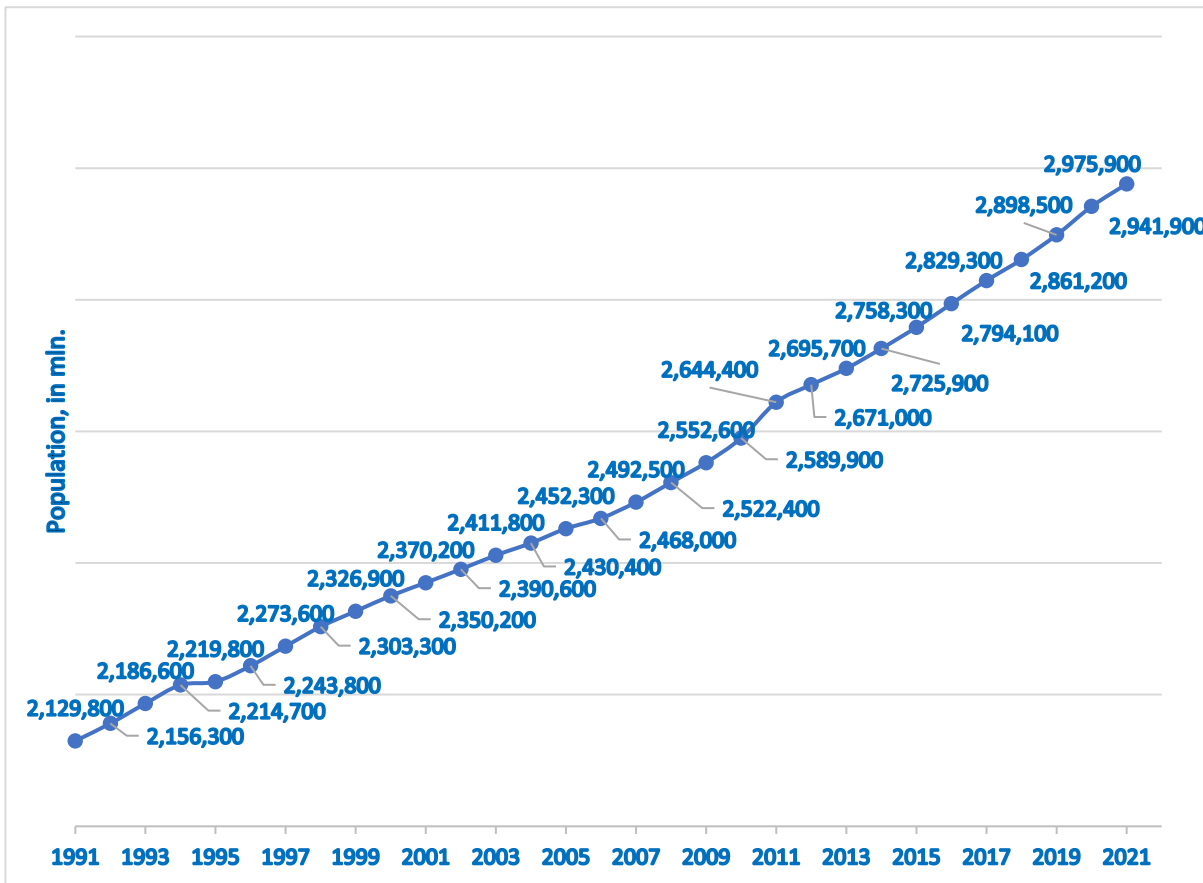


Figure 2.4. Population growth in Tashkent Province.

2.3 Annual agricultural crops area changes in Tashkent Province

Study area Tashkent Province plays an important role in the economy of the country due to the development of industry and agriculture. The total land area of the Province is 1525.8 hectares, of which 337.4 thousand hectares are irrigated lands, 434 thousand hectares are pastures and hayfields, and 81.4 thousand hectares are forests. Irrigated land accounts for 58.5% of the total agricultural land. Agriculture accounts for 59.8% of the total agricultural output and livestock for 40.2%. In 2013, a total of 355.6 thousand hectares of the Tashkent region were planted with agricultural crops, including 134.3 thousand hectares of wheat, 98.2 thousand hectares of cotton, 44.3 thousand hectares of food crops, and 78.8 thousand hectares of other crops (vegetables, melons, fruits, and vineyards) (Statistics, 2014).

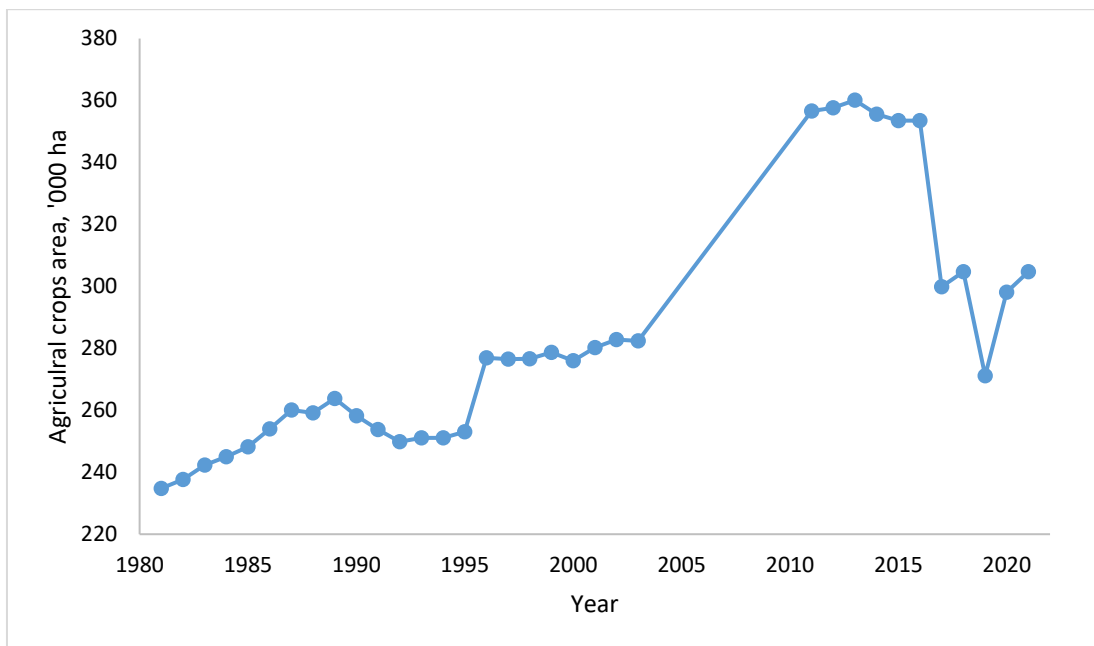


Figure 2.5. Agricultural croplands area changes in Tashkent Province.

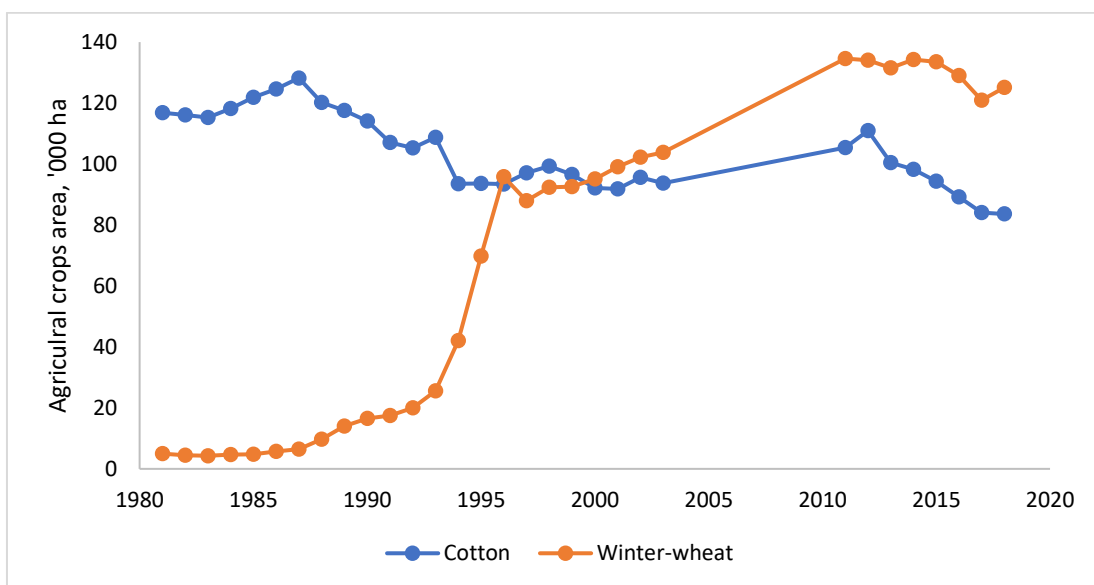


Figure 2.6. Cotton and winter-wheat area changes in Tashkent Province.

Changes in agricultural croplands area since 1981 are shown in Figures 2.5 and Figure 2.6. Analysis of agricultural croplands area changes indicates a gradual change structure of crop area until 2013 and then fluctuating until 2021 as shown in Figure 2.5. It can be the result of different land use management policies by the government. For example, for the period 1981-2018 the area of cotton decreased by about 28%, meanwhile, the area of wheat increased dramatically from 5 thousand ha up to 125.1

thousand ha. The most changes happened after getting independence from the Soviet Union in 1991 (Statistics, 2020).

2.4 Water resources of the study area

The main sources of water for Uzbekistan are the Amu Darya and the Syr Darya, which are both transboundary international rivers. The Amu Darya watershed covers 81.5% of Uzbekistan. The discharge rate of the Amu Darya watershed is 78.46 km³ /year. The amount of inflow from within Uzbekistan is 4.7 km³ /year. Discharge is highest from April to September, accounting for 77% to 80% of the total annual discharge; discharge from October to March accounts for 20% to 23% of the total. The Syr Darya watershed covers 13.5% of Uzbekistan. The discharge rate of the Syr Darya watershed is 36.57 km³ /year, and the amount of inflow from within Uzbekistan is 4.84 km³ /year. The Amu Darya supplies 63% of surface water in Uzbekistan, while the Syr Darya contributes 37%. The total available supply of surface water is 42.1 km³ /year, of which 9.5 km³ /year comes from within Uzbekistan, and 32.6 km³ /year flows in from outside the country. In other words, roughly 80% of the country's main water source, surface water, originates from other countries.

Basin hydrology analysis using GDEM data was carried out. It was found that there are 2 main river basins available in the area as shown in Figure 2.7. The Chirchik River located in Tashkent Province is the largest right midstream tributary of the Syrdarya River basin, where the population of over 3.0 million depends on water resources for irrigation and drinking water (Makhmudova and Makhmudov 2021). The highest point of the river basins in the Chirchik-Akhangaran district is the Beshtar peak (4299 m) which

is located on the Pskem ridge, which extends between the valleys of the Pskem and Chatkal rivers. (Gafforov et al.).

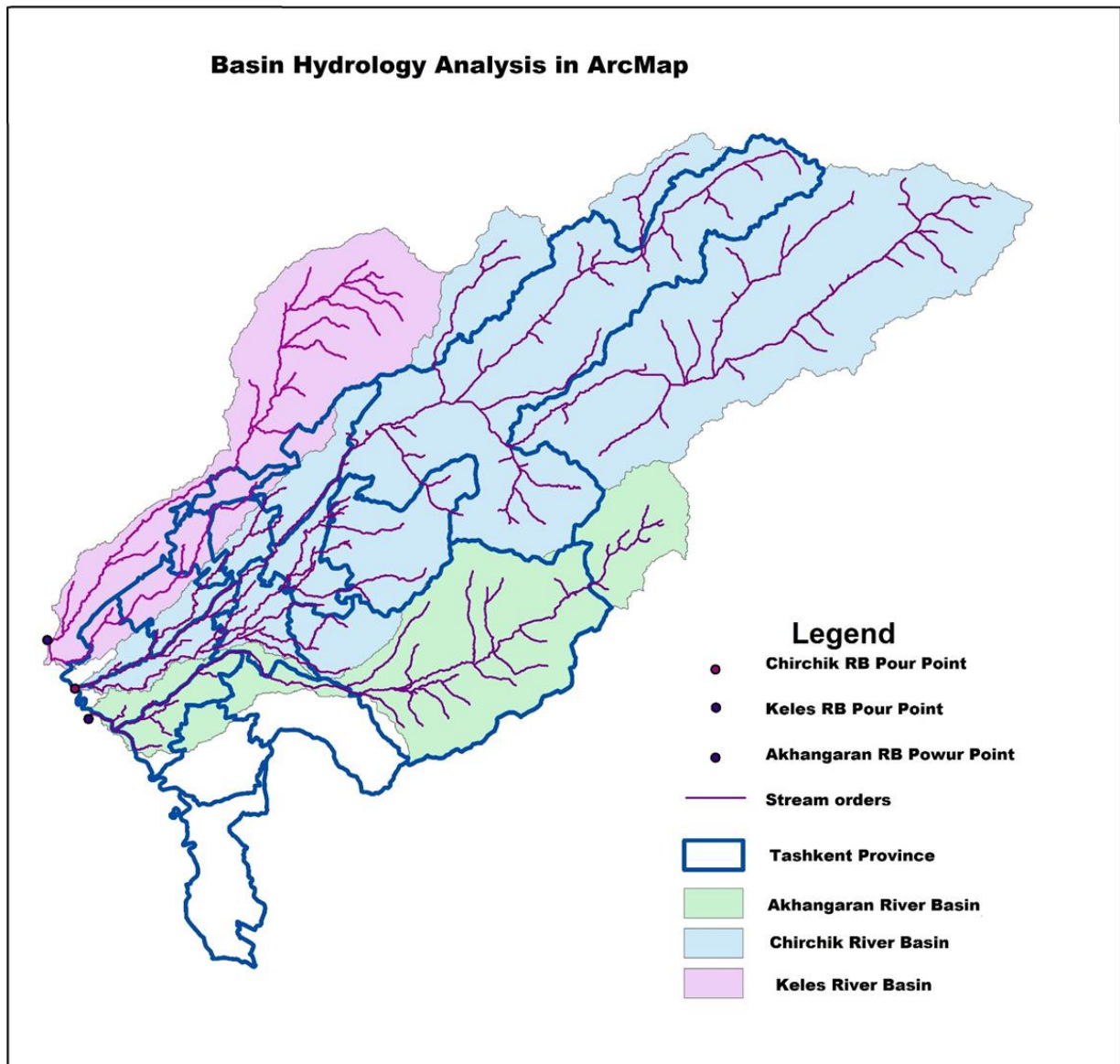


Figure 2.7. Available water basins in Tashkent Province derived from Advanced Spaceborne Thermal Emission and Reflection Radiometer (ASTER) Global Digital Elevation Model (GDEM) data (Tachikawa et al., 2011).

2.5 Soils of the study area and their quality

According to the Institute for Water Problems of Uzbekistan, the following soil types of the study area are determined as alluvial meadow, typical, meadow and dark chernozem, brown, light-brown, sierozem, and meadow steppe (Figure 2.8.). Besides, in terms of hydro-morphological series, there are grassland dark, grassland light, grassland-marsh, and marsh soils. The soils of the basin have been formed in various soil-climatic zones, such as Subnival (high mountainous light-brown soils); Humid-climate-formed type (mountainous brown woodland and mountainous brown soils); Sub-arid (dark sierozem soils); semiarid (typical sierozem soils) (Hasanov 2005).

Irrigated croplands of the Province is located in the Chirchik-Akhangaran River basin. The lands of the river basin are represented by soils from typical gray soils to light brown meadow steppe. Irrigated agriculture is developed mainly on soils that do not require reclamation to combat salinization. Pasture farming, forestry, and pasture livestock are also developed (V.G. Prikhodko 2005).

The quality of irrigated arable cropland in the Tashkent is not identical, as 40.3% of the areas are classified as “good” in terms of quality, 17.7% of the areas are classified as “best”, 36.2% are classified as “average” and 5.8% to the “below average” category. (V.G. Prikhodko 2005, p. 39) The average soil bonitet (soil quality parameter) score in the Tashkent Province is 66, which is 6 points higher than the average of the country (60). Such a comparison allows us to conclude that the irrigated cropland of the region has relatively better quality characteristics of soil fertility and a greater potential for obtaining high productivity of cultivated crops. (V.G. Prikhodko, 2005) Therefore, the soil quality of the study area is qualified as good which is one of the best in the country (Kuziev, 2018).

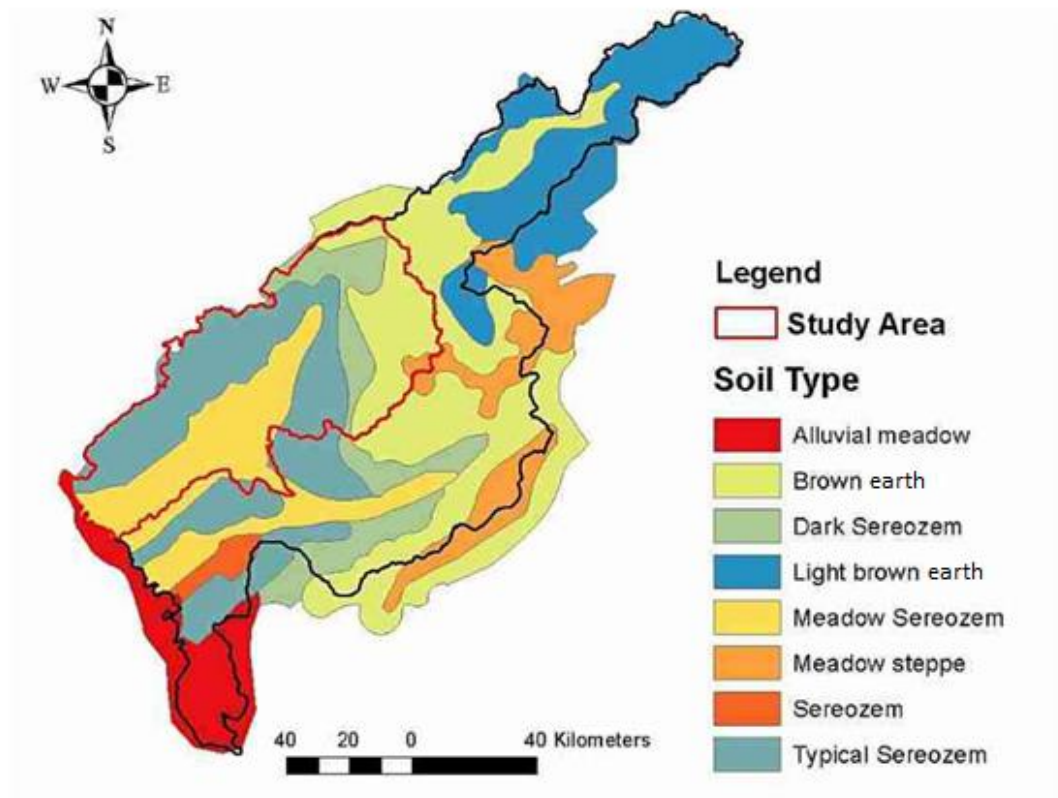


Figure 2.8. The soil types map of Tashkent province (Khurshidbek Makhmudov 2015).

3 Short Review of Climate and Land Use Change Impact on Land Degradation in Tashkent Province

Erdanaev, E.,¹ Kappas, M.,¹ Pulatov, A.² and Klinge, M.¹

¹Institute of Geography, GIS & Remote Sensing, Georg-August Universität Göttingen, Germany

E-Mail: elbek.erdanaev@geo.uni-goettingen.de, mkappas@uni-goettingen.de,
mklinge1@uni-goettingen.de

²EcoGIS Centre, Tashkent Institute of Irrigation and Melioration, Uzbekistan

E-mail: alim.pulatov@mail.ru

This chapter was published as a research article: International Journal of Geoinformatics 2015, 11(4), 39-48.

3.1 Abstract

The paper is a short review of scientific articles, local reports, and expert's opinions on land degradation caused by climate change (in particular temperature and precipitation change) and land-use change in Central Asia (CA) with a special interest in Tashkent Province and aspects of regional water management in CA to clarify future study activities. Furthermore, the paper presents the preliminary analysis of climate and land-use changes in Tashkent Province and the author's opinion about the impact of these changes on potential land degradation. Climate change analysis based on the 0.5° resolution National Centers of Environmental Prediction (NCEP) Global Forecast System Reanalysis (CFSR) weather dataset of the 35 years from 1979 to 2013 demonstrated the trend of increasing temperature and variable trend of precipitation, but small overall precipitation decreases in the croplands, pasturelands, and grasslands of the study area. Irrigated agricultural cropland increased to 7.800 ha from 1999 to 2010 to meet population demand and increase the national economy. Therefore, it is very important to carry out a comprehensive study of climate and land-use change impacts on land degradation at a regional scale using high-resolution Spatio-temporal remotely sensed data for better assessment of land degradation.

Key words: *Climate change, land-use change, land degradation, vegetation productivity, GIS and remote sensing*

3.2 Introduction

Land degradation is the decline or loss of biological or economic productivity and complexity of different types of land covers such as irrigated croplands, rain-fed lands or rangelands, pasture, forest, and woodlands in arid, semi-arid, and dry sub-humid areas, resulting from land uses and human activities (§ 5, UNCCD 1994). The term land degradation originally comes from soil degradation and therefore it is often accepted the same as soil degradation because soil degradation negatively influences plant growth. Worldwide processes like global warming, land use land cover change, as well as population increase, advance and intensify land degradation. Particularly poor countries challenge degradation processes effect more than developed countries. Overuse of natural resources in environmentally sensitive areas also accelerates the process of degradation in these countries (Kertész, 2009). Land degradation has become a major problem in all CA countries and the issue needs urgent action because of rural population engagement in agriculture and livestock, moreover, global climate and land-use changes in the region are threatening sustainable agricultural development and land management. The latest investigations showed the decrease of water resources during the last decades in CA and it is estimated to be continued according to future climate change scenarios. The CA countries depend on their rivers for drinking water, irrigation, and hydroelectric power. In Kyrgyzstan and Tajikistan as, upstream countries the rivers are used mainly for hydro-power, while downstream, in Turkmenistan, Kazakhstan, and Uzbekistan, the rivers are used for agricultural production in the summertime. Agriculture is the largest water consumer in CA and a major employer of the CA's workforce. The agricultural sector delivers a large amount of each country's gross domestic product (GDP). Improving water quality in environmentally degraded landscapes is an urgent need. CA's agricultural expansion and population growth over the past 30 years have placed a great strain on the area's water resources. Given the strong dependence of the CA's economies on irrigated agriculture, it was crucial to stabilizing interstate water exchange immediately after independence. In October 1991 the newly independent countries signed an agreement "On cooperation in the Field of Joint Management and Conservation of Interstate water resources". This agreement affirmed the continuation of formerly existing Soviet structures of interstate water allocation. Transboundary sources of water make up the

bulk of water resources useable to Uzbekistan and were used for irrigated agriculture whereas market economic principles have not been introduced to the agricultural sector in Uzbekistan (McKinney, 2004). Therefore, Uzbekistan's government had to bring up substantial budget subsidies to stabilize the maintenance of the huge water supply system. Regions under socio-hydrological stress are additionally endangered by creeping land degradation. Therefore, Uzbekistan and most of the CA countries have an urgent need for improved information systems for integrated water management under the threat of land degradation caused by climate and land-use change. Geographic Information Systems (GIS) and remote sensing techniques play an important role and they have been used in many studies for detecting minor intensities and magnitudes of land degradation because of their low cost and time efficiency compared to field measurements. Considering above all, it is crucial to study the inter-relationships between climate, ecosystem, and land-use changes using remote sensing, field observations, and modeling experiments for a better understanding of changes (Lioubimtseva and Henebry, 2005). Land degradation can be mapped by assessing spatial-temporal dynamics of land-use and land-cover changes (Kessler and Stroosnijder 2006; Lu et al. 2007, cited in Dubovyk et al. 2013). Therefore, GIS and Remote Sensing are effective tools to study land degradation at global, regional, and local scales. Land degradation assessments based on remote sensing approaches are useful in developing countries, where reliable data and financial means are limited (Dubovyk et al., 2012). GIS and remote sensing-based studies for the assessment and mapping of land degradation and desertification processes in arid and semi-arid regions are broadly recognized and well developed in a wide variety of research areas. Satellite technologies advancement together with remotely sensed image acquisition and analysis propose productive possibilities for monitoring land use and land cover change in the aforementioned fields (Khiry, 2007).

3.3 Land Degradation in CA

More than 60% of the population lives in rural areas and works in the agriculture sector in CA. Land suitable for crop production is 20% of the total agricultural land and livestock production plays an important role in the region (NASA, 2014). Land degradation of desert and semi-desert rangelands all over the whole CA region has

reached an alarming level, calling for an immediate response (Nordblom et al., 1997). Many regional and international efforts have been done to understand the reasons, magnitude, rate, and societal implications of land degradation, but these efforts have not been used effectively to address emerging issues. There are more than 16.4 million hectares of rangelands in CA, and 73% are affected by degradation of various origins, including human-induced and climate change impacts. And it is estimated that human-induced land degradation affects 7.4 million hectares (UNCCD, 2006). Overgrazing of livestock was the most serious type of degradation among all other types of degradation accounting for 44% in rangelands, followed by uprooting and cutting off vital shrubs for fuel (25%). Other degradation types, including all abiotic disturbances such as drought and wind erosion, accounted for only 30 % of total degradation (Yusupov, 2003). The study of changes in vegetation activity seasonally and annually at a regional scale in CA revealed an overall 11.35% increase and 35% of the entire vegetated area of CA exhibited upward trends in growing season NDVI from 1982 to 2003. The study concludes that a strong climate impact seasonal and growing season trends in vegetation activity in CA (Propastin et al., 2008). Net primary productivity (NPP) was derived in Kazakhstan from 2003 to 2011 by using Biosphere Energy Transfer Hydrology Model (BETHY/DLR) and results were studied regarding spatial, monthly, and inter-annual variations. The results showed mean NPP for Kazakhstan is 143 g C m² and it reaches its maximum productivity in June. Most monthly NPP anomalies occurred in northern semi-arid regions and these regions are strongly affected by climate change. And also, arid ecosystems showed lower inter-annual NPP variability in comparison with semiarid ecosystems (Eisfelder et al., 2014). Shokparova and Issanova (2013) studied sierozem soil degradation in irrigated lands of the foothills of Ile Alatau near the Targap (Almaty/Kazakhstan) by measuring soil organic matter (SOM) content, texture, and carbonate content parameters in the laboratory to determine changes between slope and plain areas. They found that soil humus content in 8° slopes is more than 1.17 times higher than in non-plowed land covered with natural vegetation and in plain areas situation is the same and more than 2 times. Intensive land use in agriculture loses soil fertility and humus content in soil horizons. It is estimated that Uzbekistan annually losses US\$ 31 million due to land degradation (World Bank, 2002, Dubovyk et al., 2013). Soil degradation affects croplands and grassland of Fergana, Kashkadarya Bukhara, and Navoi Provinces.

Agricultural croplands of Andijan, Namangan, Tashkent, and Surkhandarya Provinces are strongly affected by water erosion.

About 33 % (161.000 ha) of the area in the Khorezm Province area experienced a different magnitude of land degradation because of low productive lands bordering on the natural sandy desert, proposing that low-fertility areas should be a top place in protection planning (Dubovyk et al., 2013). The number of cattle stock has increased by 46% and sheep and goats by 25 % since 1991. Poultry stock has been increasing more than two times starting in 1997 (Yusupov et al., 2010). Sheep farming operations are mainly based on the use of summer mountain pastures, and overgrazing has a high contribution to land degradation. During the last two decades, there has been a large-scale degradation of pasture lands, due to the unsustainable pasture management in livestock farming, poor pasture maintenance, and other anthropogenic activities (Ibragimov et al., 2007). Rajabov and Thorsson (2009) studied vegetation changes in semi-desert rangeland of Uzbekistan caused by grazing using the State and Transition model to detect grazing-induced vegetation patterns by NDVI derived from satellite imagery and he found considerable vegetation changes resulting from grazing in the study area. According to local expert's observations in the national report of Goskomzemgeodezkadastr (The State Committee of the Republic of Uzbekistan on Land Resources, Geodesy, Cartography, and State Cadaster) irrigation and wind erosion, reducing soil humus content, rising ground water table and soil salinity were observed as an indicator of land degradation in Tashkent Province. Buka, Piskent, Parkent, Bustanlik, and Akhangaran districts are influenced by irrigation erosion, and Bekobod district by wind erosion, while Akkurgan, Yangiyul, and Bekabad districts are fronting soil humus content reduction. In some regions of the study area rising ground water table is increasing soil bulk density. Studying land degradation at the field level in Tashkent Province at the local level is extremely expensive and requires a huge amount of labor work. Besides, investigating inter-annual changes in recent decades is impossible due to a lack of field data.

3.4 Climate Change in CA

Climate aridity increases in CA because of higher temperatures and lower rainfall rates according to the future climate change scenarios. Future global warming may also reduce soil water content in many areas of semi-arid grassland in Asia. Heavy rainfall and increased wind speed due to climate change may increase soil water and wind erosion in some regions. Climate change accelerates the process of land degradation in semi-arid lands due to the expansion of the human population during the next decade (Sivakumar, 2007).

All the above may create difficulties for agriculture and rural livelihoods in CA, but there are no detailed studies on this issue (Sommer et al., 2013). Climate plays an important role in vegetation condition and its development over time. Much of the changes in photosynthetic activity by vegetation are being driven by climate change, especially global warming (Propastin, 2008). Comprehensive research in studying the interrelationships between climate, vegetation cover, and land-use changes will help improve our understanding of the role of CA's ecosystems in the global carbon cycle and global climate change. (Propastin, 2008). And also, climate change affects the availability of water resources and these resources are not equally distributed in CA. Tajikistan and Kyrgyzstan are located upstream and Kazakhstan, Turkmenistan, and Uzbekistan are downstream countries. Upstream countries have 80% of river runoff and consume only 16%, while the downstream countries contributed 14% of total river runoff and withdrew as much as 83% (Micklin 1988 and Chen et al., 2013). Many studies proved that glaciers in the Tien Shan and the Pamir continue to retreat and are shrinking. Most studies also confirmed the continuation of retreat and shrink, despite only a few studies conducted on mass and volume changes (Unger-Shayesteh et al., 2013). In 2000-2001, 2008 and 2011 major crop yields failed due to the decrease in water supply, upstream water use, and droughts in the last years (CACILM, 2006). Moreover, the amount of water is predicted to reduce further given the impacts of climate change and increasing demand from the continuously growing population (Lioubimtseva and Henebry, 2009, Perelet, 2007, cited in Dubovyk et al., 2013). CA countries will face temperature increases in the coming decades and the aridity index is expected to increase throughout the entire region, mostly in the western parts of Turkmenistan, Uzbekistan, and Kazakhstan. And precipitation is expected to decrease

in Uzbekistan and Turkmenistan but a medium increase is projected for winter in the eastern part of Kazakhstan and Kyrgyzstan and Tajikistan. Temperature increase can benefit northern and eastern Kazakhstan with a longer growing season, warmer winter, and little precipitation increase; however western Turkmenistan and Uzbekistan can get affected by frequent droughts and extremely high demand for irrigation water (Lioubimtseva and Henebry, 2009). Arid zones of CA is verified to be sensitive to climate change in the last 100 years, it is expected to have a negative influence on projected future temperature increase (IPCC: Climate Change, 2007 and Feng, 2013). Mountainous regions of CA are facing a frequency of flood increase due to heavy rainfall and it is hardly affecting the poorest population modelled projections show even more changes in the future. The temperature in CA may increase by 3.7°C on average by the end of this century, in particular during June, July, and August which are more important months for crops, and higher temperatures during the vegetation period increase drought risk and decline productivity of agricultural production (IPCC, 2007 and Bobojonov and Aw-Hassan, 2014). Bobojonov and Aw-Hassan, (2014) studied climate change's impact on agricultural producers in the far future by using bio-economic modeling. Modeling results showed that the sensitivity of agricultural systems of CA to climate change depends on agro-ecological zones and socio-economic aspects. During 2010-2040 climate change will benefit farmers in Uzbekistan due to good weather conditions for crop growth, but it is expected to decline during 2070-2100 because of temperature increase and water deficit, especially if irrigation water declines. The impact of climate change on wheat productivity was studied in key agro-ecological zones of CA countries by using the CropSyst model for 14 wheat varieties grown on 18 sites. The study found an increase in wheat yield by 12 % because of temperature increase which helped faster crop growth and high biomass accumulation in 14 sites but it varies between sites, soils, wheat varieties, and agronomic management. The hotter temperature during flowering increases the risk of sterility and grain yield reduction in rainfed spring areas in the north and some parts of irrigated winter wheat in the south of CA (Sommer et al., 2013).

3.5 Climate Change Analysis in Tashkent Province

Tashkent Province (figure 3.1) is located in the northeastern part of the country, between the Syr Darya River and the western part of the Tien Shan Mountains. It borders Kyrgyzstan, Tajikistan, Sirdaryo, and Namangan Provinces. Chatkal, Pskem, and Ugam mountain ranges are located in the northeastern and eastern parts of the Province (upper croplands and grasslands). There are three large water reservoirs located in the province: Charvak, Tashkent, and Akhangaran. Most of the area located in the south and southwest is a predominant plain that slopes gradually towards the Syrdarya River (lower croplands and grasslands) (The Great Soviet Encyclopedia 1979). The total land area of Tashkent Province is 1.526 Mio. ha including 816.4 thousand ha of agricultural land and 709.6 thousand ha of other land types (built-up, desert, forest, etc.). Agricultural lands consist of 305.1 thousand ha of irrigated croplands, 425.4 thousand ha of pasturelands, 35.7 thousand ha of rainfed croplands, 38.5 thousand ha of gardens, and 11.7 thousand ha of vineyards (Goskomzemgeodezcadestr, 2008). The population was 2696.1 thousand people in 2013 and the population density was 194.6 people per km². The climate is a typically continental climate with humid, relatively mild wet winters and long, hot dry summers. The mean January temperature is -1°C to -2°C and the mean July temperature is 26.8°C. The average annual precipitation is 300 mm in the plain region, 300-400 mm in the piedmont region, and 500-600 mm in the mountains. Precipitation mostly occurs in the early spring and permanent snow cover is located in the higher mountains. The

main river Syrdarya and its tributaries Chirchik and Akhangaron Rivers are fed by snow and glaciers and they are used for irrigation and hydroelectric power.

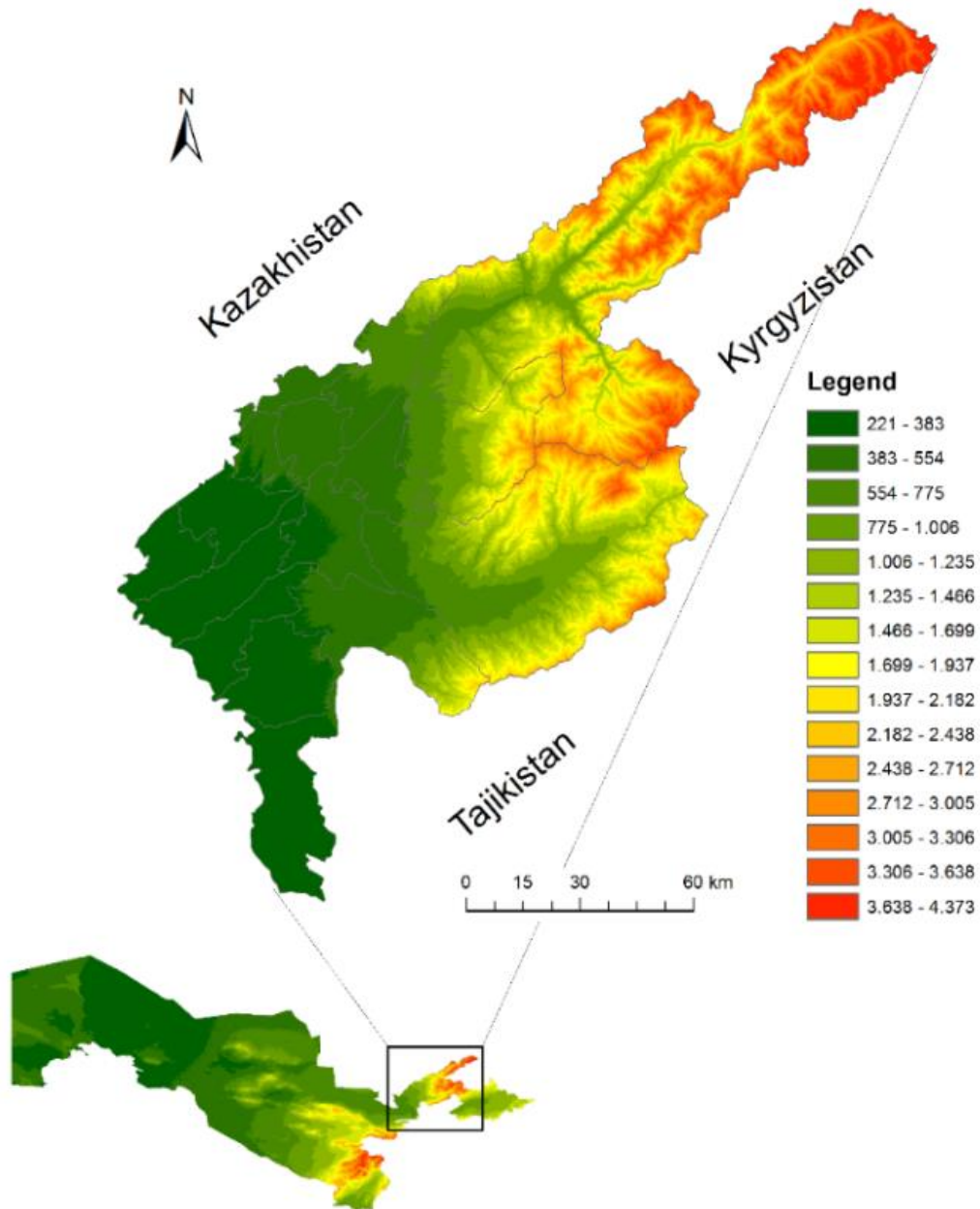


Figure 3.1. 30 m grid Digital Elevation Model (DEM) of Tashkent Province retrieved from Advanced Spaceborne Thermal Emission and Reflection Radiometer (ASTER) Global Digital Elevation Model (GDEM) (Tachikawa et al., 2011).

Climate change analysis was studied based on the data (Saha et al., 2014) of the National Centers for Environmental Prediction (NCEP) Climate Forecast System Reanalysis (CFSR) from 1979 to 2013. CFSR weather data cannot replace the accurate

weather data but it is useful where data are not available or existing data are not reliable due to random errors, especially in developing countries. (Dile et al., 2014).

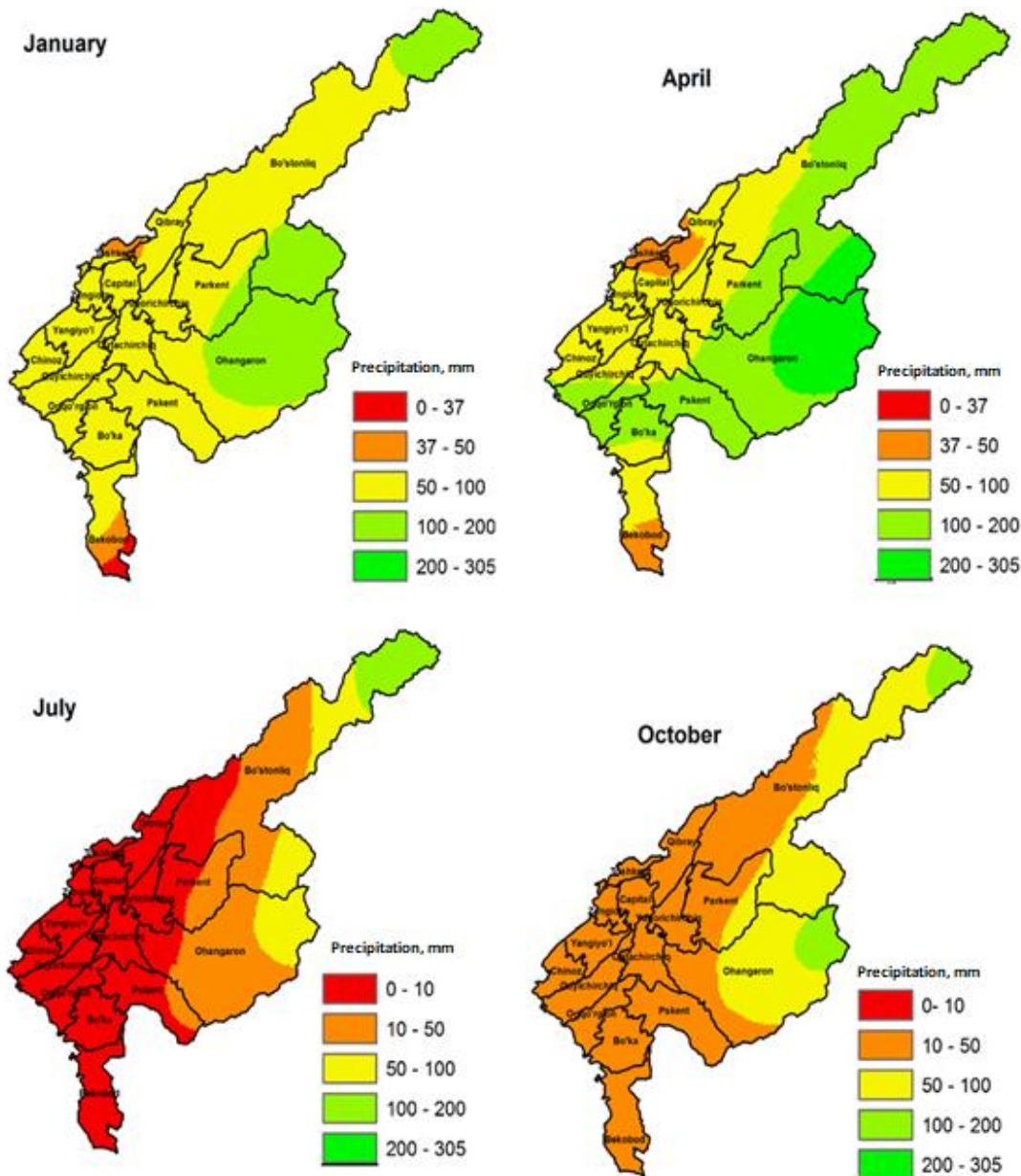


Figure 3.2. Average monthly surface precipitation over Tashkent Province interpolated by Kriging using CFSR weather data between 1979-2013.

The lack of reliable and precise data on climate and ecosystems required for regional climatic and biogeographic modeling is one of the major sources of uncertainty about vulnerability and impacts of climate and land-cover changes in arid lands of CA. (Lioubimtseva et al., 2005). Using CFSR precipitation and temperature data in the

watershed model provides better stream discharge simulations than using conventional weather data where stations are located more than 10 km from the watershed (Fuka et al., 2014) (Figure 3.2). Based on the amount of precipitation, the climate zone of Tashkent Province is divided into two regions: sub-humid and semi-arid. Precipitation exceeding 600 mm is a sub-humid zone and precipitation in the range of 300-500 mm is a semi-arid zone. Sub-humid zones are located on a slope and semi-arid zones are practiced by agriculture. The drought season lasts from June to August and during this period agricultural croplands and pasturelands receive less than 10 mm of precipitation. The results demonstrated the trend of increasing temperature and variable trend of precipitation, but little overall decrease over the croplands, pasturelands, and grasslands of the study area. The rainfall is not well distributed throughout the year; thus, pastureland and rangelands of the study area are highly influenced by the climate in drought seasons like 2000-2002 and 1995-1996.

We may expect a significant decrease of evapotranspiration in arid and semi-arid climate areas due to a lack of soil water content when the temperature rises where precipitation is not expected to increase, and thus it accelerates the process of desertification. Some scientists believe that climate change (temperature and precipitation variability) can have an advantage in the agricultural sector, because it can extend vegetation growing seasons, and a higher concentration of carbon dioxide (CO₂) can improve plant growth. But agricultural land, as well as pasturelands and grasslands in the entire study area, are dependent on irrigation and rain water respectively. Even though on a global scale the temperature is increasing slowly and the precipitation is expected to be increased slightly but we should consider that the temperature increases and precipitation decrease is very active during the summer vegetation growing period in Tashkent Province. Therefore, it is crucial to study the impacts of climate change on land degradation during the vegetation period (Figures 3.3, 3.4, 3.5).

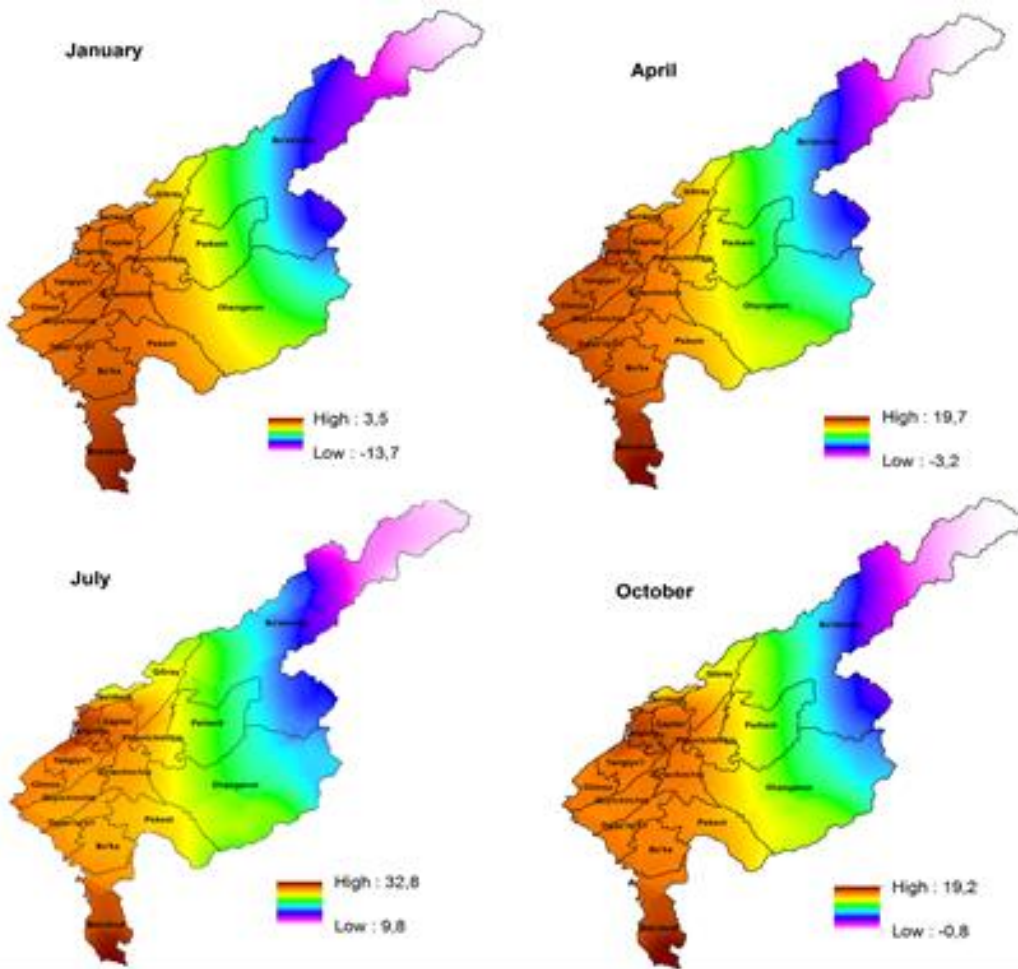


Figure 3.3. Average monthly surface temperature over Tashkent Province interpolated by Kriging using CFSR weather data from 1979 to 2013.

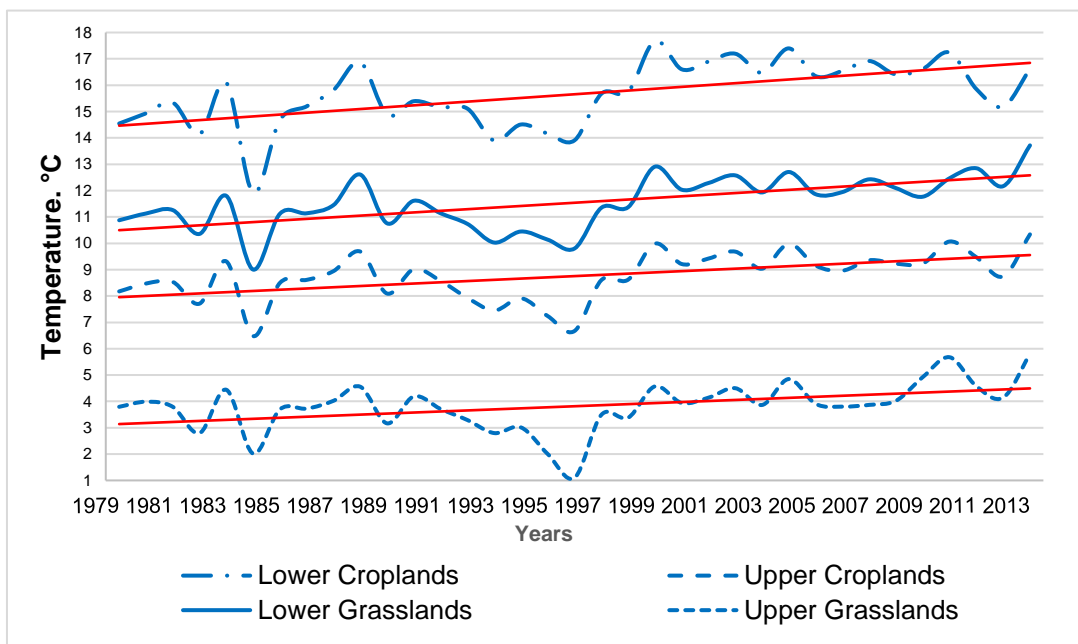


Figure 3.4. Annual average temperature change diagrams of croplands and grasslands in Tashkent Province.

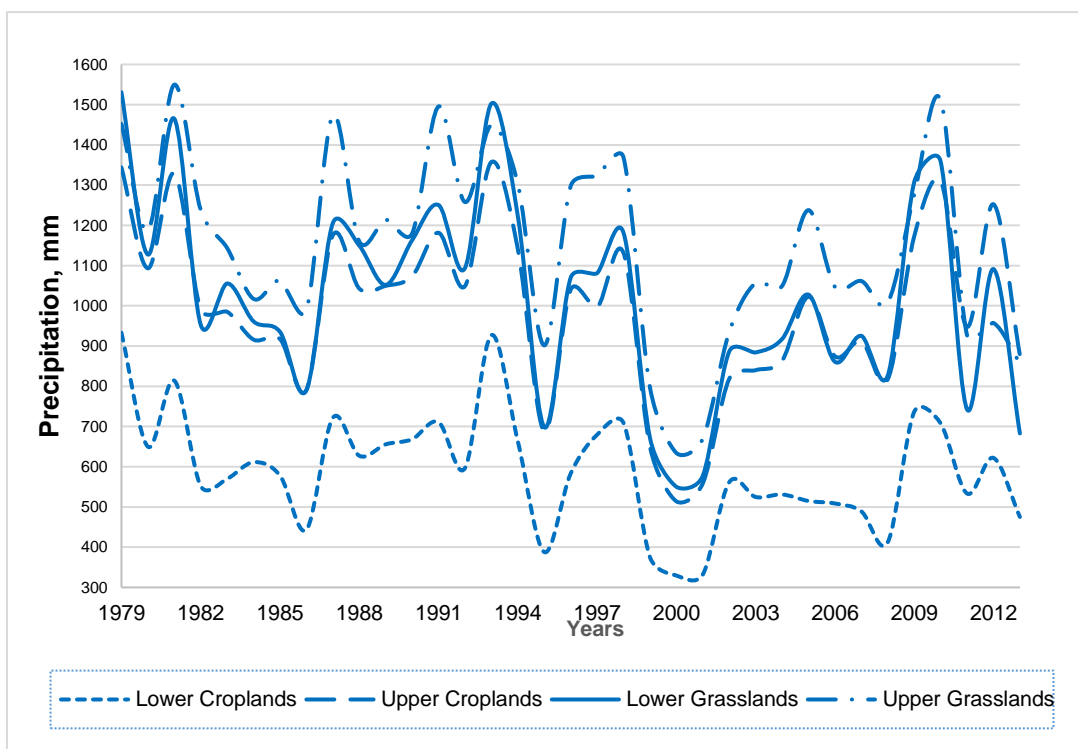


Figure 3.5. Annual precipitation changes diagrams of croplands and grasslands in Tashkent Province.

3.6 Land Use Change Analysis in Tashkent Province

Studying changes in land use and land cover is a good indicator to study the ecosystem's vulnerability and landscapes to environmental change. (Peters and Lovejoy, 1992 cited in Sivakumar, 2007). Extreme agricultural practices in the last several decades are one of the important deriving causes of land degradation and it can be seen in many parts of the world it is crucial to consider the influence of drylands climates on soil and vegetation, furthermore, it is very important to adopt uniform criteria and method to assess desertification and monitoring of dryland degradation. And also, it is fact that extensive land-use changes resulted in soil erosion in large areas in several parts of the world (Sivakumar, 2007). Irrigated land was expanded from 4.51 to 7.99 million ha from 1960 to 2000 in the Aral Basin to meet the demands of increasing population and country development (Roll et al., 2005). Land cover and land-use change analysis at a regional scale in CA were carried out through a classification approach with implemented classification tree model (C5.0) algorithm using MODIS time series for the years 2001 and 2009. And the results showed significant changes in human-induced water body alterations, seasonal precipitation affecting sparsely vegetation areas variability, and forest loss by forest fires and logging (Klein et al., 2012).

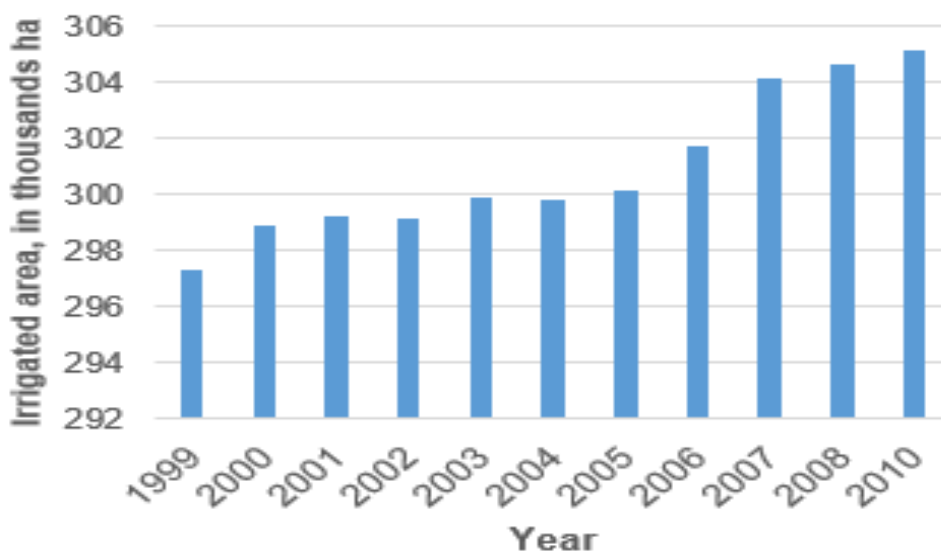


Figure 3.6. Changes in irrigated agricultural cropland between 1999 and 2010 in Tashkent Province.

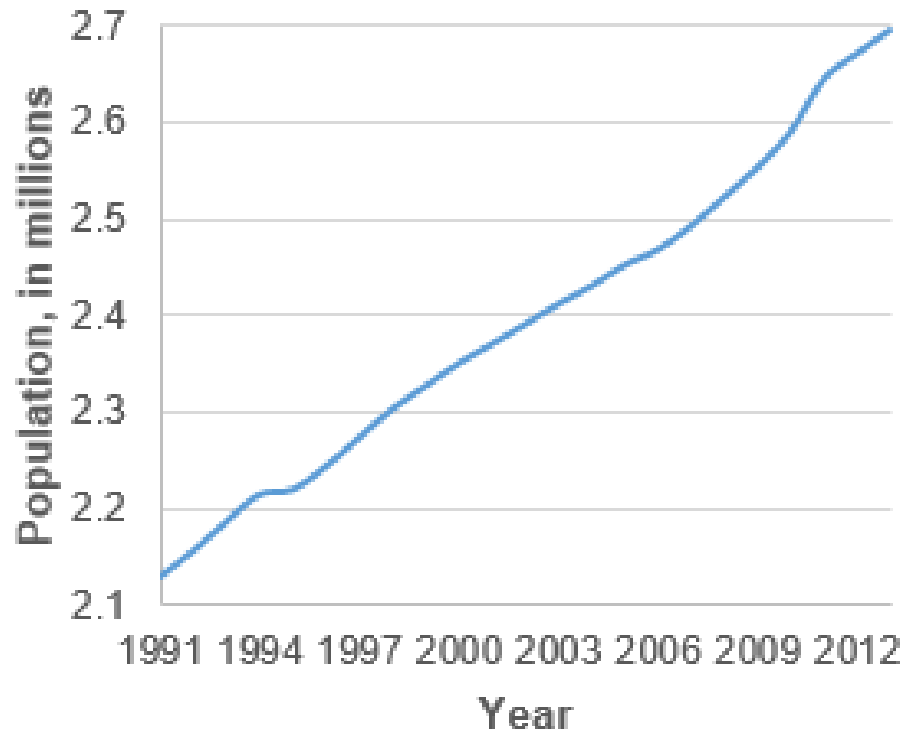


Figure 3.7. Population growth between 1991 and 2013 in Tashkent Province.

The other study of land-cover changes and degradation in the CA deserts using remote sensing and geostatistical methods was done in three key periods (the mid-late 1970s, around 1990, and 2000). The study revealed degradation existed in some areas of the region because of enhanced oil recovery and another rangeland area is getting better due to a decrease in livestock in Kazakhstan (Karnieli et al., 2008). Chen et al., (2013) studied land use land cover change and variations of ecosystem services which include net primary productivity (NPP), evapotranspiration (ET) and grain production in CA between 1990 and 2009 and they found most significant changes occurred in farmland abandonment and reclamation and farmland extent during 2000-2009. Farmland NPP was higher than natural vegetation and NPP increased with the rise of temperature in 2000 despite the decline in precipitation. The actual ET in the central area is lower than in the northern and eastern parts of CA. Besides, irrigated agricultural areas in one of the CA countries Turkmenistan expanded to 86 % equivalent to a loss of about 4500 km² previously available for natural pastures since the 1980s. Pastures close to the irrigated and populated area were not affected and vegetation cover increase was found in many places of the country. But remote pastures were affected by a higher degree of vegetation degradation, mainly because of the development of soil biogenic

crust as well as flooding and technology-related desertification that occurred around man-made structures. (Kaplan et al., 2014). Irrigated lands in Uzbekistan increased from 2.2 million ha in 1953 to 4.21 million ha in 2013, thus the long-term growth rate was about 1.5 % a year. Expansion and densification of irrigated cropland in Kashkadarya Province of Uzbekistan were studied by classification trees method using Landsat MSS and TM data from 1972/73, 1977, 1987, 1998, and 2000. Cropland extent developed from 134.800 ha to 477.000 ha between 1972/73 and 2009 and winter wheat harvesting doubled to approximately 211.000 ha from 1987 to 1998 (Edlinger et al., 2012). Irrigated cropland in Tashkent province (figure 6) has grown up from 297.3 thousand ha to 305.1 thousand ha between 1999 and 2010 (Goskomzemgeodezkadastr, 2010).

According to the State Statistical Committee of Uzbekistan, we can see an increase in food crops together with fruits, potatoes, melons, and vegetables while grain crops stay relatively stable and cotton areas slightly decreased between 2010 and 2013 (figure 8).

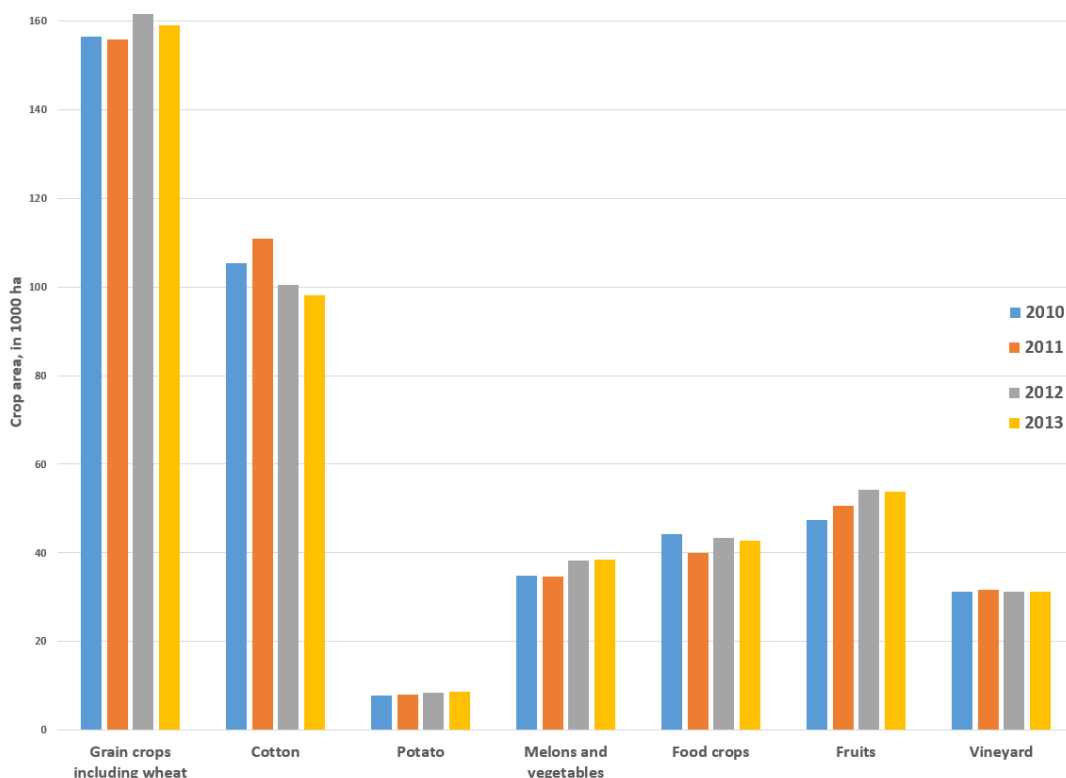


Figure 3.8. Changes in agricultural cropland area in Tashkent Province.

Population increase makes more pressure on natural resources and intensive land-use practices which causes a variety scale of land degradation in agricultural land as well as pasturelands and rangelands of Tashkent Province. Statistical data of the Province showed a 20% population increase with a 1.07 % average annual growth rate since 1991 (figure 7). The study area consists mostly of agricultural land, pasturelands, and grasslands and they play an important role in the rural population and national economy. Authors believe that each type of land use has its particular drivers of land degradation like agricultural land degradation by lack of soil water content, soil salinity, wind and water erosion, intensive land use, and pastureland as well as grasslands degradation by climate change, land-use change, overgrazing, and soil runoff.

3.7 Conclusions

Most of the carried-out research to study land degradation in CA countries used medium spatial resolution remotely sensed data such as NOAA/AVHRR and MODIS which pixels include a mixture of many land covers but they do not capture certain land degradation. And throughout reviewing research articles as well as national and international reports, it is found that study related to land degradation caused by climate and land-use changes at the local level was not carried out throughout Tashkent Province to see the inter-annual Spatio-temporal changes in land degradation caused by existing problems such as population increase, intensive agricultural practices, and water availability in last decades. At the same time modeling the relationship between climate change, land-use change, and land degradation is very important for a better understanding of interrelationships between climate, vegetation cover, and land degradation changes which helps to improve our understanding to find the main drivers of land degradation in Tashkent Province. Climate change analysis showed an increasing trend of temperature and highly variable trends in precipitation, but it indicated a small overall decrease, and the rainfall is not seasonally and quantitatively well distributed throughout the year, thus grasslands of the study area can be highly influenced by climate change in drought seasons. Furthermore, population increase is demanding more natural resources and expansion of irrigated croplands and this leads to intensive land use, overgrazing, and other environmental problems in the study area.

Using high-resolution remote sensing data is useful for informing land management decisions and understanding the interactions between land-use change, climate change, and land degradation where accurate field data of the last decades are limited.

4 The Identification of Irrigated Crop Types Using Support Vector Machine, Random Forest and Maximum Likelihood Classification Methods with Sentinel-2 Data in 2018: Tashkent Province, Uzbekistan

Erdanaev, E., * Kappas, M. and Wyss, D.

Cartography, GIS and Remote Sensing Department, Institute of Geography,
University of Göttingen, Goldschmidt Street 5, 37077 Göttingen, Germany
E-mail: elbek.erdanaev@geo.uni-goettingen.de,* mkappas@uni-goettingen.de,
daniel.wyss@uni-goettingen.de

**Corresponding Author*

This chapter was published as a research article: International Journal of Geoinformatics 2022, 11(4), 39-48.

4.1 Abstract

Accurately mapping land use and land cover including agricultural use and the state of crops at various stages is important to address specific agro-ecological challenges, implement sustainable agricultural practices, and monitor crops periodically. This study aims to provide a timely and accurate main irrigated crop types mapping at 10m resolution for Tashkent province based on multi-temporal Sentinel-2 data acquired for the growing season in 2018. This paper shows the potential use of multitemporal Sentinel-2 satellite data to derive an up-to-date irrigated crop types classification map of the study area. As single-date satellite imagery does not allow proper cropland classification, multitemporal and high-resolution Sentinel-2 data was used to capture small cropland fields and specific crop types for the vegetation period (April to October 2018). NDVI monthly profiles of crop types as well as additional 10 m resolution bands 2 and 3 were used as input data to perform and assess three classification algorithms: Support Vector Machine (SVM), Random Forest (RF), and Maximum Likelihood Classification (MLC). Accuracy assessment results showed that SVM showed the highest Overall Accuracy (OA) and Kappa Accuracy (KA). KA of

classified images for SVM were 0.90 and 0.89 for the RF algorithm. Both performed well with close values. But MLC showed a lower result of KA 0.60. The paper also compares the area of derived irrigated cropland area with data from the State Committee for Statistics of Uzbekistan for selected crop types. Values for the crops "cotton" and "wheat" derived by SVM and RF methods show a high correlation with the provided statistical data. Based on the results, the SVM classification method is recommended for further mapping and monitoring of irrigated crop types in the region when Sentinel-2 data is used.

Keywords: *Irrigated croplands, Sentinel-2, Support-vector machine, random forest, maximum-likelihood, State Statistics croplands data, Tashkent, Uzbekistan*

4.2 Introduction

(LULU) maps are of high importance for a variety of sectors in the developing world including food security, land use planning, water, and natural resources management decisions (Saah et al., 2019). Nowadays remote sensing (RS) imagery together with geoinformation systems (GIS) tools is widely used for LULC mapping. Medium and coarse resolution RS imagery provide general LULC classifications but cannot distinguish specific LUs i.e. on crop level due to similar reflectance values (Jia et al., 2018). Therefore, freely available high spatial resolution RS imagery such as Sentinel-2 is necessary to derive timely and accurate information on irrigated croplands and to better understand the impact of spectral-temporal properties of various crop types allowing control and monitoring of irrigated croplands over larger areas.

Uzbekistan is one of the Central Asian (CA) countries and is located at the heart of the Eurasian continent (Liu, 2011). Climate change in CA countries is expected to strongly impact agricultural productivity and food security in the region. Temperatures are predicted to increase by 1.7 °C and 2.6 °C and precipitation to rise by 9 % and 12 % under global warming scenarios of 1.5 °C and 2.0 °C, respectively (Li et al., 2020).

Besides, the population increase in CA is leading to higher consumption of natural resources, expansion of irrigated croplands, and intensive land-use practices (Erdanaev et al., 2015). Agriculture is one of the main sectors of Uzbekistan's economy with

agriculture, forestry, and fisheries contributing 32,40 percent of the country's total GDP in 2018. 53,20% of agricultural products belong to crop production and 46,80% to livestock. Eighty percent of the country is classified as desert or semi-desert. Agricultural land totals 20,26 million hectares including only 3.7 million hectares of irrigated agricultural land in 2018. The major crops are cotton and wheat. The share of Tashkent province towards the total volume of agricultural products, forestry, and fisheries amounts to 15.7 percent, the highest in the country (Zvi Lerman, 2019).

In Uzbekistan, accurate accounting and monitoring of land use in agriculture are very important. Unfortunately, several problems have accumulated in the field of geodesy, cartography, and cadastre in the country. The last land survey was conducted 40 years ago. The procedure for allocating agricultural land was adopted 20 years ago and does not meet modern requirements. This is evidenced by the fact that 150 thousand hectares of arable land were arbitrarily occupied in 66 districts of the state (Mirziyoyev, 2020). Several studies on LULC mapping and change detection have been carried out in Uzbekistan using RS imagery and GIS tools. (Chen et al., 2013) studied land use and land cover change and variations of ecosystem services including net primary productivity (NPP), evapotranspiration (ET), and grain production in CA between 1990 and 2009. They found out that the most significant changes were triggered through farmland abandonment and reclamation showing a significant increase in farmland between 2000 and 2009. Farmland NPP was higher than natural vegetation and NPP increased with the rise of temperature in 2000 despite a decline in precipitation. The actual ET in the central area was lower than in the northern and eastern parts of Central Asia.

Irrigated lands in Uzbekistan increased from 2.2 million ha in 1953 to 4.21 million ha in 2013, thus the long-term growth rate was about 1.5 % annually (Lerman, 2018). Expansion and densification of irrigated cropland in Kashkadarya Province of Uzbekistan were studied using classification tree methods based on Landsat MSS and TM data from 1972/73, 1977, 1987, 1998, and 2000. Cropland extent developed from 134.800 ha to 477.000 ha between 1972/73 and 2009 and winter wheat harvesting doubled to approximately 211.000 ha from 1987 to 1998 (Edlinger et al., 2012). Irrigated cropland mapping was performed using pixel-based (PB) and field-based (FB) robust non-parametric machine learning algorithms such as RF, SVM, and a

common parametric MLC using multi-temporal Landsat 8 images in Khorezm Province of Uzbekistan. Accuracy assessment results showed higher OA and kappa index (KI) for FB-RF and FB-SVM algorithms over the PB-RF, PB-SVM, and PB-MLC algorithms. The parametric FB-MLC showed the lowest OA and KI (Basukala et al., 2017). Alikhanov et al., (2020) studied LULC change in Tashkent Province between 1992-2018 using Landsat images. They found that grassland, shrubland, meadow, as well as agricultural lands, decreased from 7000km² in 1992 to 3000km² in 2008 then increased again in 2018. (Juliev et al., 2019) carried out a LULC change detection analysis between 1989-2017 in the Bostanlik District of Tashkent Province, which is located in the mountain area. They used Maximum Likelihood Classification using Landsat data with the resulting classes: snow cover, bare soil-rock, forest, waterbody, built-up areas, and agriculture. The results showed that for the last 28 years, significant changes occurred within classes of the forest, built-up areas, bare soil, and snow cover.

LULC change in the mountain areas of Tashkent Province using Landsat NDVI values as an indicator of land degradation was studied from 1989 to 2018 (Pulatov et al., 2020). Their research results showed that overgrazing had a significant effect on the mountain ecosystem of Tashkent Province with a decrease of 29 thousand ha of pastureland from 1989 until 1998, which increased again between 2008 and 2018. Gerts et al., (2020) studied agricultural land-use change in the Orta Chirchik district of Tashkent province between 1994 and 2017. The study was based on Spectral Correlation Mapper classification using Landsat and Sentinel-2 NDVI profile analysis. The results showed that the combination of both Landsat and Sentinel-1 radar data for Spectral Correlation Mapper classification increases classification accuracy. We believe that long-term change detection analysis should be performed using similar image acquisition dates or months for each year to consider vegetation phenology and specific climatic conditions. This approach is missing in the above-mentioned research and can result in misclassification and errors in LULC change detection analysis (Alikhanov et al., 2020).

Most of the published data on agricultural land use and land cover change analysis of local experts in Uzbekistan are based on the reported statistics through state organization bodies that are usually outdated and not very reliable and there is little

information available on the extent of agricultural LUs. Up to now, no study has provided a deeper understanding of spectral-temporal information derived from Sentinel-2 satellite imagery for crop classification on the provincial level in the study area. Thus, the RS approach of irrigated crop types mapping using 10 m resolution bands of Sentinel-2 data can play an important role in effective land use planning and management which are essential to assuring the sustenance of its population while fostering environmental sustainability. To achieve this approach relatively modern and robust classification algorithms such as SVM, RF and MLC can be utilized. The objective of this study aims to provide a timely and accurate irrigated crop types map for Tashkent province based on multi-temporal Sentinel-2 data acquired for the growing season in 2018. For this purpose, three supervised classification algorithms are tested and cross-evaluated. Classification results are compared with available state statistics data on crop types for future applicability and can thus provide an important basis for more sustainable development, future monitoring, planning, and decision-making.

Tajikistan in the south, and with Syrdarya Province in the south-western part (Figure 4.1).

Tashkent Province consists of 15 administrative districts and 7 cities with a population of 2.81 million in 2018 (State Statistics, 2019). The climate is a typically continental climate with humid, relatively mild wet winters and long, hot, and dry summers. The mean January temperature is -1°C to -2°C and the mean July temperature is 26.8°C . The average annual precipitation is 300 mm in the plains region, 300-400 mm in the piedmont region, and 500-600 mm in the mountains. Precipitation mostly occurs in the early spring and permanent snow cover is located in the higher mountains. The main river Syrdarya and its tributaries Chirchik and Akhangaron Rivers basins are fed by snow and glaciers and they are used for irrigation and hydroelectric power (Erdanaev et al., 2015). According to statistical data, 50,70% of the Tashkent province's population live in rural areas where most agriculture is practiced. These areas are located in low elevated lands.

4.3.2 Data Collection and Pre-Processing

The total number of 28 images during the crop growing season in 2018 which are freely available Sentinel-2 (Level-1C) multi-spectral satellite images of the study area were downloaded from the Earth Explorer website of the United States Geological Survey (USGS). Band parameters of each spectral band are given in Table 1. These products underwent radiometric and geometric corrections but were not corrected atmospherically (Drusch et al., 2012). Therefore, the images were pre-processed using the Semi-Automatic Classification plugin and the DOS1 (Dark Object Subtraction) correction tool in QGIS (Congedo, 2021) allowing the transformation of Top-Of-Atmosphere (TOA) reflectance to land surface reflectance values which is a basic requirement for multi-temporal image analysis. Generally, Sentinel-2 has a temporal resolution of approximately 5 days. But we used only the best cloud-free multi-temporal images for each month with acquisition dates covering the growing season (April to October) selected for the study area.

Table 4. 1. Band parameter of each spectral band of Sentinel – 2.

Band number	Description	Wavelengths (nm)	Spatial Resolution (m)
1	Coastal aerosol	433-453	60
2	Blue	458-523	10
3	Green	543-578	10
4	Red	650-680	10
5	Vegetation Red Edge (RE) 1	698-713	20
6	Vegetation RE 2	733-748	20
7	Vegetation RE 3	773-793	20
8	Near-Infrared (NIR)	785-900	10
8a	Narrow NIR	855-875	20
9	Water vapor	935-955	60
10	Shortwave infrared (SWIR)- Cirrus	1360-1390	60
11	SWIR 1	1565-1655	20
12	SWIR 2	2100-2280	20

Table 4. 2. Sentinel-2 data was used for image classification.

<i>Scene Path/Row</i>	April	May	June	July	August	September	October
T42TVL	20	25	24	09	03	02	02
T42TWK	12	07	06	01	05	04	04
T42TWL	12	07	06	01	05	04	04
T42TWM	12	07	06	01	05	04	04

Irrigated croplands are located in low elevated areas where irrigation canals exist. Therefore, irrigated croplands were separated from Mountain areas using high-resolution base maps in ArcMap. A total of four Sentinel -2 tiles covered the study area (Figure 2). All tiles were processed separately then mosaiced and clipped using the study area shapefile. Only 10 m resolution visible bands: 2, 3, 4, and 8 were used for image classification. Bands 4 and 8 were used for the calculation of monthly NDVI time-series data then composited creating multi-temporal NDVI images for all seven months. Visible bands 2 and 3 were also composited in the same way and combined with the NDVI composites before image classification. The images were projected to WGS 1984 Universal Transverse Mercator (UTM), Zone 42 coordinate reference

system. All classified images were smoothed to remove the noises and improve the quality of classified output.

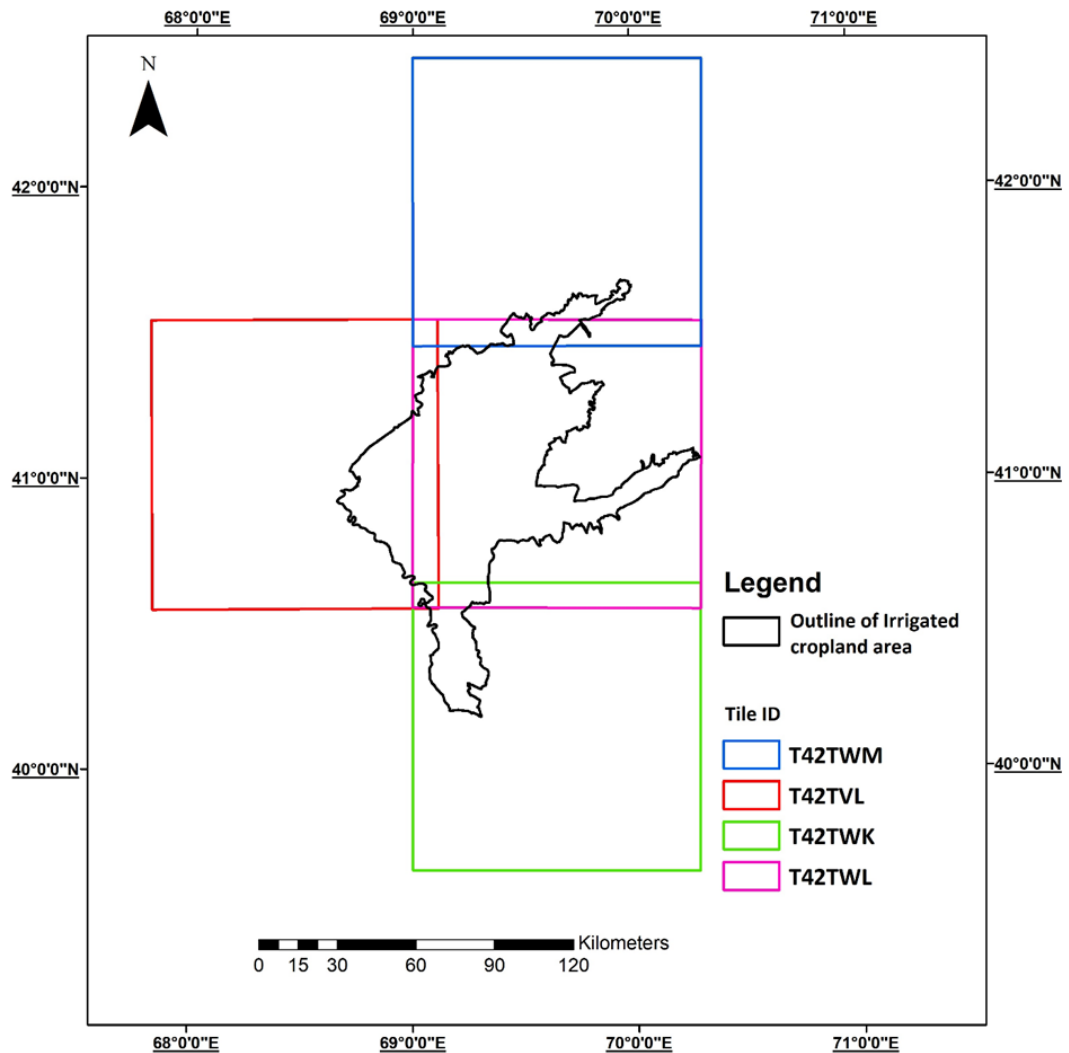
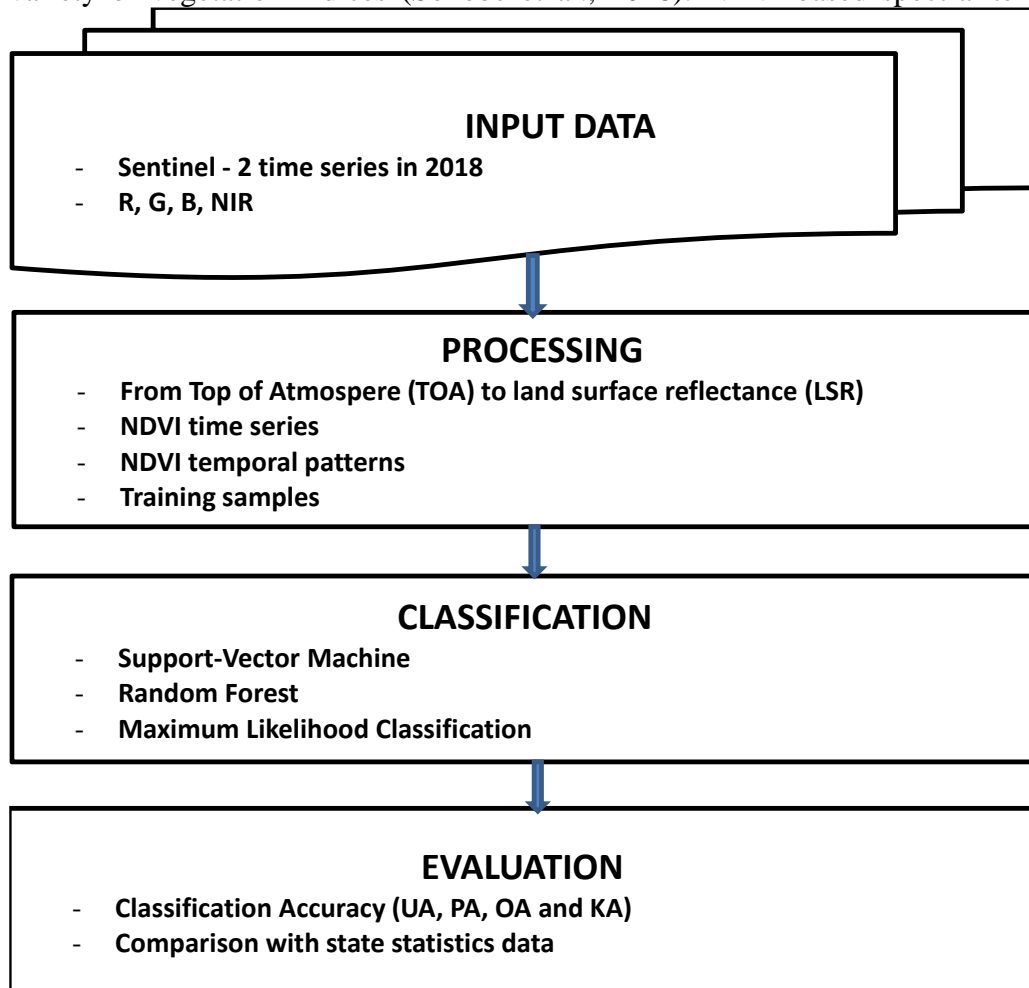


Figure 4. 2. Outline of irrigated cropland area.

4.3.3 Methodology

The methodological workflow flowchart is given in Figure 3 consisting of the following steps: 1) Preparation of input data including the download of cloud-free images and band selection; 2) data processing, including atmospheric correction (TOA to LSR conversion), creation of NDVI time series and temporal spectral profiles for specific crop types as well as delineating multitemporal training samples; 3) irrigated

cropland classification using MLC, SVM and RF algorithms; 4) evaluation of classification accuracy and comparison of classified irrigated cropland area with the State Statistics data. The identification of specific crop types can be achieved using a variety of vegetation indices (Sonobe et al., 2018). NDVI-based spectral-temporal



profiles taken during the vegetation period have a high potential to properly classify heterogeneous crops on farmland.

Figure 4. 3. Flowchart of the study methods







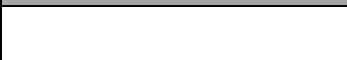

More than 85% overall accuracy can be achieved using five or more acquisition dates covering different phenological phases of vegetation, for example, the period before winter-wheat harvest and summer crops in Uzbekistan (Conrad et al., 2014). Thus, monthly NDVI profile values for the growing season between April to October were used for the delineation of training samples. In addition, multitemporal NDVI image composites in combination with composites of Band 2 and Band 3 were used as input data for supervised image classification due to their high spatial resolution of 10 m.

The high resolution of all input bands including the NDVI calculations was an important factor to derive crop-specific land use maps.

4.3.4 Training and Ground Truth data

Archived images from high-resolution satellites for ground-truthing and accuracy assessment are costly for scientists in developing countries. But freely available Google Earth (GE) images with high spatial resolution can be utilized as training samples and ground truth for mapping of LULC on a regional scale (Ahmed Ibrahim Ramz, 2015). Available GE images were also used as training and testing samples by Thanh Noi and Kappas (2017). It is recommended that the training sample size should represent approximately 0.25 percent of the study area for land cover classification of satellite images (Thanh Noi and Kappas, 2017).

Table 4. 3. Training and Ground Truthing Samples.

Class Name	Number of Pixels		Class Color
	Training Samples	Ground Truthing	
Cotton	2528	250	
Wheat	5750	500	
Rice	3038	250	
Other Crops	2248	250	
Fruits/Trees	3642	250	
Bare land	2560	250	
Others	2601	250	
Water	2899	250	

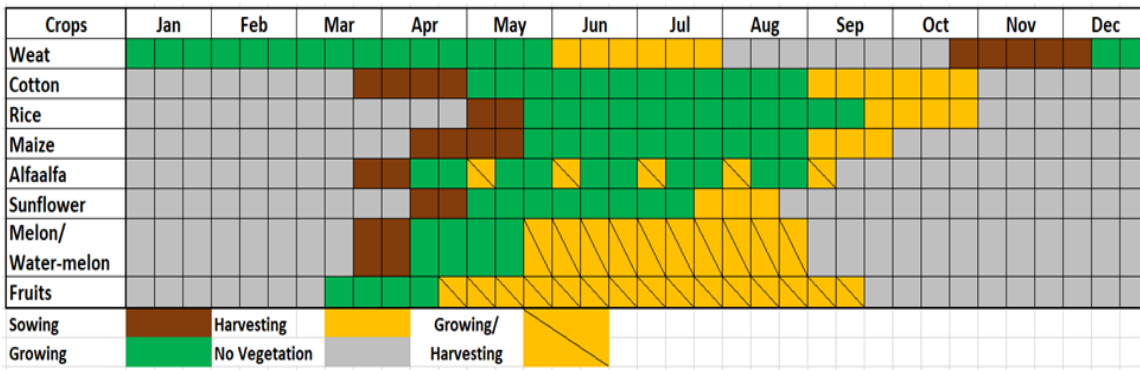


Figure 4. 4. Idealized cropping calendar of the main crop types grown in the study area based on the guidance of regional agricultural land management authority and local experts.

When the training sample sizes are large enough the performance of classifiers achieves better results (Thanh Noi and Kappas, 2017).

High accuracies are not achieved by having a large number of training samples. The main factors for ensuring higher accuracies are clarity of samples used in training, diversity of training samples, spatially equal distributed samples, and several samples (Gumma et al., 2020). To keep spatially well-distributed samples per class, 135 field samples were taken for each class except “wheat” due to crop rotation practices, requiring more training samples. Some wheat fields are given to farmworkers as a subsidy after harvest where they can use the land to grow necessary crops for themselves until the end of the harvesting season. Overall 8 classes were chosen for image classification (see Table 4.3): “Cotton”, “Wheat”, “Rice”, “Other Crops”, “Fruits/Trees”, “Bare land”, “Others”, and “Water”. “Other crops” include forage, melons, and vegetable crops. “Others” include roads, river sands, and non-vegetated areas. The class “wheat” includes winter wheat and “secondary crops” after winter wheat.

Usually, crop rotation is practiced after winter wheat is harvested such as maize, beans, and sunflowers. State statistics do not give any reports on secondary crops after winter wheat. The crops planted after winter wheat are given as a subsidy for farmworkers or as additional income sources for farmers. To check the performance of classifiers 250 ground-truthing pixel points were taken for accuracy assessment. Freely available GE

images were used for ground-truthing based on the knowledge of the cropping calendar shown in Figure 4.4.

4.3.5 Classification Methods

Nowadays, there are efficient and inexpensive GIS tools and methods available for the monitoring of LUs. In general, image classification can be grouped into three categories: a) supervised and unsupervised according to the way of learning, b) parametric and non-parametric based on data distribution assumptions, and c) hard and soft based on the number of outputs for each spatial unit. These classifiers are either based on object-oriented classification (OOC) or pixel-based classification (PBC) methods (Jawak et al., 2015). OOC has an advantage over PBC when very high and hyperspatial resolution data are used for image classification (Quynh Trang et al., 2016).

In unsupervised classifications, pixels are assigned to groups based on each pixel's similarity to other pixels (no truth, or observed, data are required). In supervised classifications, the user instructs the image processing software to specify the land cover classes of interest. For each land cover type of interest, the user creates "training samples" - places on the map that are known to be representative of that land cover type. The main problem with unsupervised classification is that spectral data will not always correspond to spectral classes and that the final grouping of clusters thus needs to be decided by the human operator. Supervised classification, on the other hand, provides more accurate classifications and also allows for more control over the classification process. Especially for large areas and diverse conditions (e.g. differing seasonality of phenology at different sea levels), extensive and thus expensive training is required (Chuvieco, 2020). Therefore, the following three supervised classification algorithms were used:

Support Vector Machine Classification: The Support Vector Machine method is an excellent classification method if the number of input variables is high (Sonobe et al., 2018). The strength of SVM is to produce good results using small training samples as well as a high level of class separability. The separation of two classes in the SVMs is

done by a hyperplane. A hyperplane is a minimum distance (also called margin) between training samples of two classes. Support vectors are the nearest spectra, which are used for identifying the hyperplane (Baghdadi and Zribi, 2016). The SVMs have four basic kernels: linear; polynomial, radial basis function, and sigmoid. In our research, we used a standard linear basic kernel which is available in ArcMap tools.

Random Forest Classification: The random Forest method is a non-parametric supervised machine learning classification method and it trains a model according to known values given by training samples. RF classifier tool in ArcMap creates models and generates predictions based on Leo Breiman's RF algorithm (Breiman, 2001). As an attribute selection measure, the RF classifier uses the Gini Index. The Index measures the impurity of an attribute related to the classes. For a given training set T, selecting one case (pixel) at random and saying that it belongs to some class C_i , the Gini index can be written as:

$$\sum \sum_{j \neq i} \left(\frac{f(C_i, T)}{|T|} \right) \left(\frac{f(C_j, T)}{|T|} \right)$$

Equation 4.1

Where $\left(\frac{f(C_i, T)}{|T|} \right)$ is the probability that the selected case belongs to class C_i . Each time a tree is grown to the maximum depth on new training data using a combination of features (Pal, 2005). In our research, the maximum number of trees was selected as 50, the maximum tree depth was 30 and the maximum number of samples per class was 1000 by default.

Maximum-Likelihood Classification: The Maximum Likelihood Classification algorithm is based on Bayes' theorem and calculates the likelihood distributions for the classes. The likelihood distributions are assumed based on multivariate normal distribution models (Richards and Jia, 2006). There should be a sufficient number of

training pixels to allow the calculation of the covariance matrix used in this algorithm. The likelihood function, described by Richards and Jia (2006), is calculated for each pixel as:

$$g_k(x) = \ln p(C_k) - \frac{1}{2} \ln \left| \sum_k \right| - \frac{1}{2} (x - y_k)^t \sum_k^{-1} (x - y_k)$$

Equation 4.2

where, C_k = land cover class k ; x = spectral signature vector of an image pixel; $p(C_k)$ = probability that the correct class is C_k ; $\left| \sum_k \right|$ = determinant of the covariance matrix of the data in class C_k ; \sum_k^{-1} = the inverse of the covariance matrix; y_k = spectral signature vector of class k .

4.3.6 Cropping Calendar

In Uzbekistan, cotton and winter wheat are the two major crops cultivated. Cotton is the most exported crop in the country, while wheat is the main grain crop in the country. Other irrigated crops are rice, watermelons, alfalfa, maize, sunflower, and fodder crops. The cropping times may differ slightly according to climate conditions. The cropping calendar was created based on the guidance of the regional agricultural land management authority and local experts of Tashkent Province, Uzbekistan (Figure 4). A similar cropping calendar was created for another region of Uzbekistan (Conrad et al., 2014). As shown most of the crops have almost similar cropping seasons in the study area. The crops cotton, rice, maize, alfalfa, sunflower, and melons are planted between the end of March and the beginning of May and harvested from July to October. Only winter wheat is sown in October and November and harvested in June and July. Fruit trees and gardens are scattered throughout the study area and it is impossible to make the comparison of the classified area of Fruits and Trees with state statistics data. Cropping calendar and vegetation growth data play an important role to take training samples for supervised classifiers.

4.4 Results

In 2018 main crops in Tashkent Province were wheat and cotton. 85 % of crops are cultivated on farmland. Cotton is planted between the end of March and April. Thus, NDVI values in May show high deviation error bars which are higher compared to June due to the growth of weeds (see Figure 5). After 40 to 50 days, at the end of June and July, flower buds start to form and cotton bolls begin to fill from July until mid-August. As a result, NDVI reaches its maximum value in August. End of August and in mid-September cotton bolls are fully open and are ready for picking. At this point, NDVI values start declining. Cotton is picked in September until mid-October. Wheat is planted end of October until the beginning of December. The vegetation period of wheat continues until June. Unfortunately, cloud-free satellite images are difficult to acquire during wintertime. After harvesting wheat, the land will be used for secondary crops or stay as furrows until the next cropping season.

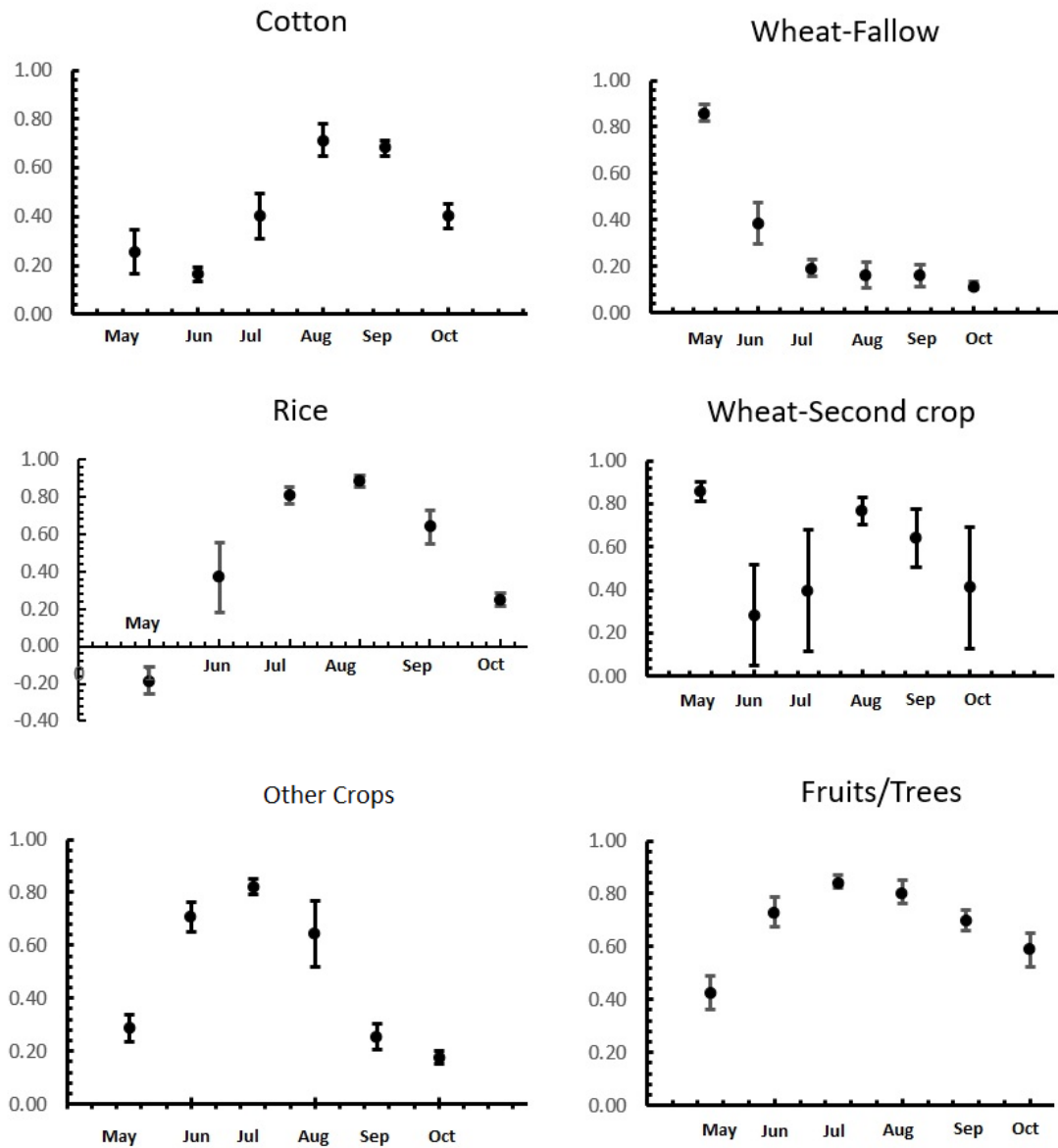


Figure 4. 5. Monthly NDVI profiles during the vegetation period in 2018 at the field level were retrieved from multitemporal Sentinel-2 data. Mean NDVI and its standard deviation error bars are also shown

Thus, NDVI values fluctuate highly during crop rotation after winter wheat. Secondary crops such as vegetables, cucurbits, potatoes, and others are sown to fulfill the food requirements of the growing population. The NDVI profiles of Rice are distinguishable because of negative values in May and peak values in July and August. Other crops are forage crops and vegetables with vegetation periods from May to August. Fruits and trees grow throughout the whole vegetation period resulting in constantly high NDVI values. These can easily be distinguished by all classification algorithms.

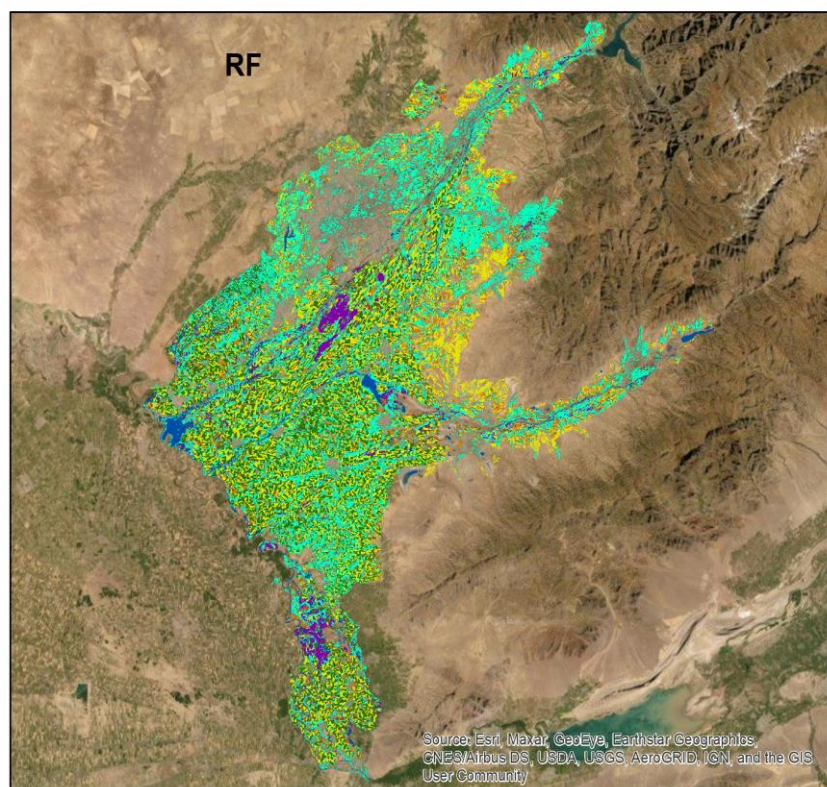
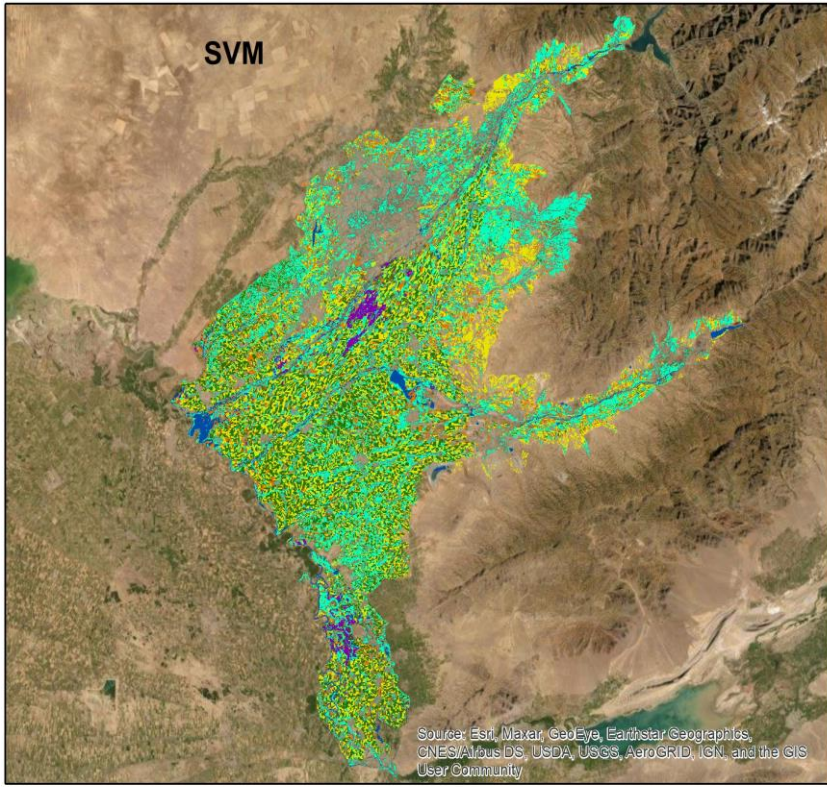


Figure 4. 6. Supervised classification methods output and the subset of Agricultural LU maps in 2018: SVM classification; RF classification; and MLC classification (Continue next page).

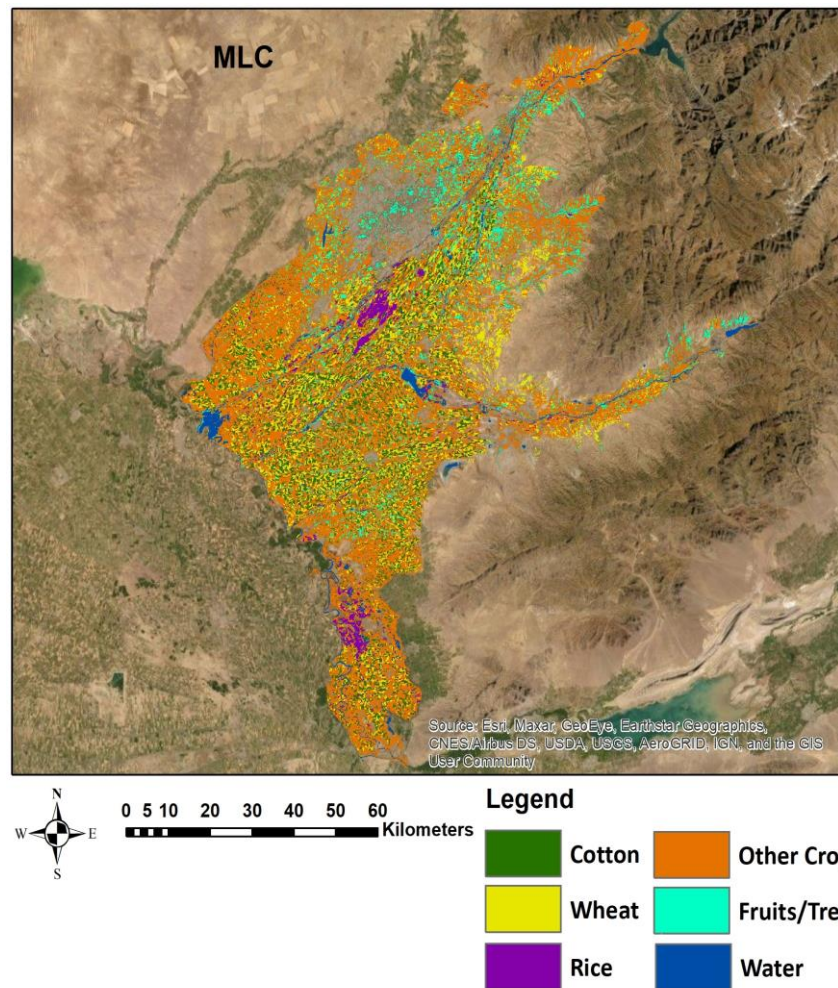


Figure 4. 6. Supervised classification methods output and the subset of Agricultural LU maps in 2018: SVM classification; RF classification; and MLC classification.

A comparison of this class with state statistics was not possible as the class includes fruits and trees of private households and private landowners. Besides, many mulberry trees are grown around croplands for sericulture. The results of high-resolution irrigated cropland classifications based on SVM, RF, and MLC methods are presented in Figure 6 and their subsets in Figure 7. It can be seen the crops “Cotton” and “Wheat” are evenly distributed across the entire province. Rice fields are located along Chrichik and Syrdarya rivers as well as main irrigated canals. The class “Other Crops” was highly misclassified using the MLC method. Visually only small differences can be seen when comparing SVM and RF classification results (Figure 4.7). Overall, the SVM-derived classification shows higher accuracy compared to RF and MLC.

4.4.1 Accuracy Assessment of Image Classification

Table 4. 4. Confusion matrices and classification methods accuracy based on ground-truthing data.

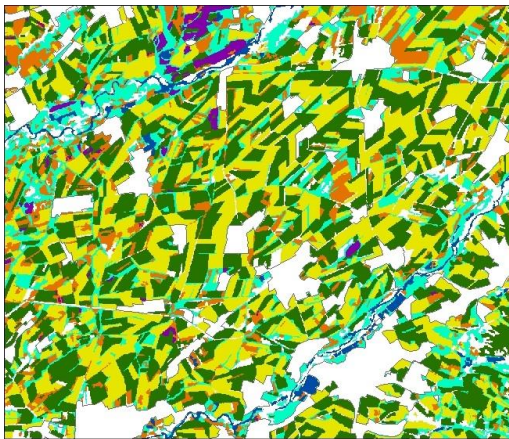
<u>Support Vector Machine Classification</u>										
	Ground Truth									
Classes	Cotton	Wheat	Rice	Other Crops	Fruits/Trees	Bare land	Others	Water	Grand Total	UA, %
Cotton	244		14		4	4			266	91.7
Wheat		462	1	2		23			488	94.7
Rice	1		225	5		2			233	96.6
Other Crops	3	18	6	238	14	2	14	2	297	80.1
Fruits/Trees	1	20		4	222	4		2	253	87.7
Bare land	1		1	1	10	204	22		239	85.4
Others						11	214	1	226	94.7
Water			3					245	248	98.8
Grand Total	250	500	250	250	250	250	250	250	2250	
PA, %	97.6	92.4	90	95.2	88.8	81.6	85.6	98		
Overall Accuracy: 91.3%										
Kappa: 0.90										
<u>Random Forest Classification</u>										
Cotton	241	1	8	5	6	5	2		268	89.9
Wheat		450	2	9		22			483	92.2
Rice	6	1	235	11	13	4			270	87.0
Other Crops	2	28	3	213	10	5		1	262	81.3
Fruits/Trees	1	20		10	220	2		2	255	86.3
Bare land				2	1	205	20	1	229	89.5
Others						7	228	2	237	96.2
Water			2					244	246	99.2
Grand Total	250	500	250	250	250	250	250	250	2250	
PA, %	96.4	90.0	94	85.2	88	82	91.2	97.6		
Overall Accuracy: 90.5%										
Kappa: 0.89										
<u>Maximum Likelihood Classification</u>										
Cotton	226		3		2	1			232	97.4
Wheat		414	1	2		16			433	84.8
Rice	9		237		5	1		1	253	93.7
Other Crops	14	57	4	247	125	14	13	4	478	51.7
Fruits/Trees	1	29		1	112				143	78.3
Bare land					6	212	4		222	95.5
Others						6	233	2	241	96.7
Water			5					243	248	98.0
Grand Total	250	500	250	250	250	250	250	250	2250	
PA, %	90.4	82.8	94.8	98.8	44.8	84.8	93.2	97.2		
Overall Accuracy: 85.5% , Kappa: 0.84										

To evaluate the derived irrigated cropland maps, an accuracy assessment was performed for each classification method. Detailed confusion matrices showing classification accuracies are given in Table 4. A total of 2250 well-distributed ground-truthing samples were taken for the accuracy assessment in Tashkent Province. The results show that the overall accuracies (OA) of SVM and RF classification algorithms are good and similarly high, whereas the MLC algorithm shows a lower OA. In the SVM confusion matrix OA was 91.3%, in RF 90.5% and in MLC 85,5%. User's accuracy (UA) and Producer's accuracy (PA) of all classes in SVM and RF algorithms were higher than 80%, but MLC showed a moderate PA of 44.8% for the class "Fruit/Trees" and 51.7% UA for the class "other crops". All other cropland classes PA and UA in MLC were higher than 78%. The highest UA for the cropland class "cotton" was achieved using MLC, for the class "wheat" and "rice" SVM showed better performances. The class "other crops" performed best using the RF algorithm. SVM shows the highest PA for the cropland classes "cotton", "wheat" and "fruit/trees" and MLC for the classes "rice" and "other crops", respectively. Kappa accuracies (KA) of classified images for SVM were 0.90 and 0.89 for the RF algorithm. Both performed well with similar values. MLC showed a lower result of KA 0.60.

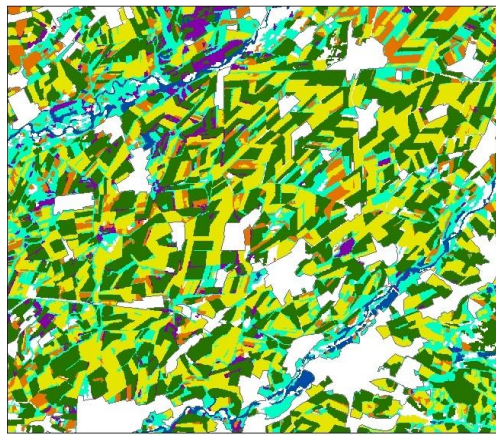
4.4.2 Comparison Sentinel Derived Cropland Products with National Statistical Data

In this study, we calculated areas of crop types for the entire Tashkent Province and compared them with the area given by statistics available from the State Statistics Committee of Uzbekistan. Figure 8 compares Sentinel-2 derived irrigated croplands areas with different supervised classification methods.

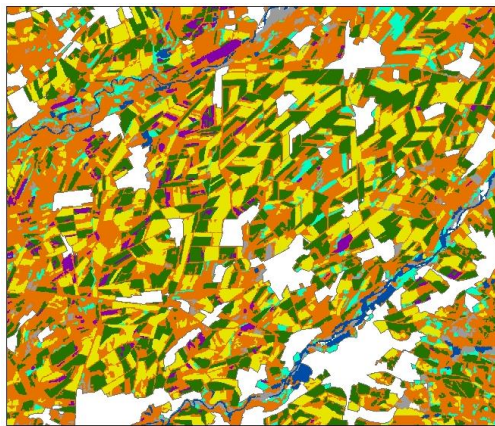
The estimated area of irrigated crop types using SVM and RF fit well with State Statistics data. The MLC classification results show the highest differences compared to state statistics and are significantly lower than state statistics data. This especially accounts for the class "other crops" due to the complexity of phenological stages during the vegetation period as shown in the NDVI monthly profiles. Other cropland classes in MLC do not significantly differ from state statistics data.



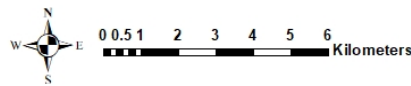
SVM



RF



MLC



Legend

- Cotton
- Wheat
- Rice
- Other Crops
- Fruits/Trees
- Bare land
- Others/Builtups
- Water

Figure 4. 7. LU map subsets from different classification methods.

In the SVM classification method, Sentinel-2 derived irrigated cropland area was 93.4 thousand ha for cotton, 120.7 thousand ha for wheat, 9.4 thousand ha for rice, and 69.6 thousand ha for other crops compared to 83.6, 125.1, 5.6, and 66.1 thousand ha of state statistics data respectively. Whereas in RF, it was 101.5 thousand ha for cotton, 122.7 thousand ha for wheat, 40.6 thousand ha for rice, and 63.1 thousand ha for other crops. MLC classified an area of 66.3 thousand ha for cotton, 82 thousand ha for wheat, 19.3 thousand ha for rice, and 224.9 thousand ha for other crops. Overall, the “cotton” and “wheat” classes show reliable results in all classification methods as both are state-order crops that can be correctly reported. Other crops' vegetation period starts in early

spring in April. At the same time, the precipitation amount is high and it can result to grow grasses on the bare lands during this period. Usually, these areas are located nearby irrigation channels, rivers, and high slope areas. Besides, after harvesting winter wheat, the second crop is cultivated by farmers which challenge the classification of this class. Therefore, the MLC method misclassified the class “Other Crops”. But SVM and RF classification methods have the privilege to distinguish this class and classified accurately.

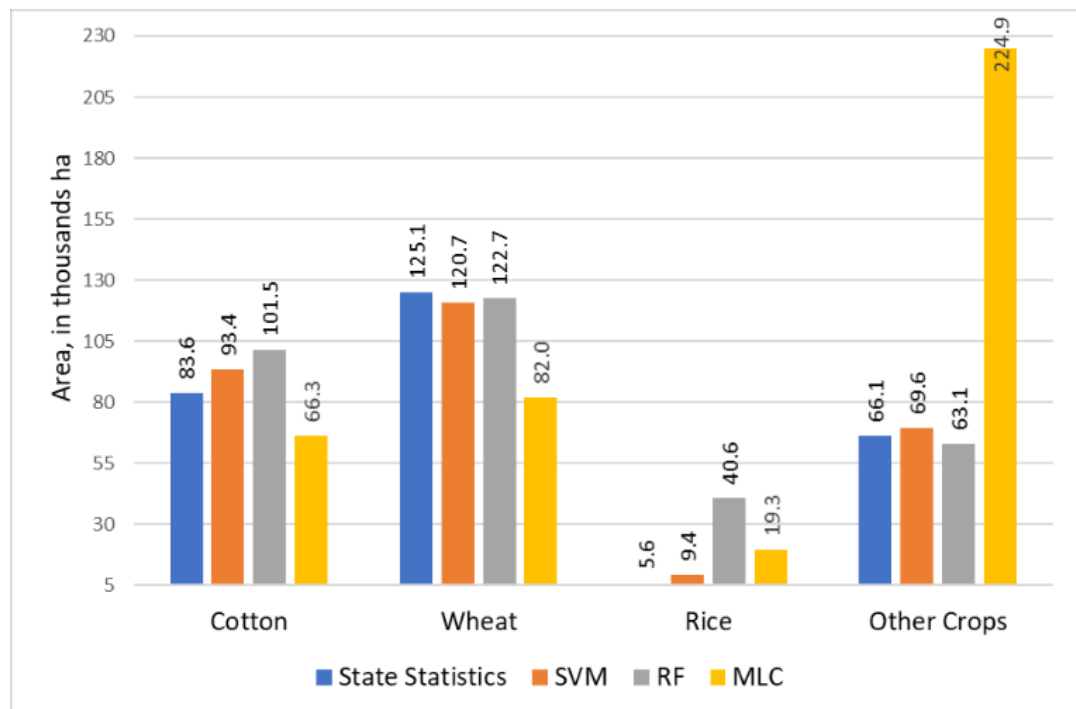


Figure 4. 8. Comparison of Sentinel 2 -derived cropland product with national statistical data

4.5 Discussion

In this paper irrigated cropland extent of Tashkent Province was mapped using high-resolution 10-m Sentinel-2 data and a comparison of supervised classification algorithms such as SVM, RF, and MLC performance was carried out. Knowledge of vegetation phenological processes and NDVI time-series data were used during the image classification process illustrating the importance of continuous satellite-based time series, capturing vegetation dynamics and plant growth characteristics to map

agricultural crop types. Results show that the use of multi-temporal datasets, in comparison to single-date imagery, provides an improved basis for the discrimination of crop types. The results are comparable to similar research conducted by Gumma et al., (2020) and Xie et al., (2019).

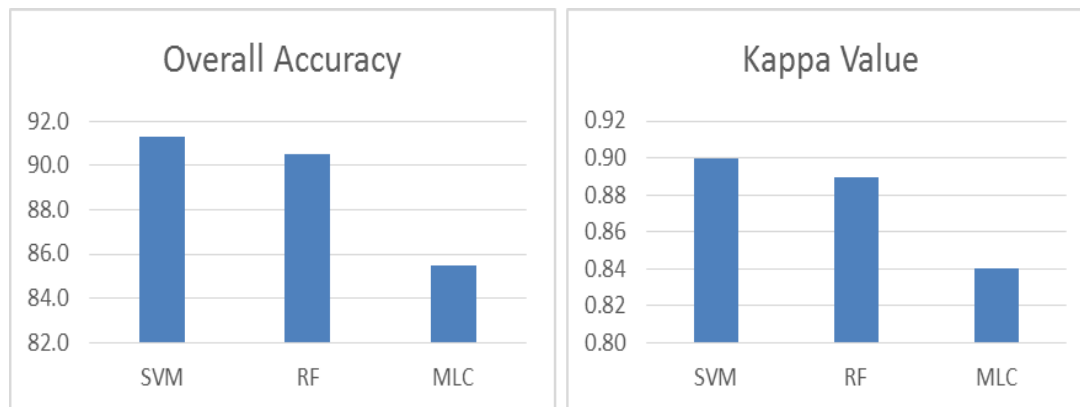


Figure 4. 9. OA and KA value of classifiers.

This study's results showed that irrigated cropland classification using SVM and RF algorithms provided the highest OA and KA compared to MLC (Figure 9). Comparable studies in other regions have shown similar results in LU mapping (Burai et al., 2015, Deilmai et al., 2014, Thanh Noi and Kappas, 2017, Xie et al., 2019). SVM and RF perform better than MLC when there is a limited number of training samples (Basukala et al., 2017). The low performance of MLC is because the capability of the MLC algorithm depends on a very accurate estimation of the average vector and the covariance matrix for each spectral class. Therefore, MLC relies on a satisfactory number of training samples per class and it performs unreasonably when a small number of training samples is used (Basukala et al., 2017). For example, when the training samples were reduced from 30 to 10 accuracy assessment was also significantly reduced from 80.78% to 52.56% (Burai et al., 2015). The lowest performance of MLC is partially due to crop types having very heterogeneous raster values in training samples, including several crops with different spatial and spectral preferences. The integration of additional imagery to provide higher temporal resolution would most probably improve classification results (Basukala et al., 2017). Unfortunately, it was impossible to get additional imagery in early spring due to the high percentage of cloud cover. Due to the high OA, KA, UA, and PA result for all

irrigated crop types, SVM and RF can be recommended for LU mapping in the region as an effective and accurate classifiers.

Accuracy assessment results of the class “rice” showed high values but its comparison with statistics data was not close for all classifiers. It might be the wrong reporting by state statistics because the local government is criticizing that the statistical data were not correctly reported previously in many cases (Shavkat Mirziyoyev, 2021). Even a few years ago rice fields area were two times high than in 2018. Besides, there some farmers plant rice crop as a secondary crop after winter wheat is harvested and it is not included in the Statistics. There should be detailed field observation to prove it. Moreover, some crops are more profitable than other crops and they can be traded on the local market except cotton due to government control (Platonov et al., 2014). As a result, there is a high demand for rice in the local market. For example, in 2020 Uzbekistan imported 13.6 thousand tons of rice but the country’s demand is about 335 thousand tons. Uzbekistan is planning to double the rice production by planting new rice sorts and introducing two crop production (Economy Uzbekistan, 2021). But the state-order crop cotton’s growing period is very long which occupies two crop production periods. Thus, rice in two-crop production might be challenging due to water shortages in the region in the future. Besides the climate of Tashkent Province is not convenient for two crop production in comparison with other regions of the country.

With the introduction of winter wheat, competition comes up between state crops and cash crops. Because state crops are not profitable for the farmers and farmers can earn additional income by planting cash crops after winter wheat (Platonov et al., 2014). Cotton is traded only by the government and wheat harvest should be given to the government as a part of the contract with the farmers. Thus, their classification results were satisfied by all classification methods it was believed the official data was correctly reported. The study showed feasible results at the Provincial level for irrigated cropland classification and a comparison of classifiers' performance with statistics data was not found in previous studies in the research object. As a first-time approach to this method, it can be a good start and should be developed in the future together with field trips and local experts' knowledge. Besides, the potential of using other indices and spectral bands of Sentinel -2 such as red edge and SWIR for cropland

classification raises important questions in the future. In this paper, it is unknown whether using other indices and spectral bands can result in better performance of irrigated cropland classification. And we intended to carry out more studies in the future, to improve the performance of different classification methods by using other indices and spectral bands.

4.6 Conclusions

The study produced a 10-m high resolution irrigated crop types product (based on Sentinel-2 data with 1 pixel = 0.01 ha). The analysis was applied based on pixels in one agricultural calendar year using SVM, RF, and MLC methods using ArcMap and open-source software QGIS. NDVI monthly profiles during the vegetation period of each class showed the potential of irrigated crop types classification. And the study of irrigated crop types mapping at the provincial level with different supervised classification methods and comparing the performance of the classifiers as well as the comparison of crop types area with official data is the first application in the region.

Among the tested methods the SVM classifier performed the highest OA and KA and produced a visually pleasant irrigated cropland map in Tashkent Province. Therefore, the authors conclude that the SVM classification algorithm was the best-suited classifier for mapping heterogeneous irrigated crop types and it can be used alternatively where digital cadastre LU maps are limited for agro-environmental assessment studies in the region. Although the RF classifier had lower accuracy than SVM, it performed better than MLC. MLC method could not yield high accuracy and handle many pixels incorrectly classified, so we do not recommend this classifier for irrigated crop types classification in the study area.

The comparison of classified crop types area with official State Statistics data showed that the state order crops “cotton”, “wheat” and the class “other crops” in SVM and RF methods were close to the official data. The area of class “rice” is higher than official data which requires additional study further or correct statistical data which also includes rice area after winter wheat. And the class “others crops” showed

unreliable results in MLC due to its complexity and heterogeneity. Comparing the area of class “fruits/trees” is complicated because private households and landowners have fruits and trees on their property. And also, many cropland fields are surrounded by mulberry trees for sericulture which is not included in the official data. Comparison of remote sensing-based irrigated cropland area with official data showed the applicability of these methods over other areas of the region which has similar agro-ecological conditions but there should also be further research with field data and using other indices or bands that can improve the estimates in rice and other crops classes.

We are also motivated to use and test other bands to derive Sentinel-2-based vegetation indices incorporating the three RE and SWIR bands in a 20 m resolution for image classification in the future.

5 Irrigated crop types mapping in Tashkent Province of Uzbekistan with remote sensing-based classification methods

Elbek Erdanaev *, Kappas Martin * and Daniel Wyss

Cartography, GIS and Remote Sensing Department, Institute of Geography, University of Göttingen, Goldschmidt Street 5, 37077 Göttingen, Germany; daniel.wyss@uni-goettingen.de

* Correspondence: elbek.erdanaev@geo.uni-goettingen.de (E.E.); mkappas@gwdg.de (K.M.);

Tel.: +49-551-39-8020 (E.E.) This Chapter was published as a research article: *Sensors* **2022**, *22*(15), 5683; <https://doi.org/10.3390/s22155683>.

5.1 Abstract

Appropriate crop type mapping to monitor and control land management is very important in developing countries. It can be very useful where digital cadaster maps are not available or use of Remote Sensing (RS) data is not utilized in the process of monitoring and inventory. The main goal of the present research is to compare and assess the importance of optical RS data in crop type classification using medium and high spatial resolution RS imagery in 2018. With this goal, Landsat 8 (L8) and Sentinel-2 (S2) data were acquired over the Tashkent Province between the crop growth period of May and October. In addition, this period is the only possible time for having cloud-free satellite images. The following four indices “Normalized Difference Vegetation Index” (NDVI), “Enhanced Vegetation Index” (EVI), and “Normalized Difference Water Index” (NDWI1 and NDWI2) were calculated using blue, red, near-infrared, shortwave infrared 1, and shortwave infrared 2 bands. Support-Vector-Machine (SVM) and Random Forest (RF) classification methods were used to generate the main crop type maps. As a result, the Overall Accuracy (OA) of all indices was above 84% and the highest OA of 92% was achieved together with EVI-NDVI and the RF method of L8 sensor data. The highest Kappa Accuracy (KA)

was found with the RF method of L8 data when EVI (KA of 88%) and EVI-NDVI (KA of 87%) indices were used. A comparison of the classified crop type area with Official State Statistics (OSS) data about sown crops area demonstrated that the smallest absolute weighted average (WA) value difference (0.2 thousand ha) was obtained using EVI-NDVI with RF method and NDVI with SVM method of L8 sensor data. For S2-sensor data, the smallest absolute value difference result (0.1 thousand ha) was obtained using EVI with RF method and 0.4 thousand ha using NDVI with SVM method. Therefore, it can be concluded that the results demonstrate new opportunities in the joint use of Landsat and Sentinel data in the future to capture high temporal resolution during the vegetation growth period for crop type mapping. We believe that the joint use of S2 and L8 data enables the separation of crop types and increases the classification accuracy.

Keywords: crop types mapping, Sentinel, Landsat, SVM, RF, NDVI, EVI, NDWI, State Statistics data, irrigated land, Uzbekistan

5.2 Introduction

Land use or land cover maps are the primary tools to manage information on the Earth's surface and the interaction between different land cover types. In this context, the need to distinguish between land cover (i.e., the physical properties of land surface) and land use (i.e., human activities making use of land) needs to be mentioned (Lambin & Geist, 2006), with this paper focusing on land use, although it is not possible to identify land use without identifying land cover. Up to the 1990s, most information on land use in Uzbekistan was derived from national mapping and surveying programs with standards of spatial as well as thematic resolution widely varying between countries and global regions (Feng & Li, 2020). While the capacity for land use mapping at a global scale had been steadily developing, starting with the first Landsat satellite in 1972, it was the opportunity to make global RS imagery more widely available via what was initially the internet and later became the world wide web that data, as well as processing capabilities and more affordable image processing software, became available to a wider range of users globally (Wulder et al., 2019). In addition

to their use in land management, land use maps are also of relevance in the context of environmental objectives such as the land use, land use change, and forestry sphere within the area of climate change politics and re-search (García-Montero et al., 2021) or biodiversity research (Cavender-Bares et al.; Stephenson, 2020).

Before the advent of RS technology, traditional cadaster data formed the basis of national land use statistics. Initially, national cadastral mapping had been introduced for taxation reasons as a basis for land ownership records as well as land use distribution (Polat, 2019; Zaragozí et al., 2019). However, in some countries of the world including the study area, adequate information is not yet available. This is due to a historical lack of cadaster systems as well as an outdated land management system. These issues related to the distribution of power between transnational (e.g., European Union), national and sub-national entities, with the latter a particularly vexing factor in countries with federal rather than centralized administrative and political systems (Schmidt-Traub, 2021).

RS data have been used widely in the field of crop phenology. Aside from crop identification, this includes the identification of crop growth stages. Usually, very coarse resolution (i.e., 100–250 m) products such as MODIS (Moderate Resolution Imaging Spectroradiometer) and VIIRS (Visible Infrared Imaging Radiometer Suite) have been widely used and proven helpful in landscape and regional level yield prediction. However, for analysis at field scale, medium (i.e., 30 m) to high (i.e., 10 m or better) resolution products, especially the Landsat series of sensors, are considered more beneficial. Unfortunately, in many regions of the world, the lack of clear (cloud-free) imagery poses a considerable challenge to widespread operational use [3]. The availability of RS imagery and relevant processing capabilities have led to a wide range of uses of RS data in agriculture. Common applications include crop growth and yield assessment, irrigation research, and information on potential crop losses due to pests and diseases (Karthikeyan et al., 2020). Similarly, agricultural land use monitoring and crop yield forecasting are listed as the main application areas (Weiss et al., 2020). The recent interest in precision farming as an approach to improve economic efficiency, reduce negative environmental impacts through minimizing the use of herbicides and pesticides, and avoid over-fertilization has led to the development of multi-data-source approaches incorporating artificial intelligence (AI) technology. Frequently noted

examples include the use of higher spatial resolution data gathered from conventional aerial sensor technology as well as sensors for the visible spectrum and passive hyperspectral sensors but also active light detection and ranging (LIDAR) or radar sensors. Other approaches include training AI with a combination of high or medium resolution RS data (e.g., Landsat or Sentinel) to allow for information of higher accuracy to be derived from low-resolution RS sensors (e.g., MODIS), which provides the benefit of more frequent return periods (García-Berná et al., 2020; Weiss et al., 2020).

The most cultivated agricultural crops are maize (corn) with global annual consumption of 1107 Mt, wheat with global consumption of 740 Mt, and rice with an annual consumption of 510 Mt (FAO, 2019). Consequently, considerable work has been conducted in the context of RS methods to improve information on these crops. The following re-search works provide a short review related to our research work. For maize, research on land use suitability for cultivation in Indonesia was carried out by (Habibie et al., 2021), using NDVI as well as SAVI based on L8 data to assess cultivation potential, although in this study the areas identified had not yet been cultivated with maize. Zhang et al. demonstrate that with appropriate methods it is possible to not just identify maize as a crop but to improve phenological analysis to allow for the differentiation between common maize (i.e., for human or animal consumption or industrial purposes) and seed maize (Zhang et al., 2020). The phenological analysis was based on different vegetation indices (VI), including NDVI, EVI, triangle vegetation index (TVI), ratio vegetation index (RVI), NDWI, difference vegetation index (DVI), and an RF classification. Furthermore, they also assessed classification accuracy using the KA and producer accuracy (PA). Satellite RS-based maize acreage estimation and prediction of maize yields based on a combination of L8 NDVI and land surface temperature (LST), data as predictors were analyzed in work published by (Ahmad et al., 2020) using ground-truthing plots for supervised classification. These results are also of particular interest due to more frequent extreme weather situations, due to climate change, expected to lead to higher variations in yield.

Climate change and phenological reactions of agriculture crops were also the main focus of research carried out by (Chen et al., 2020), focusing on the spring phenology re-sponse of winter wheat to pre-season weather data based on long-time climate

records as well as NOAA-AVHRR NDVI time-series data from 1981 to 2015. Results demonstrated the approach to be more suited to assess more long-term climate change developments rather than short-term seasonal reactions and also highlighted the potential of using long-term time series data available from historical RS records. However, Wang et al. arrived at different results using the spring frost damage index to identify spring frost damage using a combination of historic weather data and MODIS RS data (Wang et al., 2020).

Given its importance as a staple crop in many of the most populated regions of the world, considerable work has also been carried out using RS data in the context of rice farming. For the identification of rice, different classification methods including supervised and unsupervised classification as well as phenological indicators have been used successfully with newer work focusing on AI approaches. For yield prediction, sophisticated methods need to be used, given the required differentiation between irrigated, rain-fed, or upland paddy fields. Given these complexities, additional data such as digital elevation models (DEM) need to be used. For more precise crop yield prediction, complex crop models using additional input, e.g., canopy height from LIDAR data (manned air-craft or UAV) are required (dela Torre et al., 2021).

To summarize, the use of RS for identifying not just the most important crops but also for analyzing phenological development details within farmed areas with these crops has been widely used with recent approaches combining RS and machine learning (ML) technology.

Classical unsupervised classification is based on a statistical analysis of natural groupings of data, typically using cluster-based approaches to analyze the degree of similarity of data correlation between different bands within pixels. Classic supervised classification is based on the same principle but uses training areas to provide ex ante information on areas of different land-cover types. Training areas are classified either using ground-truth data or through visual interpretation by a human operator. The main problem with unsupervised classification is that spectral data will not always correspond to spectral classes and that the final grouping of clusters needs to be decided by the human operator. Supervised classification, on the other hand, provides more accurate classifications and also allows for more control over the classification

process. Especially for large areas and diverse conditions (e.g., differing seasonality of phenology at different sea lev-els), extensive and thus expensive training is required (Chuvieco, 2020).

In this context, the main goal of this research is to test the capability of using S2 and L8 sensor data for mapping precise and accurate main irrigated crop types using ML algorithms SVM and RF. To achieve this goal, the following specific objectives were developed: (i) to map and compare the performance of ML algorithms such as SVM and RF for main irrigated croplands by crop types with medium and high-resolution L8 and S2 data; (ii) to test different index combinations such as NDVI, EVI, NDWI1, and NDWI2 as input data to derive crop type classification; (iii) to compare the area of all derived agricultural land use maps with the OSS data from the State Committee for Statistics of Uzbekistan. The other parts of this research work are structured as follows: Section 5.3 describes the study area, presents the data description, and theoretical background of methodologies of ML classifiers for crop types mapping, Section 5.4 describes the results and provides a discussion of the results. Lastly, Section 5.5 draws some conclusions and the future direction.

5.3 Materials and methods

5.3.1 Study area

This study focuses on the Tashkent province within the central Asian country Uzbekistan. Agricultural land makes up for about 62% of the total land area, the majority of this being pasture, while only about 10% of the national land area of some 425 km² is available as arable land (CIA, 2021). Tashkent Province was formed in 1938 as part of the Uzbek Soviet Socialist Republic and is located in the northeast of Uzbekistan between 40.18 N and 42.29 N and 68.64 E and 71.27 E of the Greenwich meridian or between the western part of the Tien Shan mountains and Syrdarya river. The Province borders Kazakhstan in the north and north-west, with Kyrgyzstan in the north-east, Namangan Province in the east, Tajikistan in the south, and with Syrdarya Province in the south-western part (Erdanaev et al., 2015). Since arable land is located

only in the lower areas of the province, the analysis only focused on these regions (see Figure 5.1.)

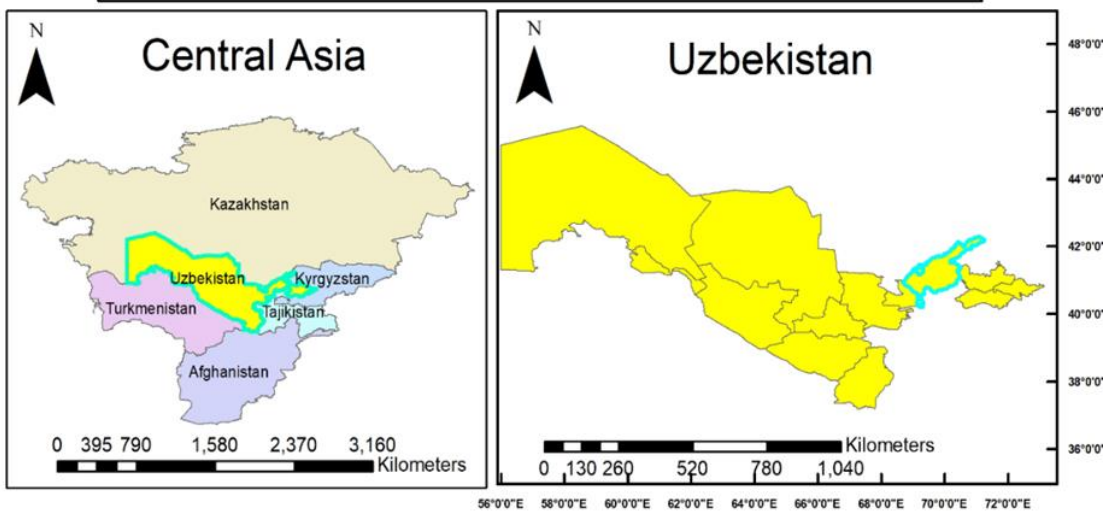
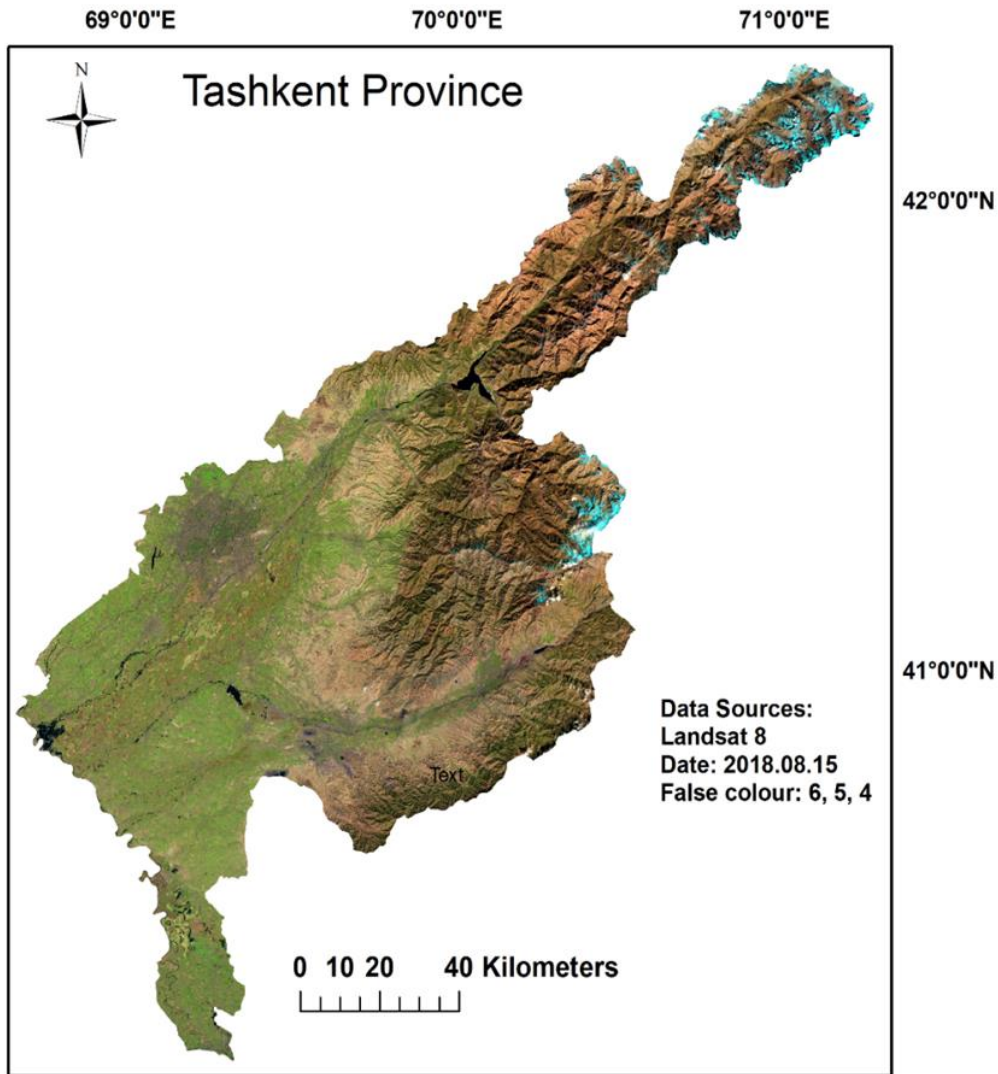


Figure 5. 1. Location of the study region

“The climate is a typically continental climate with humid, relatively mild wet winters and long, hot, and dry summers. The mean January temperature is -1°C to -2°C and the mean July temperature is 26.8°C . The average annual precipitation is 300 mm in the plains region, 300–400 mm in the piedmont region, and 500–600 mm in the mountains. Precipitation mostly occurs in the early spring and permanent snow cover is located in the higher mountains. The main river Syrdarya and its tributaries Chirchik and Akhangaron Rivers basins are fed by snow and glaciers and they are used for irrigation and hydroelectric power (Erdanaev, E., Kappas, M., Pulatov, A. and Klinge, M, 2015)”. In Uzbekistan, wheat is cultivated on about 40% of irrigated lands, cotton is around 36% and the remaining 24% is other crops (fruits, vegetables, livestock, and various cereals). In the Tashkent province, cotton and wheat occupied over 61% percent of the total cultivated area in 2018 (UzGosKomStat, 2019).

5.3.2 Data

S2 and L8 tiles covering the relevant study region were downloaded from the USGS Earth Explorer (USGS, 2020a) site for multiple dates of vegetation growth period from May to October 2018. In addition, only cloud-free images are available during this time. An overview of the satellite imagery dates for different months is provided in Table 5.1. In total, 4 tiles of S2 (T42TVL, T42TWK, T42TWL, T42TWM) and 3 tiles (153/031, 154/031, 153/032) of L8 were downloaded and processed separately before merging. All tile id numbers of S2 start with T (Toulouse) and the second two numbers 42 is the Universal Transverse Mercator (UTM) zone, next T is the latitudinal chunk, and the last two letters denote the position of the tiles. L8 tiles path and row numbers show the location of Tashkent province.

Table 5.1. S2 and L8 tiles were downloaded for the classification.

Month	S2 Multispectral Imaging (MSI)				L8 Operation Land Imager (OLI)		
	Date				Date		
	T42TVL	T42TWK	T42TWL	T42TWM	153/031	154/031	154/032
May	25	7	7	7	28	3	3
June	24	6	6	6	13	20	20
July	9	1	1	1	15	22	22
August	3	5	5	5	16	7	7
September	2	4	4	4	1	8	8
October	2	4	4	4	3	26	26

The specification of spectral bands for the two sensor systems used in the analysis can be observed in Table 5.2.

Table 5.2. Specifications of spectral bands for S2 MSI (ESA, 2021) and L8 OLI (USGS, 2020b).

Band Number	S2 MSI			L8 OLI		
	Description	Wave- Lengths (nm)	Spatial Resolution (m)	Description	Wave- Lengths (nm)	Spatial Resolution (m)
1	Coastal aerosol	433–453	60	Coastal aerosol	433–453	30
2	Blue	458–523	10	Blue	450–515	30
3	Green	543–578	10	Green	525–600	30
4	Red	650–680	10	Red	630–680	30

5	Vegetation Red Edge 1	698–713	20	NIR	845–885	30
6	Vegetation Red Edge 2	733–748	20	SWIR 1	1570–1650	30
7	Vegetation Red Edge 3	773–793	20	SWIR 2	2100–2300	30
8	Near- Infrared (NIR)	785–900	10	Panchromatic	500–680	15
8a	Narrow NIR	855–875	20			
9	Water vapor	935–955	60	Cirrus	1360–1390	30
10	SWIR-Cirrus	1360–1390	60	Thermal Infrared (TIRS) 1	10,600–11,200	100
11	SWIR 1	1565–1655	20	Thermal Infrared (TIRS) 2	11,500–12,500	100
12	SWIR 2	2100–2280	20			

One of the significant problems in crop type mapping in this research is the lack of quality training data. Because of ideal ground reference data limitation, historical Google Earth images in 2018 (February, April, June, July, August, and October) available in Google Earth Pro desktop application (Google LLC, version 7.3.2.5776, Göttingen, Germany) was used as an alternative for validation pixel samples collection. It is based on prior knowledge of crop phenology and cropping calendar (Erdanaev, E., Kappas, M. and Wyss, D., 2022). The spatial distribution of training and validation samples is displayed in Figure 5.2, and the numerical information is given in Table 5.3.

Table 5.3. Numerical information on training and validation data.

Land Use	Training (Polygons/Pixels)	Validation (Pixels)
Cotton	150/2528	250
Wheat	300/5750	500
Rice	150/3038	250
Other Crops	150/2248	250
Fruits/Trees	150/3642	250
Bare land	150/2560	250
Others	150/2601	250
Water	150/2899	250

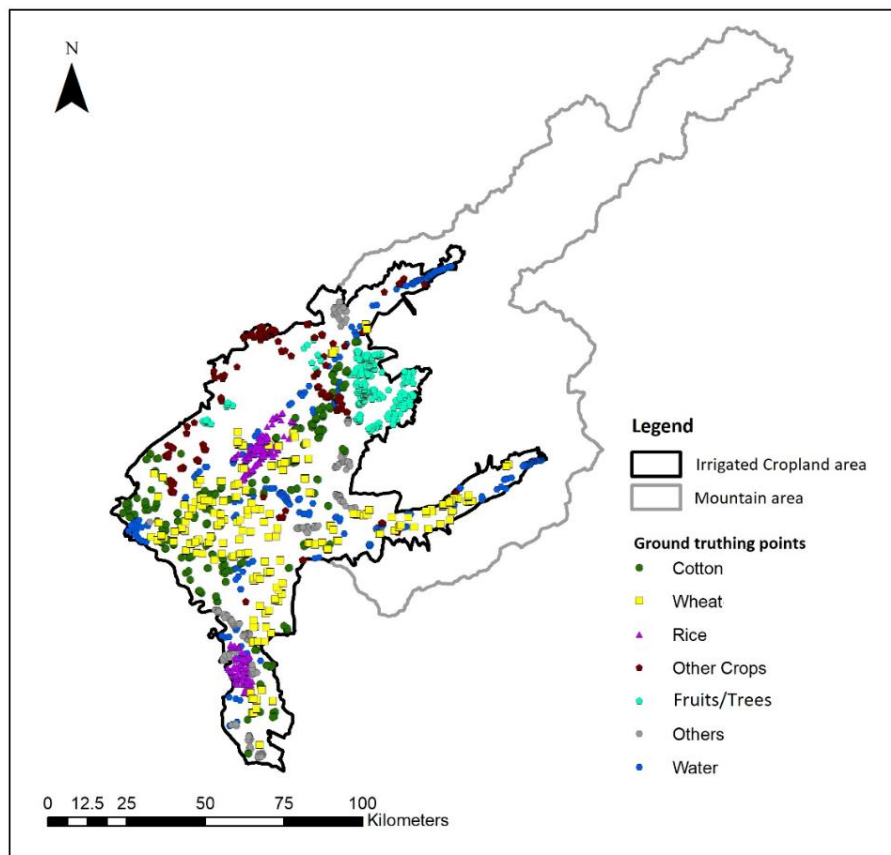


Figure 5.2. Location of training and ground-truthing samples.

The OSS data (UzGosKomStat, 2019) about the sown area by crop types across provinces of the country in 2018 issued by the State Committee of Statistics of Uzbekistan is used for comparative analysis with derived remote sensing-based crop types area.

5.3.3 Methodology

5.3.3.1 Data Preprocessing

After downloading S2 imagery, the SWIR 1 and SWIR 2 bands were resampled to 10 m resolution. Both L8 and S2 data were then atmospherically corrected from Top of Atmosphere Reflectance (TOA) to Surface Reflectance (SR). This was conducted using the Dark Object Subtraction (DOS1) tool of the Semi-Automatic Classification Plugin (SCP) of the QGIS GIS package (Clemente et al., 2020). Then, all tiles of S2 and L8 merged for every month separately, and subset to study area. Reflectance values were then used to calculate NDVI (Rouse, J.W., Haas, R.H., Schell, J.A. and Deering, D.W., 1974), EVI (Alfredo Huete et al., 1999), NDWI1 (Gao, 1996) from SWIR 1, and NDWI2 from SWIR 2. In the end, we have obtained monthly temporal profiles of NDVI, EVI, NDWI1, and NDWI2 as input data for ML classifiers.

Before classification built-up areas were manually digitized as polygons and the shapefile was used to mask these areas.

Training data was used to train SVM and RF classifiers. Both classifiers were then used to classify the main irrigated crop type maps. This was performed for 5 combination variants using different indices such as (1) NDVI, (2) EVI, (3) EVI-NDVI used together, (4) NDWI1, and (5) NDWI2 data.

The resulting land use maps were then assessed for accuracy using OA, PA, UA, and KA using validation data for reference.

5.3.3.2 Indexes

Four spectral vegetation indices, NDVI (Rouse, J.W., Haas, R.H., Schell, J.A. and Deering, D.W., 1974), EVI (Alfredo Huete *et al.*, 1999), NDWI1 (Gao, 1996) from

SWIR 1, and NDWI2 from SWIR 2 were calculated using the surface reflectance values. These indices were formulated by using the following equations:

$$NDVI = \frac{\rho_{NIR} - \rho_{Red}}{\rho_{NIR} + \rho_{Red}} \quad (\text{Equation 5.1})$$

$$EVI = 2.5x \frac{\rho_{NIR} - \rho_{Red}}{\rho_{NIR} + 6 * \rho_{Red} - 7x\rho_{Blue} + 1} \quad (\text{Equation 5.2})$$

$$NDWI1 = \frac{\rho_{NIR} - \rho_{SWIR1}}{\rho_{NIR} + \rho_{SWIR1}} \quad (\text{Equation 5.3})$$

$$NDWI2 = \frac{\rho_{NIR} - \rho_{SWIR2}}{\rho_{NIR} + \rho_{SWIR2}} \quad (\text{Equation 5.4})$$

where ρ_{Blue} , ρ_{Red} , ρ_{NIR} , ρ_{SWIR1} , and ρ_{SWIR2} are the surface reflectance values of Band 2 (blue, 0.45–0.51 μm), Band 4 (red, 0.64–0.67 μm), Band 5 (near-infrared, 0.85–0.88 μm), Band 6 (SWIR1, 1.57–1.65 μm), and Band 7 (SWIR2, 2.11–2.29 μm) in the Landsat-8 LOI and Sentinel-2 images, respectively (Table 5.2).

The approach is displayed in Figure 5.3.

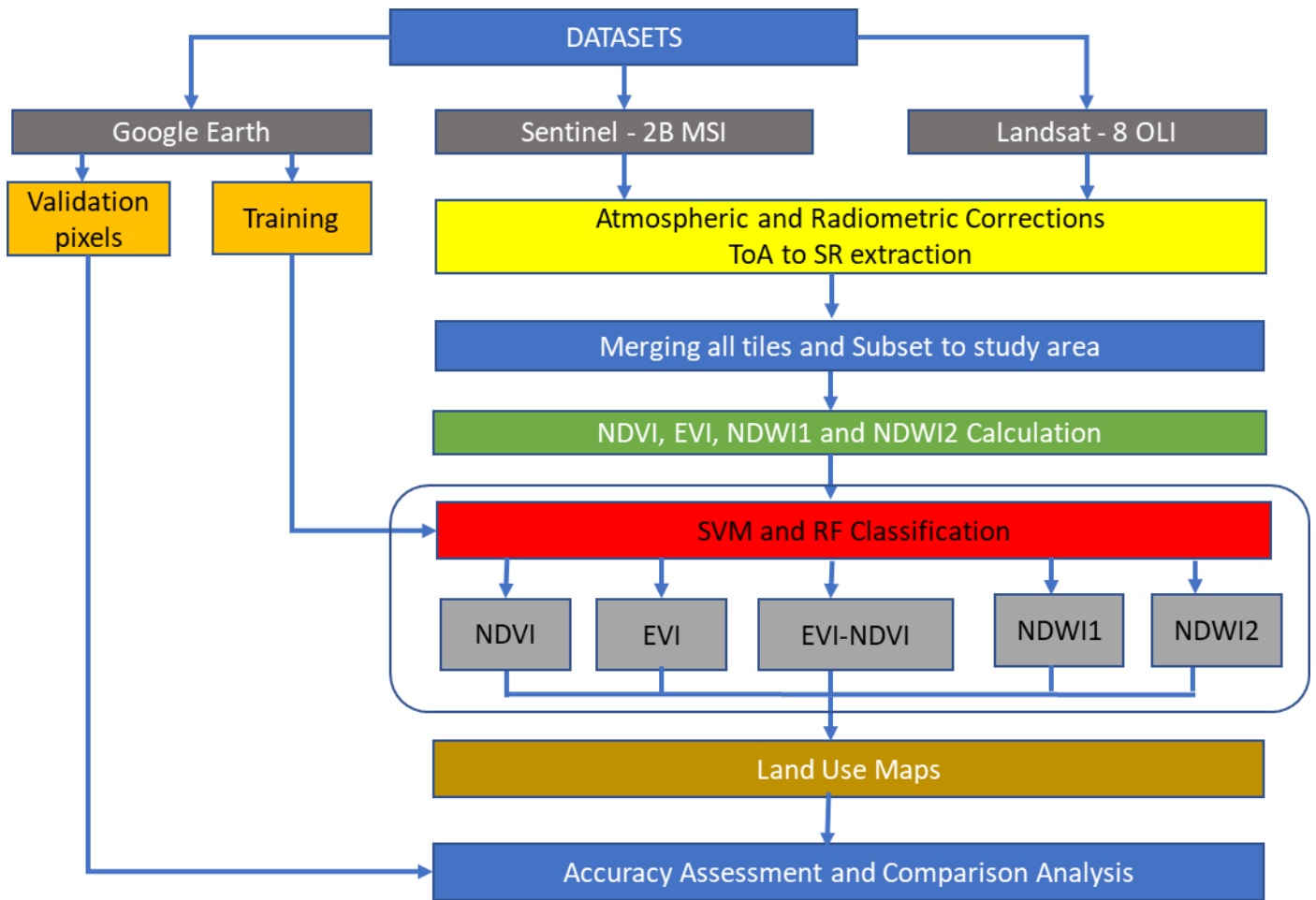


Figure 5.3. Methodology applied for this research

5.3.3.3 ML Algorithms

SVM is a statistical learning method, which was first published by (Vapnik, 1982). The SVM training algorithm is designed to identify a hyperplane separating a dataset into predefined discrete classes based on training examples. The decision boundary minimizing misclassifications is considered the optimal separation hyperplane. This is identified through an iterative learning process separating first training patterns and then simulation data with the same configurations (Zhu & Blumberg, 2002).

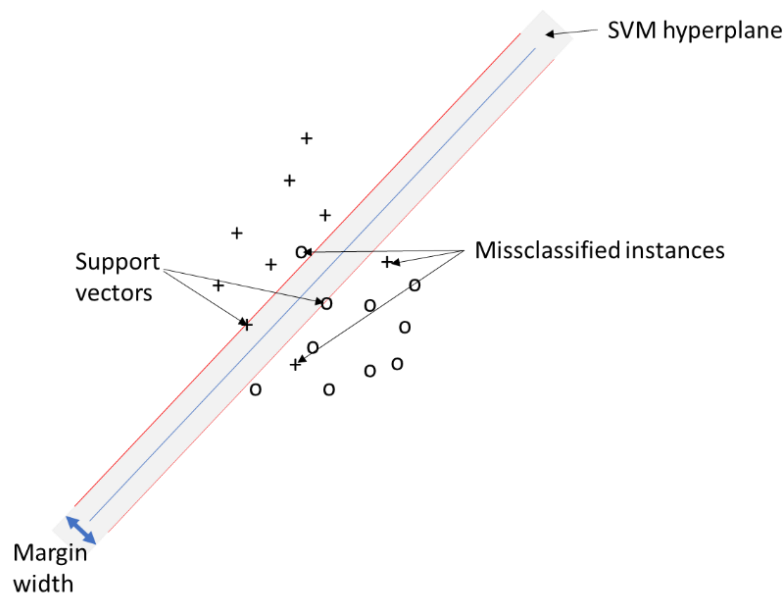


Figure 5.4. Linear SVM example adapted from (Burges, 1998).

In RS, individual pixels are represented as pattern vectors consisting of numerical measurements for each frequency band. In addition, other discriminative measurements based on spatial pixel relationships (e.g., texture) may also be elements of the feature vector. The hyperplane of maximum margin is defined by the subset of points lying on the margin of the classes. In Figure 5.4, the concept is illustrated as a linear SVM based on the simple example of a two-class classification problem. In RS practice, more complex SVMs are applied using multi-class classifiers as kernel functions. A major advantage of SVMs is that they also work well with small training datasets while achieving higher classification accuracy than conventional approaches (Breiman, 2001). Another advantage is the fact that SVM allows generalizing accuracy acquired from finite training patterns to unseen data.

The main challenge for the use of SVM in RS is constituted by the choice of kernel functions. In this context, the radial-bias function and polynomial functions have been demonstrated to produce different results (Zhu & Blumberg, 2002). In this research, we used a linear kernel function in which the algorithm creates a hyperplane to separate the classes.

The RF method was first introduced by (Breiman, 2001). It is based on a combination of tree predictors in which each tree depends on the values of an independently

sampled random vector, where all trees in the forest have the same distribution. For the set-up of an RF model, the base of the method, constituted by the two parameters, the number of trees n and the number of features in each split m_{try} , are required. According to (Breiman, 2001), a random forests consists of tree-structured classifiers $\{h(x, \Theta_k), k = 1, \dots\}$. In this $\{\Theta_k\}$ independent, there are identically distributed random vectors. Accurate classification is determined by each tree casting a unit vote. In RF classifiers, the number of features used at each node and the number of trees grown are user-defined parameters. Thus, at each node only selected features are assessed. In the classification of a dataset, each case is assessed in each tree. Accurate classification is determined by the majority vote from all trees (Pal, 2005).

The concept is illustrated in Figure 5.5. A are input samples. B and C are decision trees within an RF D, assigning the sample to one of two branches based on the rule at each decision point. In both B and C, the sample is assigned to the red class. Consequently, the combined output result E of the RF is also the red class. The RF has strong predictive performance. In addition, results inform each feature's level in contributing to class prediction (Denisko & Hoffman, 2018).

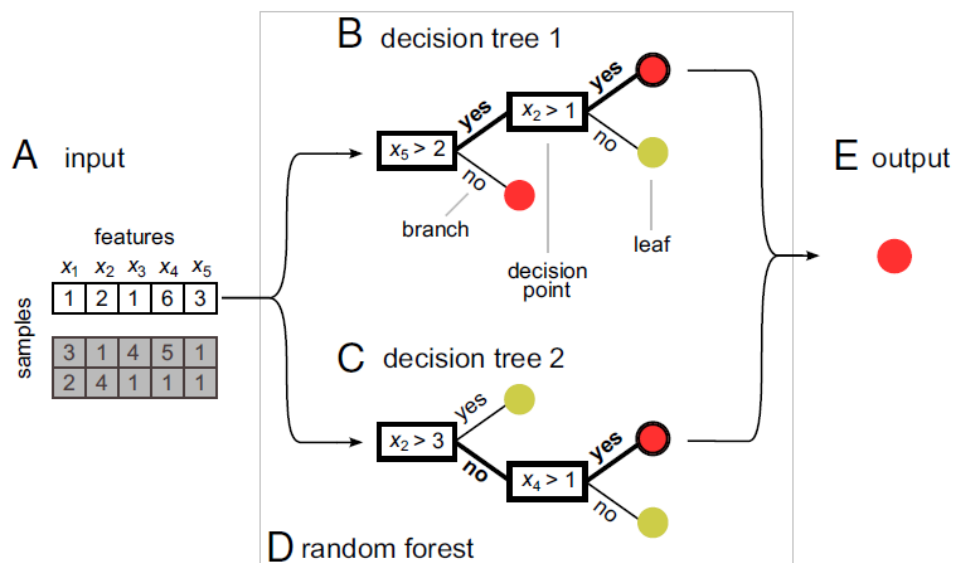


Figure 5.5. RF concept adapted from (Denisko & Hoffman, 2018).

Comparing SVM and RF, (Denisko & Hoffman, 2018) concludes that they achieve comparable accuracy. The fact that RF only requires two parameters to be set, whereas SVM requires several user-defined parameters constitutes an advantage of RF over

SVM (Thanh Noi & Kappas, 2017). RF classifier tool in ArcMap creates models and generates predictions based on Leo Breiman’s RF algorithm (Breiman, 2001). Another advantage of RF is the ability to handle data with missing values and unbalanced data, as well as categorical data, which SVM lacks. In addition, RF allows for the detection of outliers through proximity analysis. The main difference though is that RF can also be used for unsupervised classification. These advantages of RF notwithstanding, (Nitze, I., Schulthess, U., & Asche, H., 2012), consider SVM with the polynomial kernel as well as radial-basis function to be superior to RF, with RF performing inferior to SVM, if only single satellite coverage is used.

5.3.3.4 Accuracy of RS Classification

To assess the performance of each classifier with different satellite sensors and indices combination, the confusion matrices were calculated in ArcMap. Confusion matrices can be used to describe the classification algorithm’s performance.

The increased use of digital RS data and various semi-automated or fully-automated classification methods has led to an increased interest in classification accuracy. OA is the simplest statistic, describing the number of all correctly classified pixels by the total number of pixels used for accuracy assessment within the error matrix. In addition, producer’s accuracy (PA) describes the probability that a reference pixel has been correctly classified (and thus not omitted); the user’s accuracy (UA) describes the probability of pixels within a specific class, which have been correctly classified and divided by the total number of pixels assigned to that class. Another common measure of accuracy is KA, which is calculated by the kappa index of agreement KHAT equation (Congalton, 1991):

$$\hat{K} = \frac{N \sum_{i=1}^r x_{ii} - \sum_{i=1}^r (x_{i+} x_{+i})}{N^2 - \sum_{i=1}^r (x_{i+} x_{+i})} \quad \text{Equation 5.1}$$

Where:

r: number of rows in the matrix

x_{ii} : number of observations in row i and column i

x_{i+} , x_{+i} : marginal totals of row i and column i

N : total number of observations.

KA value can be divided into three categories; a value greater than 0.80 represents strong agreement; a value between 0.40–0.80 represents moderate agreement; and a value below 0.40 represents poor agreement (Congalton, 1991).

5.4 Results

5.4.1 Results from land use classification

Results from the land use classification for different combinations of sensor, classifier, and index are presented in Figure 5.6 (S2-data and SVM classifier), Figure 5.7 (S2-data and RF classifier), Figure 5.8 (L8-data and SVM classifier), and Figure 5.9 (L8-data and RF classifier). For comparison in each figure the OSS data are also presented.

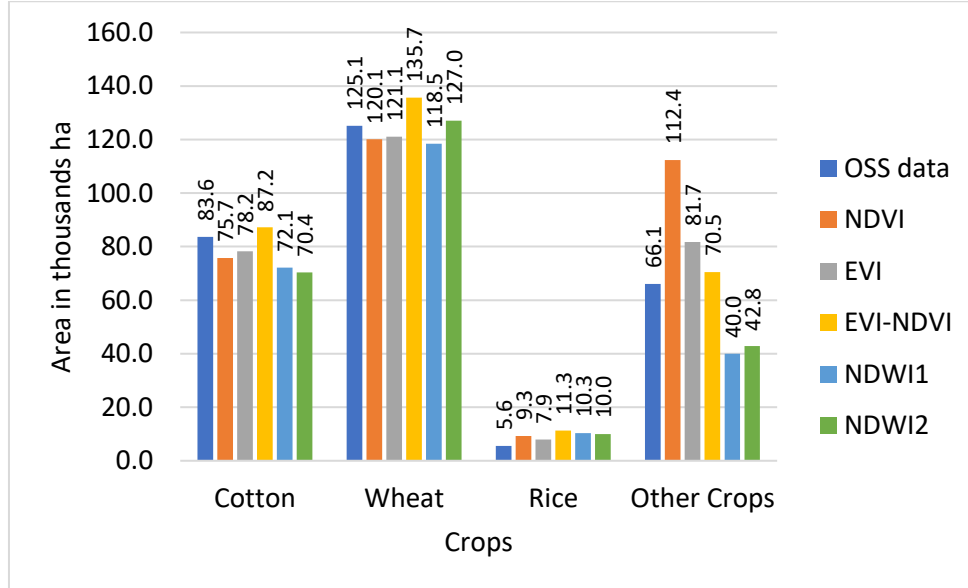


Figure 5.6. Comparison of classified crop types area with OSS data for RF classifier with S2 sensor.

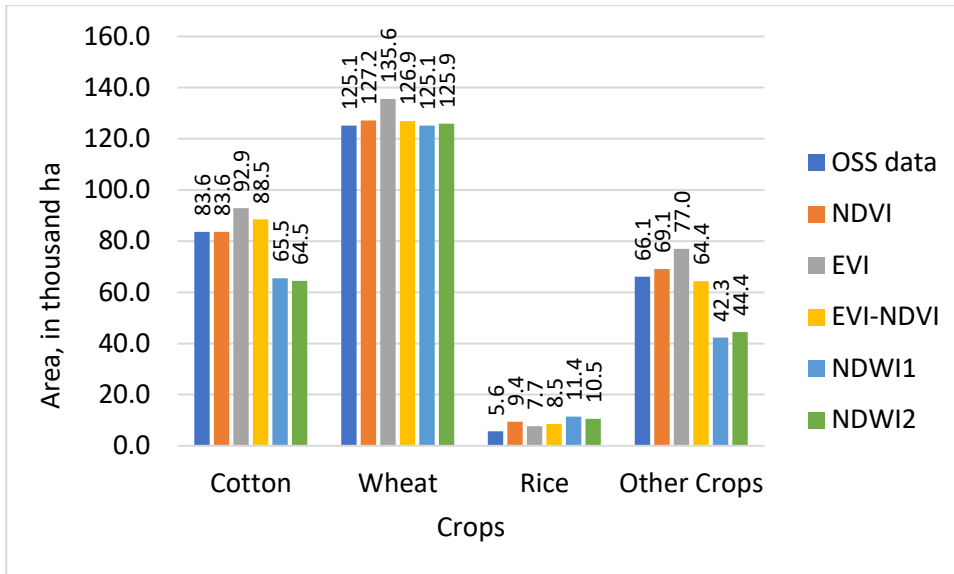


Figure 5.7. Comparison of classified crop types area with OSS data for SVM classifier with S2 sensor.

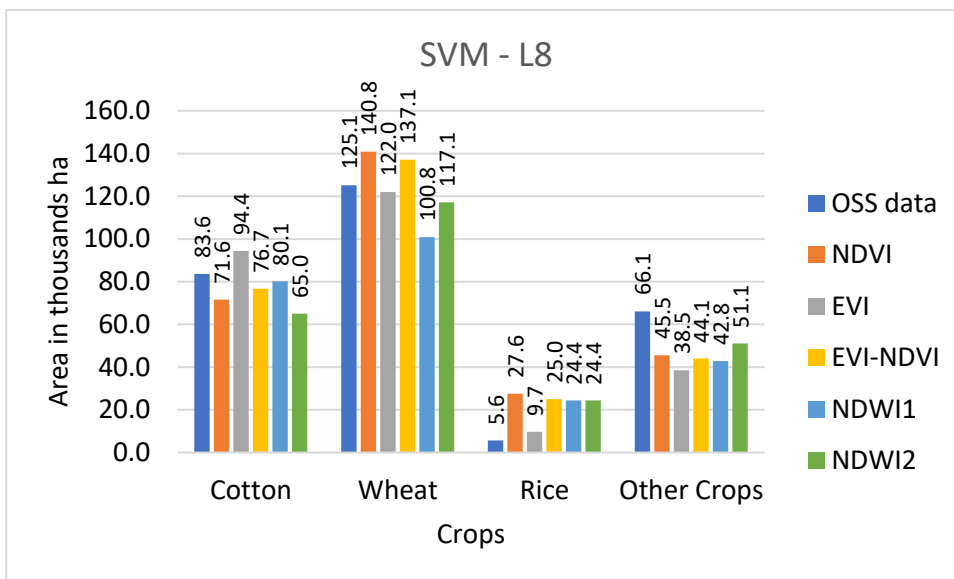


Figure 5.8. Comparison of classified crop types area with OSS data for SVM classifier with L8 sensor.

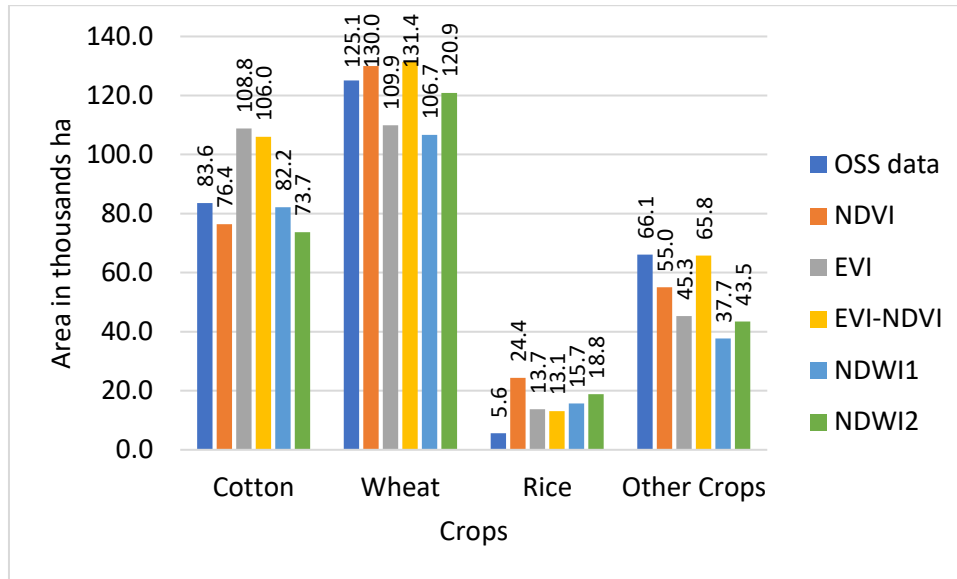


Figure 5.9. Comparison of classified crop types area with OSS data for RF classifier with L8 sensor.

With winter wheat being the most abundant crop in the study region, classification results for this crop might have a higher influence on the overall result. Figure 5.6 shows that wheat results based on S2-SVM indices are very close to OSS and each other. Figure 5.7, however, shows that except for EVI-NDVI this is also true for S2-RF. From Figure 5.8, it can be observed that there are higher differences between the different indices as well as between individual indices and OSS. However, what is also evident from Figures 5.8 and 5.9 is that the SVM and RF classifiers tend to classify rice paddies area with a probability of difference between 190% to almost 500% compared to the area given by OSS. This can be the result of wetlands being classified as rice fields and needs to be investigated further in detail. Besides, the rice is also planted after harvesting winter wheat as a second crop which is not included and recorded by OSS. This is because the study area is located where the upstream water resources are formed and it has more access to the water resources than other areas of the country.

As can be observed from Figure 5.9, there are differences between OSS data and classification results for each of the sensor-classifier-index combinations. These differences appear to be particularly high for land use classes for which OSS shows comparatively low values. To analyze this in more detail, differences between individual classification results and OSS were calculated and presented in Table 5.4.

Table 5.4. Differences between classification results and OSS (1000 ha).

S2-SVM						
		NDVI	EVI	EVI-NDVI	NDWI1	NDWI2
Cotton		0	-9.3	-4.9	18.1	19.1
Wheat		-2.1	-10.5	-1.8	0	-0.8
Rice		-3.8	-2.1	-2.9	-5.8	-4.9
Other crops		-3	-10.9	1.7	23.8	21.7
	AM	-2.2	-8.2	-2.0	9.0	8.8
	WA (OSS):	-0.4	-2.5	-0.5	2.7	2.6
S2-RF						
		NDVI	EVI	EVI-NDVI	NDWI1	NDWI2
Cotton		7.9	5.4	-3.6	11.5	13.2
Wheat		5	4	-10.6	6.6	-1.9
Rice		-3.7	-2.3	-5.7	-4.7	-4.4
Other crops		-46.3	-15.6	-4.4	26.1	23.3
	AM	-9.3	-2.1	-6.1	9.9	7.6
	WA (OSS):	-1.6	-0.1	-1.7	31	2.1
L8-SVM						
		NDVI	EVI	EVI-NDVI	NDWI1	NDWI2
Cotton		12	12	-10.8	6.9	3.5
Wheat		-15.7	-15.7	3.1	-12	24.3
Rice		-22	-4.1	-19.4	-18.8	-18.8
Other crops		20.6	27.6	22	23.3	15
	AM	-1.3	4.9	-1.3	-0.2	6.0
	WA (OSS):	0.2	0.7	0.7	0.5	3.8
L8-RF						
		NDVI	EVI	EVI-NDVI	NDWI1	NDWI2
Cotton		7.2	7.2	-25.2	-22.4	1.4
Wheat		-4.9	-4.9	15.2	-6.3	19
Rice		-18.8	-8.1	-7.5	-10.1	-13.2
Other crops		-1.4	3.8	-4.3	-2.6	7.5
	AM	-1.35	3.75	-4.3	-2.6	7.45
	WA (OSS):	0.6	1.2	-0.2	-0.7	3.5

For each classification method, the arithmetic means (AM), as well as a WA using OSS area as weights, were calculated. Since using the AM value for the differences, the results in a disproportionate influence of differences for land use classes with a low share of overall land use (i.e., particularly rice); therefore, it was decided to focus on the WA results, as shown in Table 5.4.

Based on the results, the smallest absolute value difference WA 0.1 thousand ha was demonstrated for the S2-sensor data using the RF classifier and EVI index, whereas for the SVM classifier with S2 data, the smallest absolute value difference WA result, 0.4 thousand ha, is obtained using the NDVI.

For L8-sensor data, the smallest absolute value difference result of 0.2 thousand ha was obtained by using the EVI-NDVI with RF method or NDVI with SVM method.

To compare classification results for different sensor-classifier-index combinations, subsets of land use maps in the middle of the study area located in Figure 5.10 for the SVM classifier and Figure 5.11 for the RF classifier. The location of subsets is shown in Figures 5.12 and 5.13. The subset area was chosen due to its location along the main river Chirchik and the availability of all main cultivated crops inside. Visual analysis of these comparisons indicates that results appear similar for both sensors' data with differences depending on the classifier and index method. The results from the NDWI2 demonstrate a very high amount of areas classified as water compared to other index methods.

Since OSS data are based on planning data compiled by the Ministry of Agriculture and Resources of Uzbekistan, Tashkent, Uzbekistan, rather than on an assessment of the actual cultivation situation, a high level of similarity for classification results with these data is not necessarily an indicator of the quality of the classification result. Therefore, results for classification accuracy are presented and analyzed in the next section.

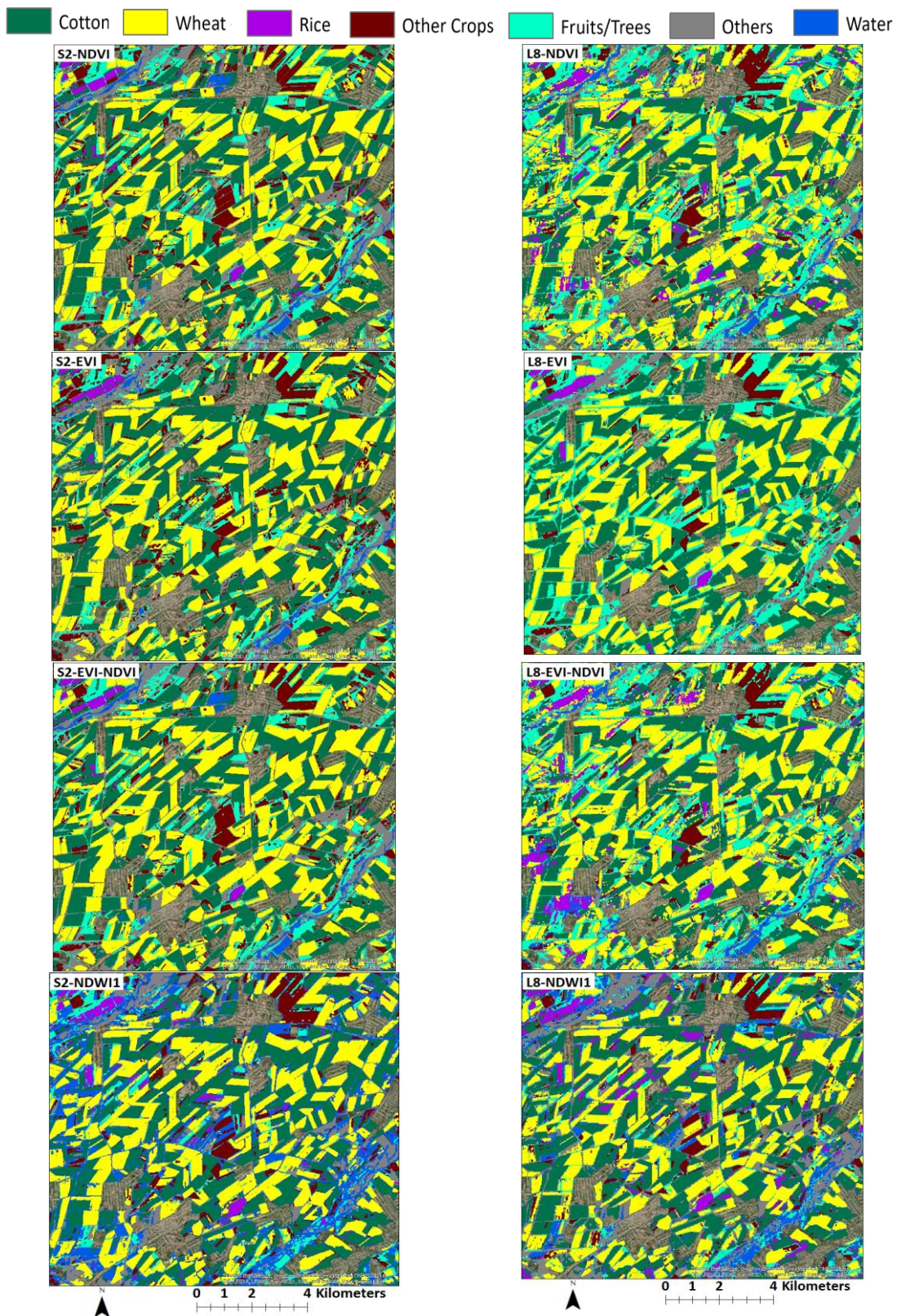


Figure 5.10. Subsets of land use maps derived from different indices using the SVM classification method for both S2 (**left**) and L8 (**right**).

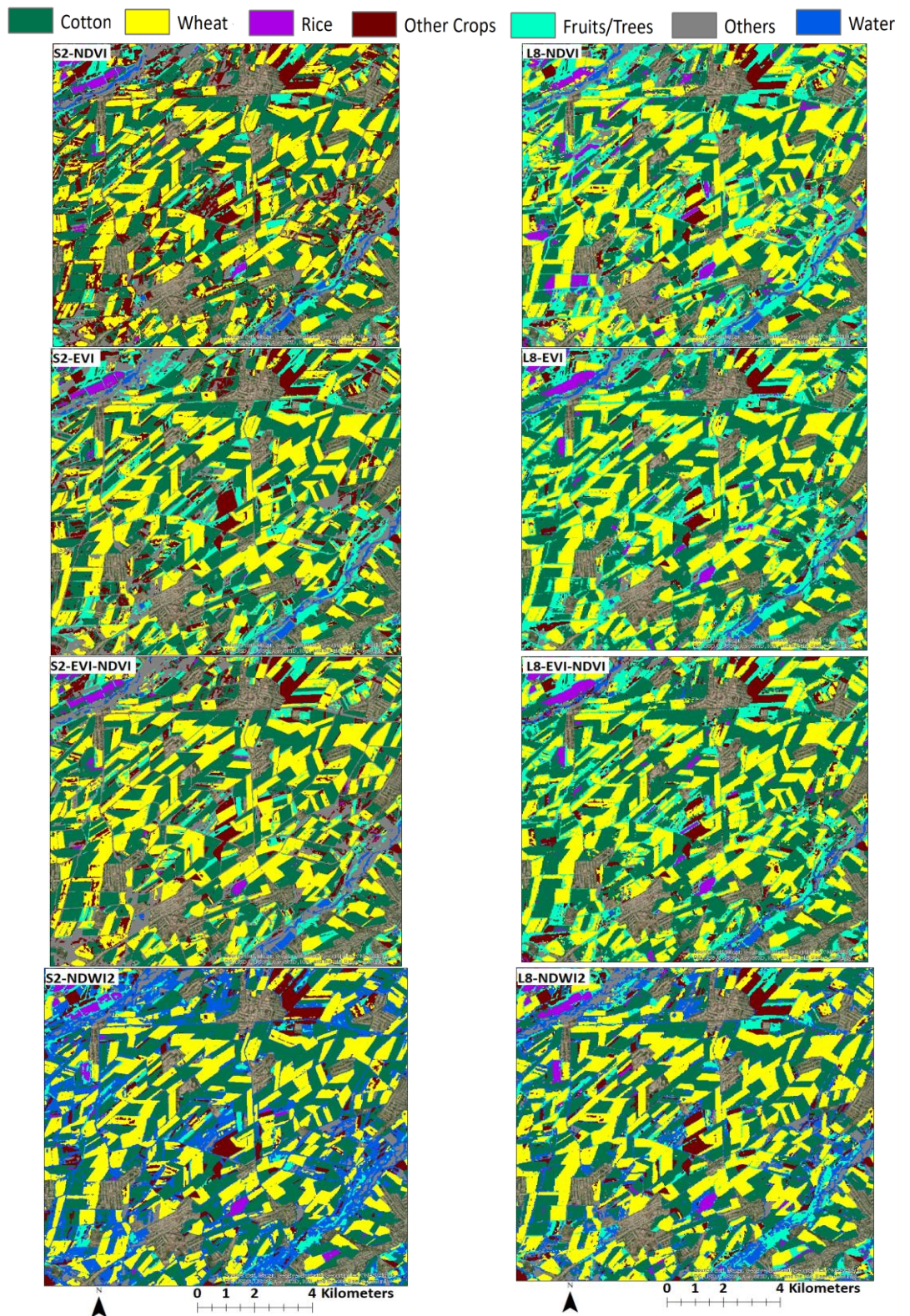


Figure 5.11. Subsets of LU maps derived from different indices using the RF classification method for both S2 (**left**) and L8 (**right**).

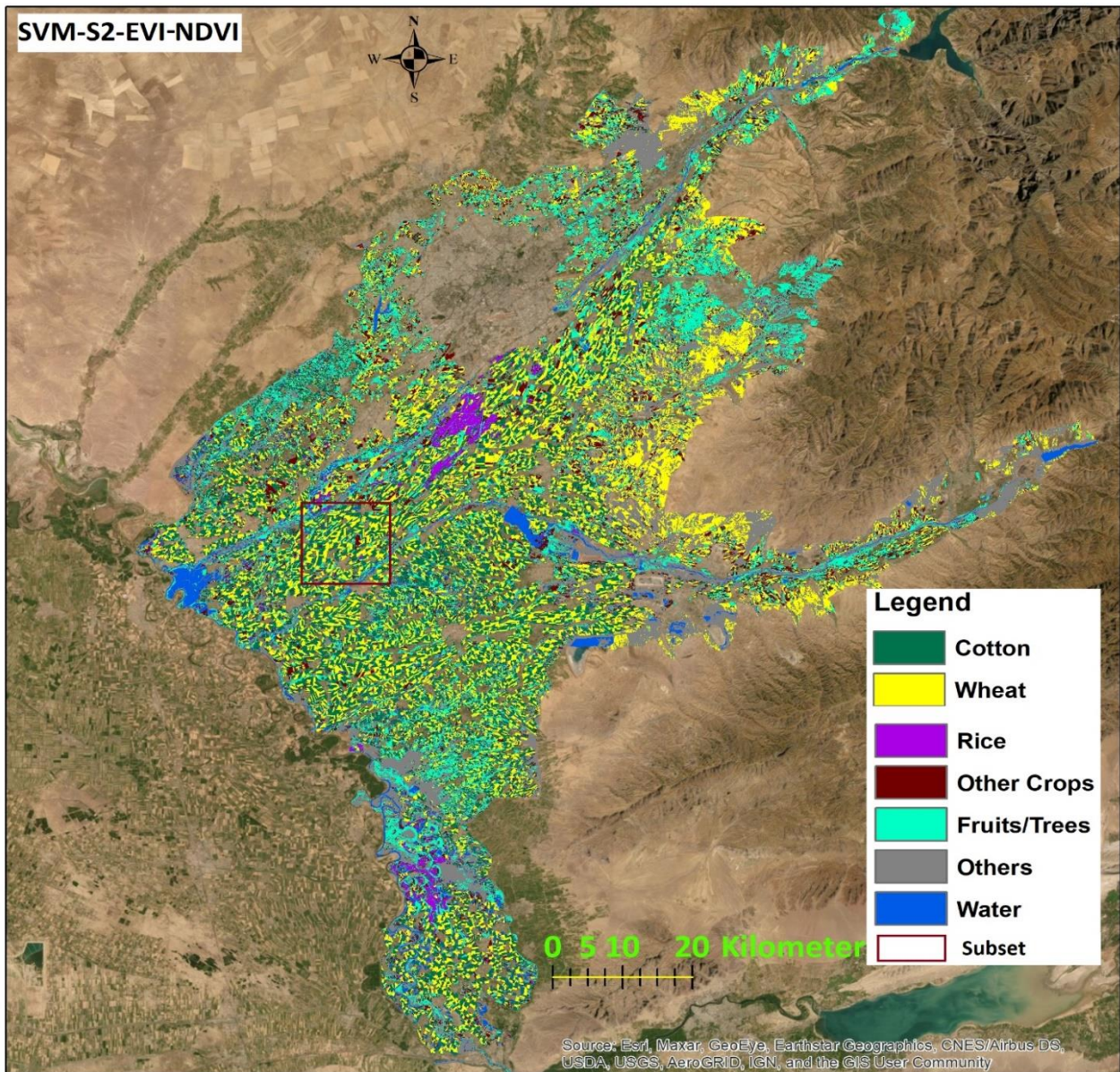


Figure 5.12. Classification result of S2-SVM-EVI-NDVI (highest OA 88% for SVM).

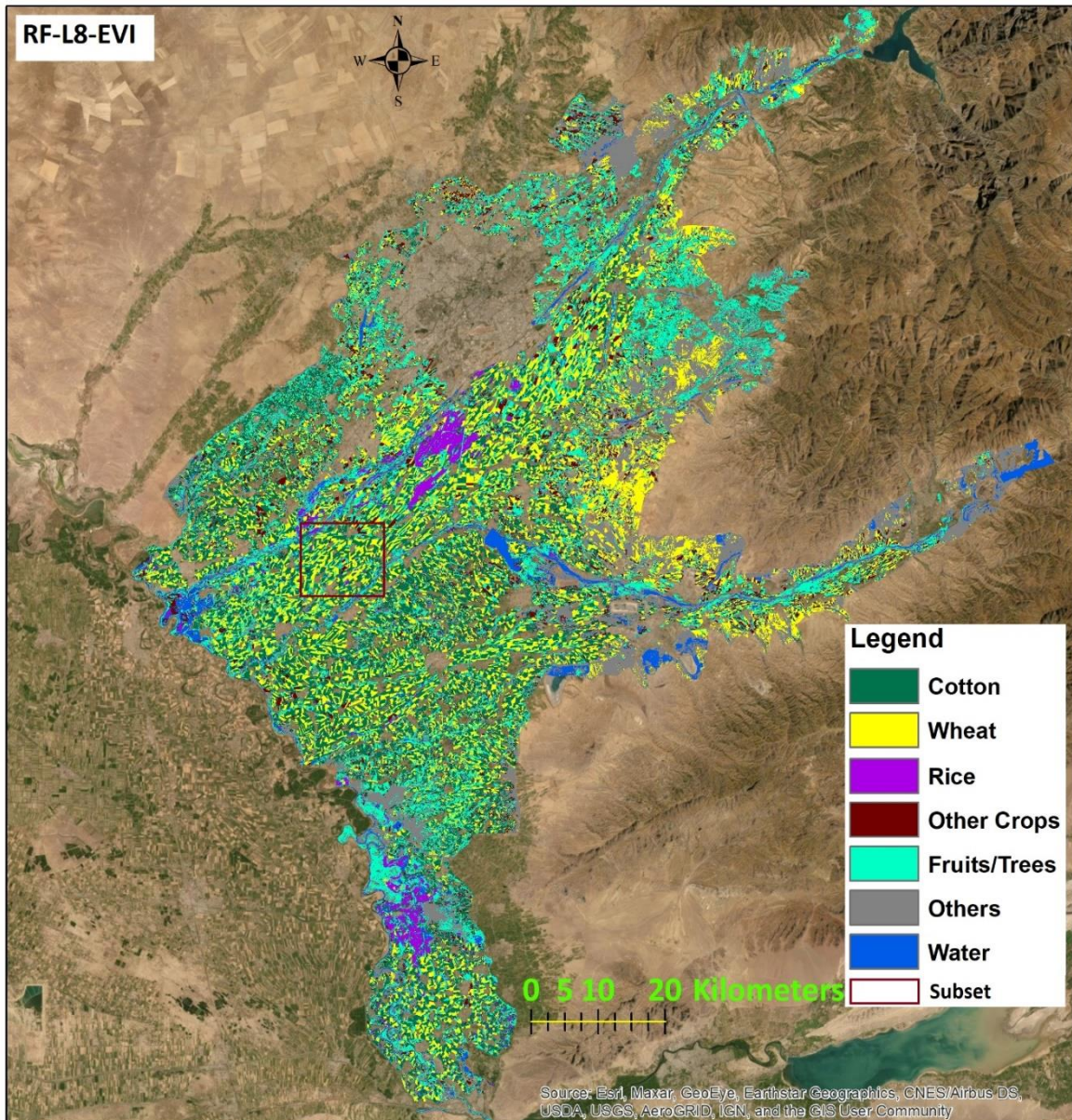


Figure 5.13. Classification result of L8-RF-EVI (highest OA 90% for RF).

5.4.2 Results for classification accuracy

Classification accuracy (CA) was assessed using ground-truthing samples derived from historical Google Earth data. Results for OA, UA, PA, and KA are presented in Table 5.5 for the SVM classifier and in Table 5.6 for the RF classifier.

Table 5.5. Accuracy assessment (in %) results of SVM classifier.

Classes	NDVI				EVI				EVI-NDVI				NDWI1				NDWI2			
	UA		PA		UA		PA		UA		PA		UA		PA		UA		PA	
	S2	L8	S2	L8	S2	L8	S2	L8	S2	L8	S2	L8	S2	L8	S2	L8	S2	L8	S2	L8
Cotton	84	75	94	73	74	85	96	92	87	78	97	81	93	86	92	82	90	90	90	85
Wheat	87	85	92	81	86	78	92	89	88	82	91	83	92	93	93	90	95	89	91	89
Rice	93	75	78	68	97	94	70	94	95	83	80	74	90	83	92	85	92	84	88	87
Other crops	76	79	80	86	84	86	80	60	78	78	80	76	87	80	86	72	84	78	89	72
Fruits/trees	87	81	88	89	81	69	87	88	86	81	89	88	71	76	78	80	73	83	74	81
Others	89	84	83	85	92	65	75	86	89	91	83	82	92	87	82	90	94	85	86	83
Water	97	88	95	92	98	99	98	31	98	85	96	93	76	72	75	80	76	74	87	83
AM	88	81	87	82	87	82	85	77	89	83	88	82	86	82	85	83	86	83	86	83
OA-S2	87				86				88				86				87			
OA-L8	82				79				82				83				84			
KA-S2	85				84				86				84				84			
KA-L8	78				75				79				80				81			

Table 5.6. Accuracy assessment (in %) results of RF classifier.

Classes	NDVI				EVI				EVI-NDVI				NDWI1				NDWI2			
	UA		PA		UA		PA		UA		PA		UA		PA		UA		PA	
	S2	L8	S2	L8	S2	L8	S2	L8	S2	L8	S2	L8	S2	L8	S2	L8	S2	L8	S2	L8
Cotton	81	77	91	84	77	88	92	95	77	89	94	95	94	90	95	90	93	90	94	90
Wheat	91	90	87	84	86	94	89	92	91	92	93	87	92	94	92	92	94	89	93	90
Rice	94	83	76	76	96	94	68	97	92	94	76	97	90	90	94	88	94	90	93	90
Other crops	72	83	85	84	70	87	78	85	84	76	78	79	88	86	78	77	90	85	84	71
Fruits/trees	82	81	86	89	81	78	85	81	81	85	81	87	70	76	76	83	76	79	81	84
Others	89	86	84	82	85	92	73	91	85	96	86	82	95	95	80	86	93	92	82	75
Water	97	91	97	98	97	93	97	90	99	89	97	99	65	75	74	86	75	68	86	85
AM	87	84	87	85	85	89	83	77	87	89	86	89	85	87	84	86	88	85	88	84
OA-S2	86				84				87				85				88			
OA-L8	85				90				89				87				84			
KA-S2	84				81				85				82				86			
KA-L8	82				88				87				84				81			

As can be observed from Table 5.5, UA and PA vary considerably between land use classes for the SVM classifier. The AM across all land use classes is in the range of

84% to 89% for all sensor-ML algorithm-index combinations. The highest mean UA value for the SVM classifier is 89% for S2-EVI-NDVI. The highest mean UA value for L8 is 83% for NDWI1 and NDWI2, followed by 82% for NDVI and EVI-NDVI.

Looking at Table 5.6 and using OA and KA as measures, these two classification accuracy indicators are higher for the S2 than the L8 sensor data using the SVM classifier. In comparison to this, when looking at Table 5.6 at OA for results from the RF classifier and S2 and L8, this relationship is less pronounced, with OA showing higher values for S2 than L8 for NDVI, and NDWI2, whereas OA for L8 has taken on higher values than S2 for EVI, EVI-NDVI, and NDWI1. KA shows the same relationships between sensor data for both SVM and RF.

Results presented in Tables 5.5 and 5.6 indicate that RF with L8 data results in higher OA values than SVM with L8 data. However, for S2 data, results from SVM show higher OA values than with RF.

The highest OA of 88% resulted for S2 was achieved when EVI-NDVI was used, as well as the highest KA. A map displaying the classification result is shown in Figure 5.12. In addition, the highest OA of 90% for L8 data was achieved with EVI. A map displaying the classification result is shown in Figure 5.13.

For the RF classifier in Table 5.6, results for UA and PA also differ considerably between land use classes and sensors. AM values across all land use classes for each satellite datasets-ML algorithms calculation are in the range of 82% to 88%. The highest mean value of 89% resulted for EVI-L8, EVI-NDVI-PA-L8, and EVI-NDVI-UA-L8. The highest mean UA value for S2-data is 88% for NDWI2 followed by 87% for EVI-NDVI. The highest PA value is 83% for L8-NDWI2 at 83% and L8-EVI-NDVI. As can be observed from Tables 5.5 and 5.6, OA is the highest, at 90%, for the combination L8-RF-EVI, followed by L8-RF-EVI-NDVI, at 89%, and S2-SVM-EVI-NDVI and L8-RF-NDWI2, both 88%. The values for KA, on the other hand, are highest for L8-RF-EVI at 88%, followed by L8-RF-EVI-NDVI at 87. Generally, the values for KA show a wider range from 75 to 88 than those for OA, which range from 84 to 90. The mapping result for the combination L8-RF-EVI is displayed in Figure 5.13.

5.5 Discussion

In this study, high-resolution S2 data, as well as medium-resolution L8 data were analyzed using different vegetation and water indices to derive main irrigated crop types mapping. Two widely used ML classifiers of SVM and RF methods were used to recommend appropriate classification methods to map high-resolution spatial crop types in the semi-arid area of Tashkent province, Uzbekistan, because SVM and RF classifiers perform better results for cropland classification when compared with other classification methods such as Maximum Likelihood Classification, Classification and Regression Trees, Naive Bayes, etc. (Basukala *et al.*, 2017; Clemente *et al.*, 2020).

5.5.1 Performance of ML Classifiers

Comparison of accuracy assessment analysis indicates that the highest OA 90%, as well as KA 88%, was achieved using L8 sensor data with RF classifier and EVI used as input data. For the SVM classifier, the highest OA 88% as well as KA 86% resulted from using S2 data and EVI-NDVI used as input data. Thus, regarding the accuracy assessment analysis, results from this paper do not provide a definitive answer on whether S2 or L8 is a better dataset for crop types classification, as the OA and KA result rather depends on the classifiers (SVM or RF) than the type of sensor (medium-resolution L8 or high-resolution S2) used. However, we can conclude that in terms of accuracy assessment, the RF classifier performs slighter better than SVM. This result also agrees with other studies (Saini & Ghosh, 2018; Azeez *et al.*, 2020; Bofana *et al.*, 2020; Virnodkar *et al.*, 2021).

Thus, the conclusion made by Nitze *et al.* (Nitze, I., Schulthess, U., & Asche, H., 2012) that SVM performs superior to RF if used with single satellite coverage is not supported by the results presented in this paper. In conclusion, the results demonstrate that both classifiers perform well, with comparable results in terms of classification accuracy, which are made in (Breiman, 2001), to be supported.

5.5.2 Using Different Indices and Their Performance

Using the spectral indices alone improves the classification accuracy. When spectral indices are used together with reflectance values for crop type classification, it negatively impacts classification accuracy due to large sets of correlated variables. The reflectance including bands Blue, Red, NIR, SWIR1, and SWIR2 spectral indices are very useful for the identification of crop types and can achieve high classification accuracy (Kobayashi *et al.*, 2020). Based on that recommendation, four indices of NDVI, EVI, NDWI1, and NDWI2 performance were studied using different satellite datasets and ML algorithms.

The highest values of OA and KA resulted when EVI and EVI-NDVI were used in crop type classifications, as shown in Figures 5.14 and 5.15. Using the L8 dataset's EVI, EVI-NDVI, and NDWI1 with RF classifier yielded higher OA values of 90%, 89%, and 87%, respectively. It also applies to KA values as well. The lowest OA and KA values resulted in an SVM classifier of L8 datasets for all indices.

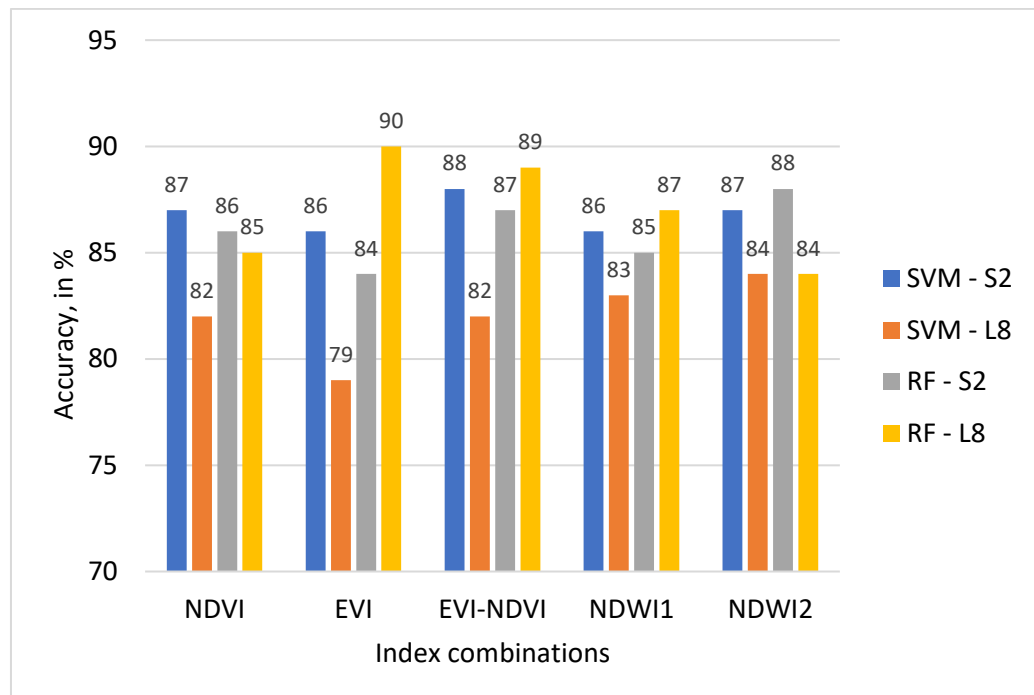


Figure 5.14. OA of SVM and RF classifiers on different indices and satellites.

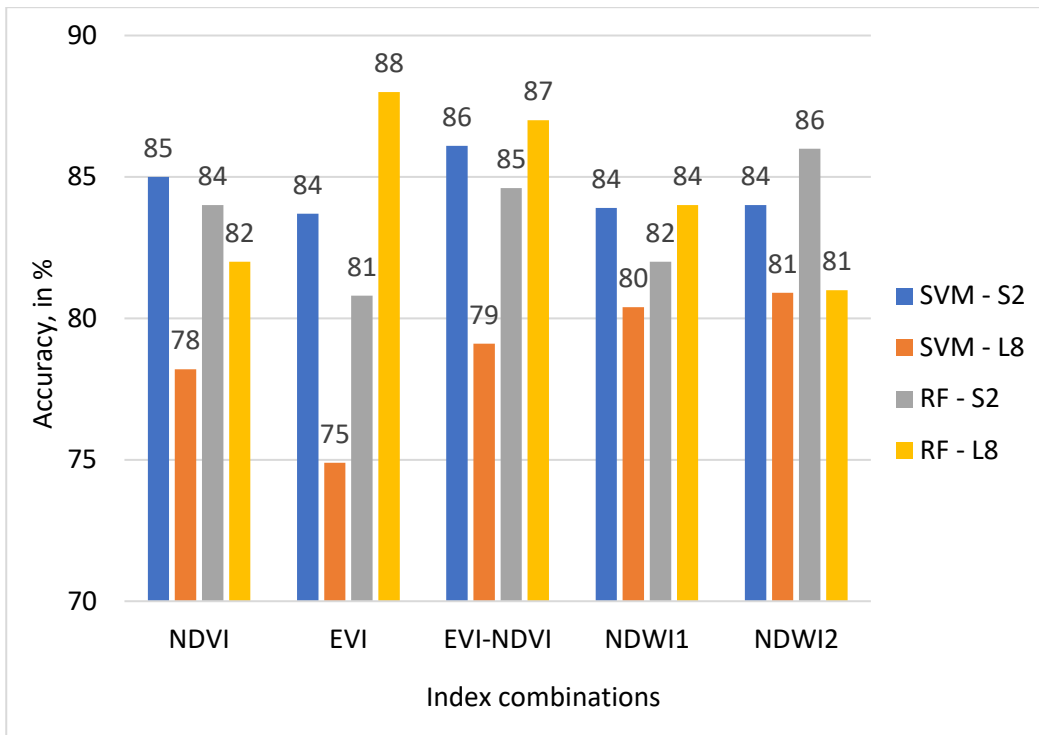


Figure 5.15. KA of SVM and RF classifiers on different indices and satellites.

For NDWI1 and NDWI2, a visual assessment of classified images in Figures 5.10 and 5.11 indicates that these indices tended to overclassify water areas, which could explain the overall bigger areas classified to these classes because NDWI is very sensitive to changes in the water content of vegetation canopies and soil water content (Gao, 1996). Due to irrigation of crops in the early crop growing period, the soil water content influences the classification accuracy, which resulted in many misclassified pixels as water. NDVI and EVI resulted in overall slightly better accuracy values than NDWI1 and NDWI2. Vegetation indices, which include NIR, have a great contribution to identifying crop types (Palchowdhuri *et al.*, 2018; Saini & Ghosh, 2018; Sonobe *et al.*, 2018). The other research studies compared the performance of EVI and NDVI for image classifications; it was found that their performance is equally good, with a slight overperformance of each other's (Wardlow & Egbert, 2010; HAO *et al.*, 2020). The most important factor is crop phenology knowledge and crop growth period consideration during training and validation samples (Pan *et al.*, 2021). At the very beginning of the crop growing season (March–April), the classification achieves relatively low accuracies, and it significantly increases when satellite images are obtained between May and June until the OA reaches its highest value in July (Vuolo

et al., 2018; Demarez *et al.*, 2019). However, when the combination of multiple sensor datasets is used for crop type classification, it improves the classification accuracy due to its high temporal resolution, which captures more datasets throughout the vegetation growth period (Yi *et al.*, 2020; Pan *et al.*, 2021; Song *et al.*, 2021).

5.5.3 Comparing Derived Main Crop Types Area with OSS Data

Cropland areas derived from this study were compared with OSS data at the provincial level. The other studies also compared calculated croplands area with OSS data at national and regional levels (Oliphant *et al.*, 2019; Gerts *et al.*, 2020; Asam *et al.*, 2022; Erdanaev, E., Kappas, M. and Wyss, D., 2022). In Figure 5.16, a comparison of the total area classified for the land use categories of cotton, wheat, rice, and other crops is displayed by the sensor, classifier, and index and compared to the equivalent figures from OSS.

The comparison of the total area classified for the land use categories of cotton, wheat, rice, and other crops with OSS data in Figure 5.16 shows that with exception of the S2-RF sensor-classifier combination, classifications based on NDVI are closest to OSS and also comparatively close to each other regarding the total classified area. NDWI1 and NDWI2 also demonstrate similar total classified area results for all sensor-classifier combinations, but at roughly 250 thousand ha both show smaller total areas than OSS data. The total area of classifiers NDVI-S2-RF, EVI-S2-SVM, EVI-NDVI-L8-RF, and EVI-NDVI-S2-RF are recorded in OSS.

The mapped areas of the crop classes in this study area, overall, do well with OSS data at the provincial level, with on average 1% deviation in coverage resulting with L8 sensor datasets using RF-EVI and SVM-EVI-NDVI methods, as shown in Table 5.7. A similar result was also found in the work of Asam *et al.*, 2022 (Asam *et al.*, 2022). The deviation between 1% to 13% resulted from the EVI and NDVI used by all ML classifiers and sensor datasets. The close values are also found in the research of Oliphant *et al.*, 2019 (Oliphant *et al.*, 2019). The lowest deviation values of 8% to 14% (less than OSS data) were found using NDWI1 and NDWI2 by all ML classifiers and sensor datasets.

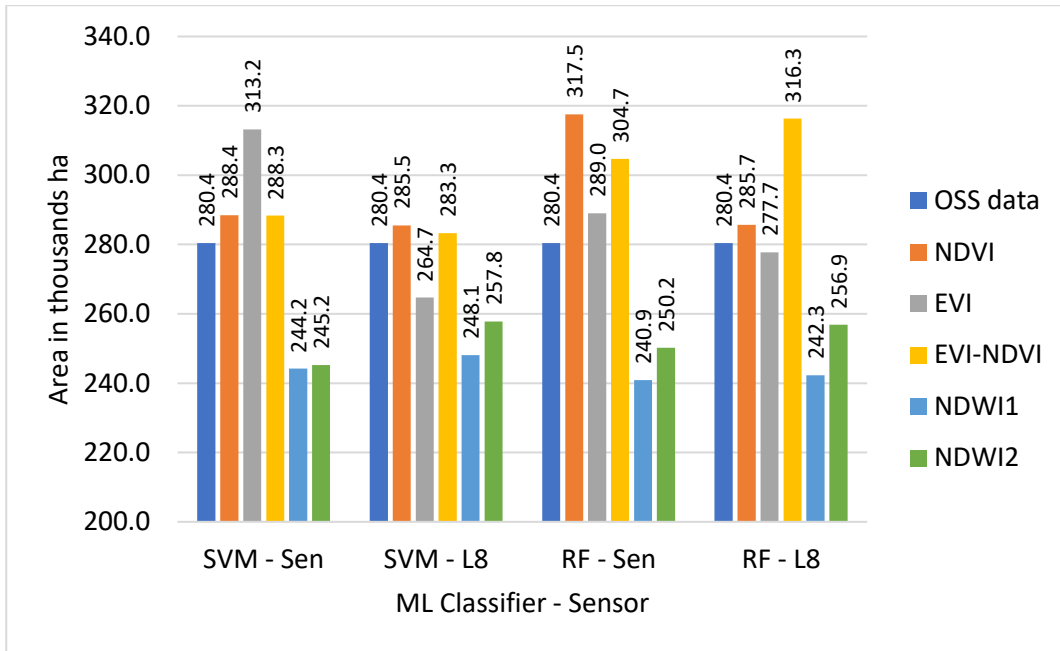


Figure 5.16. Difference between the total area of OSS data and classified area by sensors, classifiers, and indices.

Table 5.7. Deviation (in %) between the total mapped crop areas and OSS data (280.4 thousand ha).

Classifier- Sensor	Indices Combination				
	NDVI	EVI	EVI-NDVI	NDWI1	NDWI2
SVM-S2	3	12	3	-13	-13
SVM-L8	2	-6	1	-12	-8
RF-S2	13	3	9	-14	-11
RF-L8	2	-1	13	-14	-8

5.5.4 Theoretical and Practical Implications of the Research

Land information systems access for local or regional land administration highly influences the way a state operates and the policies they develop. Recognizing land uses by land administration is a major funding source such as tax, stamp duty on property transfers, etc. (Virnodkar et al., 2021). Derived irrigated crop types maps can be utilized by regional land administration offices to monitor the spatial extent of crops

location and its monitoring as well as modeling and predicting crop yields and production by different models.

5.5.5 Limitations and Recommendations

Training and validation sampling points were taken based on the best knowledge of crop development phenology, cropping calendar, monthly NDVI profiles during the crop growth period, and historical google earth images. However, it is lacking the field observation data. In this research, we focused on creating a map of major crops such as cotton, wheat, rice, other crops, and fruits/trees, which are recorded by state statistics. The “Other crops” class consists of multiple minor crops, and we are motivated to continue our research to classify these classes by crop types in the future. Besides, we recommend creating detailed second crop maps, which is vital for public land management authority and local government to make decisions on a crop location that is suitable for soil quality and food security stability.

5.6 Conclusions

In this study, S2 and L8-based time series data in 2018 served as the input for mapping irrigated crop types using different vegetation indices such as NDVI, EVI, NDWI1, and NDWI2 by SVM and RF ML algorithms.

Regarding the comparability of medium (30 m) to high (10 m) resolution RS data, the results have demonstrated that both sensor products provide comparable outcomes concerning total area classified as well as accuracy assessment results. This is confirmed by the fact that the classification results demonstrating the highest OA results for SVM and RF, respectively, have been produced with different sensors. A closer analysis of OA, KA, UA, and PA, too, has demonstrated that RS imagery from both sensors is of comparable quality. Differences in accuracy results vary higher based on the vegetation indices used than on sensor data. KA values vary between 75% to 88% in all indices. The lowest KA values were achieved in all indices with the SVM

classifier of L8 sensor data. The highest KA values of 88% and 87% were achieved with the RF classifier of L8 data when EVI and EVI-NDVI were used, respectively.

We can also have a similar conclusion regarding the difference between RS-based-derived crop types area and OSS area. The lowest absolute WA using OSS area as weight, between areas classified per respective OSS category is 0.1 thousand ha for S2-RF-EVI classification and 0.2 thousand ha for L8-SVM-NDVI classification. Thus, classified maps can be used by global cropland mapping projects or any other ecological models that require specific crop types mapping. The recent successful launch of Landsat-9 will successfully continue the Landsat data suite and enable new opportunities in the joint use of Landsat and Sentinel data to capture high temporal resolution during the vegetation growth period.

The comparison of classified map areas for the main crops of cotton, wheat, and other crops demonstrated very reliable results when NDVI and EVI-NDVI were used with S2 sensor data. Therefore, S2 high resolution and temporal data can be utilized in the future to create LU maps to calculate crop water and irrigation requirements by using a variety of climate-hydrology models. Besides, created crop types map of agricultural areas can be used to inform decision-makers of local administration offices to develop policies to assure food security, valuable ecological resources, and services where digital data do not exist or missing.

The performance of both ML classifiers with S2 and L8 sensor data resulted in not being satisfactory for the rice crop due to the mixture of this class with second crops after winter wheat, which was due to a similar sowing time and growth period. Another limitation of this research relates to other crops classes, where other crop classes include a variety of crops; some of these crops might have similar growth periods and spectral properties to each other. This can influence on the OA of the classifiers, and we recommend further studying the separating of other crop types in the future.

6 General conclusions, limitations, and recommendations

6.1 Summary findings

The focus of this thesis is to map precise and accurate irrigated croplands extent product of Tashkent Province in Uzbekistan using different supervised classification methods in 2018. To achieve this goal, Sentinel - 2 and Landsat - 8 satellite data were utilized by well-known classifiers algorithms SVM, RF, and MLC. GIS and Remote sensing tools were used for the study analysis. The most important findings and main conclusions of the specific objectives are presented in this chapter:

- i. Reviewing scientific articles, local reports, and expert's opinions showed only a limited amount of research was published that mapped agricultural croplands by crop types using multi-temporal satellite data during the vegetation period, and also, compared and evaluated the performance of RF, SVM, and MLC with different indices using Sentinel-2 and Landsat-8 imagery, especially in Tashkent Province of Uzbekistan. Most of the carried-out research to study land use land cover, and land degradation used medium spatial resolution remotely sensed data such as NOAA/AVHRR, MODIS, and Landsat and which may pixels include a mixture of many land covers but they do not capture certain croplands by crop types. Last 35 years climate change data analysis showed an increasing trend of temperature and highly variable trends in precipitation and it is predicted to rise temperature by 1-2 degrees in the future. We expect an increase in precipitation and water resources for certain times of period due to climate change and the shrinking of Glaciers in the Tien Shan and Pamir mountains then a decrease in water resources in the region. That's why we intended to create a specific crop types map that can play an important role in land management policies under climate change scenarios.

- ii. Classification of main irrigated crop types was carried out using multi-temporal Sentinel-2 data in 2018. As input data, calculated monthly NDVI profiles together with bands 2 and 3 at 10 m resolution were selected. Three classifier algorithms SVM, RF, and MLC were used for the classification process. Among the tested methods the SVM and RF classifiers produced a visually pleasant and realistic irrigated cropland map in Tashkent Province. Performance test results showed that SVM showed the highest OA and KA. KA of classified images for SVM were 0.90 and 0.89 for the RF algorithm. Both performed well with close values. But MLC showed a lower result of KA 0.60. Based on the results, SVM and RF classifiers were recommended to test and compare different sensor types and indices for the appropriate crop types mapping in the research area.
- iii. Recommended classification algorithms SVM and RF were utilized to map irrigated croplands by using Sentinel - 2 and Landsat - 8 sensors data to compare the performance and recommend the suitable method for crop type classification. Four indices NDVI, EVI, NDWI1, and NDWI2 were calculated using blue, green, near-infrared, SWIR 1, and SWIR 2 bands and used as input data. All input data resampled at 10 m resolution and SVM and RF respectively have been produced irrigated crop types map with different sensors and indices. Detailed analysis of OA, KA, UA, and PA, too, has shown that RS imagery from both sensors is of comparable quality. Differences in accuracy results vary higher based on the vegetation indices used than on sensor data. KA values vary between 75% to 88 % in all indices. The lowest KA values were achieved in all indices with the SVM classifier of L8 sensor data. The highest KA values 88% and 87% were achieved with the RF classifier of L8 data when EVI and EVI-NDVI were used respectively. Using NDWI 1 and NDWI 2 which uses SWIR 1 and SWIR 2 bands is not achieved good results in both accuracies point and area comparison. And also, visually it was found that many misclassified water pixels throughout the study area. It is because all cropland in the study area is irrigated and irrigation water in the early crop development process can influence the classification of croplands as water surface by

water indices. Thus, we do not recommend using these indices for cropland classification using both sensor type and classifiers.

- iv. All derived crop types class areas were compared with official State Statistics data for validation. Firstly, SVM, RF, and MLC results showed that the state order crops “cotton”, “wheat” and the class “other crops” in SVM and RF methods were close to the official data. The area of class “rice” was higher than the official data in all classifiers. And the class “others crops” showed unreliable results in MLC due to its complexity and heterogeneity. Comparing the area of class “fruits/trees” is complicated because private households and landowners have fruits and trees on their property. And also, many cropland fields are surrounded by mulberry trees for sericulture which is not included in the official data. Secondly, using calculated NDVI, EVI, NDWI 1, and NDWI 2 values of Sentinel – 2 and Landsat – 8 sensors data showed that the arithmetic average difference values of main crops cotton, wheat, and other crops showed very reliable results when NDVI and EVI-NDVI used with Sentinel - 2 sensor data. Therefore, the same conclusion needs to be drawn. The lowest absolute weighted average using state statistics area as weight, between areas classified per respective state statistics category is 0.1 thousand ha for S2-RF-EVI classification and 0.2 thousand ha for L8-SVM-NDVI classification. Thus, classified maps using NDVI, EVI, and NDVI-EVI can be used by global cropland mapping projects or any other ecological models which require specific crop types mapping.
- v. Concerning the comparability of medium (30 m) to high (10 m) resolution RS data, results have shown that both sensor products provide comparable identical outcomes concerning total area classified as well as accurate results. This is confirmed by the fact that the classification results showing the highest OA results for SVM and RF respectively have been produced with different sensors. Thus, logically we can conclude that using medium-level (30 m) sensor data is sufficient and thus to be recommended since using lower resolution data reduces the amount of data as well as the requirement for processing resources. With Landsat data at 30 m resolution

being available since the launch of Landsat 4 & 5 in 1982, time series analysis based on the method suggested in this paper is possible for the period 1982 to today. For data collected by Landsat 1-3 since 1972 at 79 m x 79 m resolution additional analysis is required using historical land-use data to draw further conclusions. The recent successful launch of Landsat-9 will successfully continue the Landsat data suite and enable new opportunities in the joint use of Landsat and Sentinel data to capture high temporal resolution during the vegetation growth period.

6.2 Limitations

In this study, the application of GIS and Remote Sensing techniques has proven as an effective means for mapping irrigated croplands by crop types and produced some meaningful information about the spatial extent of the overall crop area in Tashkent Province of Uzbekistan. But it involves some inherent limitations due to resources and finance limits, such as:

- training and ground-truthing points were taken based on the best knowledge of crop development phenology, monthly NDVI profiles during the crop growth period, and historical google earth images. But it is lacking the field observation data. Provided data remotely were not reliable and useful for a research purpose;
- the crops growing together at the same time make the spectral separation difficult, which may influence the performance of classifiers. Therefore, more images by time duration can solve the problem via increasing temporal resolution. For example, combining both Sentinel and Landsat sensor images for this purpose as the results were identical;
- it was found that the performance of all classifiers for the rice crop is less reliable due to state statistics reports limitation. Rice crops planted after winter wheat as well as rice fields of seed farming should also include in statistical

data. Then we can have a proper area comparison results similar to state statistics for rice;

- another limitation of this research relates to the “other crops” class where other crops include a variety of crops. And some of these crops might have similar growth periods and spectral properties like main crops cotton and wheat. This can influence the overall accuracy of the classifiers and we recommend studying deeper and further investigation on separating other crop types individually;
- after winter wheat is harvested, usually the practice of a second crop is adopted to reduce the poverty. The crops harvested as a second crop are an additional outcome or subsidy for poor people or farm workers. And these crops are not recorded in the statistics or controlled and managed by the government. There, we think the second crop after winter wheat should be classified separately and investigated deeply to make a clear vision of the extent of the second crop for sustainable crop management policies.

6.3 Recommendations

Irrigated croplands classification using GIS and Remote sensing techniques together with Sentinel and Landsat data were found to be very effective in the semi-arid area of the Tashkent Province in Uzbekistan. Among tested four indices NDVI and EVI or using both together proposed to be very useful to derive irrigated crop types map in the region. SVM and RF classification algorithms were the best-suited classifiers for mapping heterogeneous irrigated crop types and they can be used alternatively where digital cadaster LU maps do not exist for agro-environmental assessment studies in the region. Besides, derived irrigated crop types maps can be utilized by regional land administration offices to monitor the spatial extent of crop distribution, location, and its monitoring as well as modeling and predicting crop yields and production by different models.

In this study, we focused to create a map of major crops such as cotton, wheat, rice, other crops, and fruits/trees which are recorded by state statistics. “Other crops” class consists of multiple minor crops and we are motivated to continue our research to classify these classes by crop types in the future. Besides, we recommend creating detailed second crop maps which is vital for public management authority and local government to make decisions to plant proper crops which is suitable for the soil quality.

Since the performance and area comparison analysis of Sentinel 2 and Landsat 8 achieved comparable close results, we recommend using them combined to increase seasonal temporal resolution which will help to distinguish the crops' spectral properties and to increase the accuracy of classification. It will also increase the chance of getting cloud-free images during the vegetation growth period.

References

- Ahmad I., Singh A., Fahad M. & Waqas M.M. (2020) Remote sensing-based framework to predict and assess the interannual variability of maize yields in Pakistan using Landsat imagery. *Computers and Electronics in Agriculture*, 178, 105732. DOI: 10.1016/j.compag.2020.105732.
- Ahmed Ibrahim Ramzi, V., 2015, Ground Truth and Mapping Capability of Urban Areas in Large Scale Using GE images. *Proc. Earth Resources and Environmental Remote Sensing/GIS Applications VI*, Vol. 9644, <https://doi.org/10.1117/12.2193727>.
- Alfredo Huete, Chris Justice & Wim van Leeuwen (1999) MODIS vegetation index (MOD13). Algorithm theoretical basis document., 3, 295–309.
- Alikhanov, B., Alikhanova, Sh., Oymatov, R., Fayzullaev, Z. and Pulatov, A, 2020, Land Cover Change in Tashkent Province During 1992 – 2018. *IOP Conf. Ser.: Mater. Sci. Eng.*, Vol. 883, DOI: 10.1088/1757-899X/883/1/012088.
- Asam S., Gessner U., Almengor González R., Wenzl M., Kriese J. & Kuenzer C. (2022) Mapping Crop Types of Germany by Combining Temporal Statistical Metrics of Sentinel-1 and Sentinel-2 Time Series with LPIS Data. *Remote Sensing*, 14, 2981. DOI: 10.3390/rs14132981.
- Azeez N., Yahya W., Al-Taie I., Basbrain A. & Clark A. (2020) Regional Agricultural Land Classification Based on Random Forest (RF), Decision Tree, and SVMs Techniques. In: *Fourth International Congress on Information and Communication Technology: ICICT 2019*, London. Volume 1 / Xin-She Yang, Simon Sherratt, Nilanjan Dey, Amit Joshi, editors (ed. by X.-S. Yang, S. Sherratt, N. Dey & A. Joshi), pp. 73–81. Springer, Springer.
- Baghdadi, N. and Zribi, M., 2016, *Optical Remote Sensing of Land Surfaces. Techniques and Methods (Eds.)*. London, Oxford: ISTE Press Ltd.; Elsevier Ltd (Remote sensing observations of continental surfaces set).
- Basukala A.K., Oldenburg C., Schellberg J., Sultanov M. & Dubovyk O. (2017) Towards improved land use mapping of irrigated croplands: performance

- assessment of different image classification algorithms and approaches. *European Journal of Remote Sensing*, 50, 187–201. DOI: 10.1080/22797254.2017.1308235.
- Bobojonov, I. and Aw-Hassan, A., 2014, Impacts of Climate Change on Farm Income Security in CA: An Integrated Modeling Approach. *Agriculture, Ecosystems and Environment*, 188, 245-255.
- Bofana J., Zhang M., Nabil M., Wu B., Tian F., Liu W., Zeng H., Zhang N., Nangombe S.S., Cipriano S.A., Phiri E., Mushore T.D., Kaluba P., Mashonjowa E. & Moyo C. (2020) Comparison of Different Cropland Classification Methods under Diversified Agroecological Conditions in the Zambezi River Basin. *Remote Sensing*, 12, 2096. DOI: 10.3390/rs12132096.
- Breiman, L., 2001, Random Forests. *Machine Learning*, Vol. 45(1), 5–32. DOI: 10.1023/A:-1010933404324.
- Burai, P., Deák, B., Valkó, O. and Tomor, T., 2015, Classification of Herbaceous Vegetation Using Airborne Hyperspectral Imagery. *Remote Sensing*, Vol. 7(2), 2046–2066. DOI: 10.3390/rs70202046.
- Burges C.J.C. (1998). *Data Mining and Knowledge Discovery*, 2, 121–167. DOI: 10.1023/A:1009715923555.
- Cavender-Bares J., Gamon J.A. & Townsend P.A. The Use of Remote Sensing to Enhance Biodiversity Monitoring and Detection: A Critical Challenge for the Twenty-First Century, 1–12. DOI: 10.1007/978-3-030-33157-3_1.
- Chen X., Wang W., Chen J., Zhu X., Shen M., Gan L. & Cao X. (2020) Does any phenological event defined by remote sensing deserve particular attention? An examination of spring phenology of winter wheat in Northern China. *Ecological Indicators*, 116, 106456. DOI: 10.1016/j.ecolind.2020.106456.
- Chen, X., Bai, J., Li, X., Luo, G., Li, J. and Li, B. L., 2013, Changes in Land Use/Land Cover and Ecosystem Services in Central Asia during 1990–2009. *Current Opinion in Environmental Sustainability*, Vol. 5(1), 16–127. DOI: 10.1016/j.cosust.2012.12.005.

- Chuvieco E. (2020) Fundamentals of satellite remote sensing: An environmental approach / Emilio Chuvieco. CRC Press, Boca Raton.
- CIA. (2021). *Uzbekistan*. Central Intelligence Agency. Retrieved 14.11.2021 from <https://www.cia.gov/the-world-factbook/countries/uzbekistan/>
- Clemente J.P., Fontanelli G., Ovando G.G., Roa Y.L.B., Lapini A. & Santi E. (2020) GOOGLE EARTH ENGINE: APPLICATION OF ALGORITHMS FOR REMOTE SENSING OF CROPS IN TUSCANY (ITALY). The International Archives of the Photogrammetry, Remote Sensing and Spatial Information Sciences, XLII-3/W12-2020, 291–296. DOI: 10.5194/isprs-archives-XLII-3-W12-2020-291-2020.
- Climate Adaptation Platform (2021): Climate adaptation and mitigation plan for climate change in Uzbekistan. Available online at <https://www.preventionweb.net/news/climate-adaptation-and-mitigation-plan-climate-change-uzbekistan#:~:text=Climate%20change%20has%20reduced%20the,drop%20of%2011%20per%20cent.,updated%20on%208/21/2021,checked%20on%205/1/2022.>
- Congalton R.G. (1991) A review of assessing the accuracy of classifications of remotely sensed data. *Remote Sensing of Environment*, 37, 35–46. DOI: 10.1016/0034-4257(91)90048-B.
- Congedo, L., 2021, Semi-Automatic Classification Plugin: A Python Tool for the Download and Processing of Remote Sensing Images in QGIS. *JOSS*, Vol. 6(64), DOI: 10.21105/joss.03172.
- Conrad, Ch., Dech, S., Dubovyk, O., Fritsch, S., Klein, D., Löw, F., Schorcht, G. and Zeidler, J., 2014, Derivation of Temporal Windows for Accurate Crop Discrimination in Heterogeneous Croplands of Uzbekistan Using Multitemporal RapidEye Images. *Computers and Electronics in Agriculture*, Vol. 103, 63–74. DOI: 10.1016/j.-compag.2014.02.003.
- Deilmai, B. R., Ahmad, B. B. and Zabihi, H., 2014, Comparison of Two Classification Methods (MLC and SVM) to Extract Land Use and Land Cover in Johor Malaysia.

IOP Conf. Ser.: Earth Environ. Sci., Vol. 20, DOI: 10.1088/1755-1315/20/1/012052.

dela Torre D.M.G., Gao J. & Macinnis-Ng C. (2021) Remote sensing-based estimation of rice yields using various models: A critical review. *Geo-spatial Information Science*, 24, 580–603. DOI: 10.1080/10095020.2021.1936656.

Demarez V., Helen F., Marais-Sicre C. & Baup F. (2019) In-Season Mapping of Irrigated Crops Using Landsat 8 and Sentinel-1 Time Series. *Remote Sensing*, 11, 118. DOI: 10.3390/rs11020118.

Denisko D. & Hoffman M.M. (2018) Classification and interaction in random forests. *Proceedings of the National Academy of Sciences of the United States of America*, 115, 1690–1692. DOI: 10.1073/pnas.1800256115.

Dile, Y. T. and Srinivasan, R., 2014, Evaluation of CFSR Climate Data for Hydrologic Prediction in Data-Scarce Watersheds: An Application in the Blue Nile River Basin. *Journal of American Water Resources Association*, 50(5), 1226-1241.

Djanibekov, Nodir (2019): Farm Restructuring in Uzbekistan: How Did It Go and What is Next? World Bank.

Djumaboev, K.; Hamidov, A.; Anarbekov, O.; Gafurov, Z. 2017. Collective action in the irrigation sector of Uzbekistan: a case study of water consumers' associations (WCAs) in the Karshi Steppe. Colombo, Sri Lanka: International Water Management Institute (IWMI). 39p. doi: 10.5337/2018.200.

Drusch, M., Del Bello, U., Carlier, S., Colin, O., Fernandez, V., Gascon, F., Hoersch, B., Isola, C., Laberinti, P., Martimort, P., Meygret, A., Spoto, F., Sy, O., Marchese, F. and Bargellini, P., 2012, Sentinel-2: ESA's Optical High-Resolution Mission for GMES Operational Services. *Remote Sensing of Environment*, Vol. 120, 25–36, DOI: 10.1016/j.rse.2011.11.026.

Dubovyk, O., Gunter M., Conrad, C. and Khamzina, A., 2012, Object-Based Cropland Degradation Identification: A Case Study in Uzbekistan. *In the Proceedings SPIE Remote Sensing*, Edinburgh, United Kingdom.

- Dubovyk, O., Menz, G., Conrad, C., Kan, E., Machwitz, M. and Khamzina, A., 2013, Spatio-Temporal Analyses of Cropland Degradation in the Irrigated Lowlands of Uzbekistan using Remote-Sensing and Logistic Regression Modeling. *Environmental Monitoring and Assessment*, 185(6), 4775-4790.
- Economy Uzbekistan, 2021, Uzbekistan Eyes to Double Rice Production this Year. Available online at <https://www.thetribune.com/uzbeki-stan-eyes-to-double-rice-production-this-year/>.
- Edlinger, J., Conrad, C., Lamers, J., Khasankhanova, G. and Koellner, T., 2012, Reconstructing the Spatio-Temporal Development of Irrigation Systems in Uzbekistan Using Landsat Time Series. *Remote Sensing*, Vol. 4(12), 3972–3994. DOI: 10.3390/rs4123972.
- Eisfelder, C., Klein, I., Niklaus, M. and Kuenzer, C., 2014, Net Primary Productivity in Kazakhstan, its Spatio-Temporal Patterns and Relation To Meteorological Variables. *Journal of Arid Environments*, 103, 17-30.
- Erdanaev, E., Kappas, M. and Wyss, D. (2022) The Identification of Irrigated Crop Types Using Support Vector Machine, Random Forest and Maximum Likelihood Classification Methods with Sentinel-2 Data in 2018: Tashkent Province, Uzbekistan. *International Journal of Geoinformatics*, 18, 37–53. DOI: 10.52939/ijg.v18i2.2151.
- Erdanaev, E., Kappas, M., Pulatov, A. and Klinge, M., 2015, Short Review of Climate and Land Use change Impact on Land Degradation in Tashkent Province. *International Journal of Geoinformatics*, Vol. 11(4), 39-48.
- ESA. (2021). *Sentinel 2 Product Specification Document*. European Space Agency. <https://sentinel.esa.int/documents/247904/685211/Sentinel-2-Products-Specification-Document>
- FAO. (2019). *World Food Situation*. Food and Agriculture Organization of the United Nations. <http://www.fao.org/worldfoodsituation/csdb/en/>

- FAOSTAT (2020a): Cotton production by country. Available online at <https://worldpopulationreview.com/country-rankings/cotton-production-by-country>, updated on 2020, checked on 6/9/2022.
- FAOSTAT (2020b): Wheat production by country. Available online at <https://worldpopulationreview.com/country-rankings/wheat-production-by-country>, updated on 2020, checked on 5/5/2022.
- Feng M. & Li X. (2020) Land cover mapping toward finer scales. *Science Bulletin*, 65, 1604–1606. DOI: 10.1016/j.scib.2020.06.014.
- Feng, Z. D., 2013, Hydrological and Ecological Responses to Climatic Change and to Land-Use/Land-Cover changes in CA. *Quaternary International*, 311, 1-2.
- Fuka, D. R., Walter, M. T., MacAlister, C., Degaetano, A. T., Steenhuis, T. S. and Easton, Z. M., 2014, Using the Climate Forecast System Reanalysis as Weather Input Data for Watershed Models. *Hydrological Processes*, 28(22), 5613-5623.
- Gafforov, Khusein Sh.; Bao, Anming; Rakhimov, Shavkat; Liu, Tie; Abdullaev, Farkhod; Jiang, Liangliang et al.: The Assessment of Climate Change on Rainfall-Runoff Erosivity in the Chirchik–Akhangaran Basin, Uzbekistan.
- Gao B.-c. (1996) NDWI—A normalized difference water index for remote sensing of vegetation liquid water from space. *Remote Sensing of Environment*, 58, 257–266. DOI: 10.1016/S0034-4257(96)00067-3.
- Gao, B.-C. (1995). Normalized difference water index for remote sensing of vegetation liquid water from space. *Imaging Spectrometry*,
- García-Berná J.A., Ouhbi S., Benmouna B., García-Mateos G., Fernández-Alemán J.L. & Molina-Martínez J.M. (2020) Systematic Mapping Study on Remote Sensing in Agriculture. *Applied Sciences*, 10, 3456. DOI: 10.3390/app10103456.
- García-Montero L.G., Pascual C., Martín-Fernández S., Sanchez-Paus Díaz A., Patriarca C., Martín-Ortega P. & Mollicone D. (2021) Medium- (MR) and Very-High-Resolution (VHR) Image Integration through Collect Earth for Monitoring Forests and Land-Use Changes: Global Forest Survey (GFS) in the Temperate FAO

- Ecozone in Europe (2000–2015). *Remote Sensing*, 13, 4344. DOI: 10.3390/rs13214344.
- Gary M. Senseman, Calvin F. Bagley, Scott Tweddale (1995): Accuracy Assessment of the Discrete Classification of Remotely-Sensed Digital Data for Landcover Mapping.
- Gerts J., Juliev M. & Pulatov A. (2020) Multi-temporal monitoring of cotton growth through the vegetation profile classification for Tashkent province, Uzbekistan. *GeoScape*, 14, 62–69. DOI: 10.2478/geosc-2020-0006.
- Gumma, M. K., Thenkabail, P. S., Teluguntla, P. G., Oliphant, A., Xiong, J., Giri, C., Pyla, V., Dixit, V. and Whitbread, A. M., 2020, Agricultural Cropland Extent and Areas of South Asia Derived Using Landsat Satellite 30-m Time-Series Big-Data Using Random Forest Machine Learning Algorithms on the Google Earth Engine cloud, *GIScience and Remote Sensing*, Vol. 57(3), 302-322, DOI: [10.1080/154816-03.2019.1690780](https://doi.org/10.1080/154816-03.2019.1690780).
- Habibie M.I., Noguchi R., Shusuke M. & Ahamed T. (2021) Land suitability analysis for maize production in Indonesia using satellite remote sensing and GIS-based multicriteria decision support system. *GeoJournal*, 86, 777–807. DOI: 10.1007/s10708-019-10091-5.
- HAO P.-y., TANG H.-j., CHEN Z.-x., MENG Q.-y. & KANG Y.-p. (2020) Early-season crop type mapping using 30-m reference time series. *Journal of Integrative Agriculture*, 19, 1897–1911. DOI: 10.1016/S2095-3119(19)62812-1.
- Hasanov D. N., (2005). Development of Hydrogeology and engineering geology in Uzbekistan, *Gidroingeo*, Tashkent, Uzbekistan.
- Huete, A., Justice, C., & Van Leeuwen, W. (1999). MODIS vegetation index (MOD13). *Algorithm theoretical basis document*, 3(213), 295-309.
- Ibragimov, N., Evett, S. R., Esanbekov, Y., Kamilov, B. S., Mirzaev, L. and Lamers, J. P. A., 2007, Water use Efficiency of Irrigated Cotton in Uzbekistan under Drip and Furrow Irrigation. *Agricultural Water Management*, 90(1-2), 112-120.

- Jawak, S. D., Devliyal, P. and Luis, A. J., 2015, A Comprehensive Review on Pixel Oriented and Object Oriented Methods for Information Extraction from Remotely Sensed Satellite Images with a Special Emphasis on Cryospheric Applications. *Advances in Remote Sensing*, Vol. 4(3), 177-195. DOI: 10.4236/ars.2015.43015.
- Jean-Marc Faurès, Jippe Hoogeveen and Jelle Bruinsma: THE FAO IRRIGATED AREA FORECAST FOR 2030. Available online at <http://www.fao.org/ag/agl/aglw/aquastat/main/index.htm>.
- Jia, Yuanxin; Ge, Yong; Ling, Feng; Guo, Xian; Wang, Jianghao; Le Wang; Chen, Yuehong; Li, Xiaodong, 2018, Urban Land Use Mapping by Combining Remote Sensing Imagery and Mobile Phone Positioning Data. *Remote Sensing*, Vol. 10(3), DOI: 10.3390/rs10030446.
- John, A. and Richards, X., J., 2006, *Image Classification Methodologies. Remote Sensing Digital Image Analysis*. Berlin/Heidelberg: Springer-Verlag, 295–332.
- Juliev, M., Pulatov, A., Fuchs, S. and Hübl, J., 2019, Analysis of Land Use Land Cover Change Detection of Bostanlik District, Uzbekistan. *Pol. J. Environ. Stud.*, Vol. 28(5), 3235–3242. DOI: 10.15244/pjoes/94216.
- Kaplan, Sh., Blumberg, D. G., Mamedov, E. and Orlovsky, L., 2014, Land-use change and Land Degradation in Turkmenistan in the Post-Soviet era. *Journal of Arid Environments*, 103, 96-106.
- Karnieli, A., Gilad, U., Ponzet, M., Svoray, T., Mirzadinov, R. and Fedorina, O., 2008, Assessing Land-Cover change and Degradation in the CAn Deserts using Satellite Image Processing and Geostatistical Methods. *Journal of Arid Environments*, 72(11), 2093-2105.
- Karthikeyan L., Chawla I. & Mishra A.K. (2020) A review of remote sensing applications in agriculture for food security: Crop growth and yield, irrigation, and crop losses. *Journal of Hydrology*, 586, 124905. DOI: 10.1016/j.jhydrol.2020.124905.
- Kertész, A., 2009, The Global Problem of Land Degradation and Desertification. *Hungarian Geographical Bulletin*, 58(1), 19-31. Klein, I., Gessner, U. and Kuenzer,

- C., 2012, Regional Land Cover Mapping and change Detection in CA using MODIS Time-Series. *Applied Geography*, 35(1-2), 219-234.
- Kessler, C. A., & Stroosnijder, L., 2006, Land degradation assessment by farmers in Bolivian mountain valleys. *Land Degradation & Development*, 17(3), 235–248. Cited in Dubovyk, O., Menz, G., Conrad, C., Kan, E., Machwitz, M. and Khamzina, A., 2013, Spatio-Temporal Analyses of Cropland Degradation in the Irrigated Lowlands of Uzbekistan using Remote-Sensing and Logistic Regression Modeling. *Environmental Monitoring and Assessment*, 185(6), 4775-4790.
- Khiry, M. A., 2007, Spectral Mixture Analysis for Monitoring and Mapping Desertification Processes in Semi-arid Areas in North Kordofan State, Sudan. PhD Thesis, *Institute of Photogrammetry and Remote Sensing*, Technische Universität Dresden, Dresden, Germany.
- Khurshidbek Makhmudov (2015): DEVELOPMENT OF THE CALCULATION METHODS OF HYDROLOGICAL PARAMETERS FOR THE SUSTAINABLE WATER MANAGEMENT IN ARID RIVER BASIN. Ph.D. Kyushi University, Japan, checked on 1/14/2016.
- Kobayashi N., Tani H., Wang X. & Sonobe R. (2020) Crop classification using spectral indices derived from Sentinel-2A imagery. *Journal of Information and Telecommunication*, 4, 67–90. DOI: 10.1080/24751839.2019.1694765.
- Kuziev, K. F.: Regional distinctions of agricultural development in Uzbekistan under limited water resources.
- Lambin E.F. & Geist H., editors (2006) *Land-use and land-cover change: Local processes and global impacts* / Eric F. Lambin, Helmut Geist (eds.). Springer, Berlin, INew York.
- Landis, J. Richard; Koch, Gary G. (1977): The Measurement of Observer Agreement for Categorical Data. In *Biometrics* 33 (1), p. 159. DOI: 10.2307/2529310.
- Li, Z., Fang, G., Chen, Y., Duan, W. and Mukanov, Y., 2020, Agricultural Water Demands in Central Asia under 1.5 °C and 2.0 °C Global Warming. *Agricultural Water Management*, Vol. 231, DOI: 10.1016/j.agwat.2020.106020.

- Lioubimtseva, E. and Henebry, G. M., 2009, Climate and Environmental change in Arid CA: Impacts, Vulnerability and Adaptations. *Journal of Arid Environments*, 73(11), 963-977.
- Lioubimtseva, E., Cole, R., Adams, J. M. and Kapustin, G., 2005, Impacts of Climate and Land-Cover changes in Arid Lands of CA. *Journal of Arid Environments*, 62(2), 285-308.
- Liu, M. Y., 2011, Central Asia in the Post–Cold War World. *Annu. Rev. Anthropol.*, Vol. 40(1), 115–131. DOI: 10.1146/annurev-anthro-081309-145906.
- Liu, Shuang; Luo, Geping; Wang, Hao (2020): Temporal and Spatial Changes in Crop Water Use Efficiency in Central Asia from 1960 to 2016. In *Sustainability* 12 (2), p. 572. DOI: 10.3390/su12020572.
- Lu, D., Batistella, M., Mausel, P., & Moran, E., 2007, Mapping and monitoring land degradation risks in the Western Brazilian Amazon using multitemporal Landsat TM/ETM+ images. *Land Degradation & Development*, 18(1), 41–54. Cited in Dubovyk, O., Menz, G., Conrad, C., Kan, E., Machwitz, M. and Khamzina, A., 2013, Spatio-Temporal Analyses of Cropland Degradation in the Irrigated Lowlands of Uzbekistan using Remote-Sensing and Logistic Regression Modeling. *Environmental Monitoring and Assessment*, 185(6), 4775-4790.
- M. S. Boori, R. Paringer, K. Choudhary, A. Kupriyanov, R. Banda (Ed.) (2018): Land cover classification and build spectral library from hyperspectral and multi-spectral satellite data: A data comparison study in Samara, Russia. IV International Conference on "Information Technology and Nanotechnology": Image Processing and Earth Remote Sensing (2210).
- Makhmudova, Dildora; Makhmudov, Hurshid (2021): Analysis and assessment method of the Chirchik river flow for water supply and water use. In *E3S Web Conf.* 264, p. 1045. DOI: 10.1051/e3sconf/202126401045.
- Malik, Tassawar Hussain; Ahsan, Muhammad Zahir (2016): Review of the cotton market in Pakistan and its future prospects. In *OCL* 23 (6), D606. DOI: 10.1051/ocl/2016043.

- Mantero, P., Moser, G., & Serpico, S. B. (2005). Partially supervised classification of remote sensing images through SVM-based probability density estimation. *IEEE Transactions on Geoscience and Remote Sensing*, 43(3), 559-570.
- McKinney, Daene C., 2004, Cooperative management of transboundary water resources in Central Asia. In: Daniel Burghart & Theresa Sabonis-Helf (eds) *In the Tracks of Tamerlane: Central Asia's Path to the 21st Century*. Washington, DC: National Defense University, 187–220.
- NASA, 2014, NASA LCLUC Science Team Meeting on Land Use and Water Resources in CA. *The Earth Observer*, 26(2), 14-19.
- Nations Online Project. <https://www.nationsonline.org/oneworld/map/uzbekistan-administrative-map.htm>. Accessed 04.05. 2022.
- Nitze, I., Schulthess, U., & Asche, H. (2012) COMPARISON OF MACHINE LEARNING ALGORITHMS RANDOM FOREST, ARTIFICIAL NEURAL NETWORK AND SUPPORT VECTOR MACHINE TO MAXIMUM LIKELIHOOD FOR SUPERVISED CROP TYPE CLASSIFICATION, 35–40.
- Nordblom, T., Shomo, F. and Gintzburger, G., 1997, Food and Feed Prospects for Resources in CA. In Demmet, M. (ed.), *CA Regional Livestock Assessment Workshop*, Tashkent, Uzbekistan, Management Entity, Small Ruminant CRSP, University of California, USA, 226.
- Oliphant A.J., Thenkabail P.S., Teluguntla P., Xiong J., Gumma M.K., Congalton R.G. & Yadav K. (2019) Mapping cropland extent of Southeast and Northeast Asia using multi-year time-series Landsat 30-m data using a random forest classifier on the Google Earth Engine Cloud. *International Journal of Applied Earth Observation and Geoinformation*, 81, 110–124. DOI: 10.1016/j.jag.2018.11.014.
- Pal, M. (2007). Random forest classifier for remote sensing classification. *International Journal of Remote Sensing*, 26(1), 217-222. <https://doi.org/10.1080/01431160412331269698>

- Pal, M., 2005, Random Forest Classifier for Remote Sensing Classification. *International Journal of Remote Sensing*, Vol. 26(1), 217–222. DOI: 10.1080/01431160412331269698.
- Palchowdhuri Y., Valcarce-Diñeiro R., King P. & Sanabria-Soto M. (2018) Classification of multi-temporal spectral indices for crop type mapping: a case study in Coalville, UK. *The Journal of Agricultural Science*, 156, 24–36. DOI: 10.1017/S0021859617000879.
- Pan L., Xia H., Zhao X., Guo Y. & Qin Y. (2021) Mapping Winter Crops Using a Phenology Algorithm, Time-Series Sentinel-2 and Landsat-7/8 Images, and Google Earth Engine. *Remote Sensing*, 13, 2510. DOI: 10.3390/rs13132510.
- Perelet R., 2007, Fighting climate change: human solidarity in a divided world (Human Development Report). UNDP, New York. Cited in Dubovyk, O., Menz, G., Conrad, C., Kan, E., Machwitz, M. and Khamzina, A., 2013, Spatio-Temporal Analyses of Cropland Degradation in the Irrigated Lowlands of Uzbekistan using Remote-Sensing and Logistic Regression Modeling. *Environmental Monitoring and Assessment*, 185(6), 4775-4790.
- Peters, R.L., Lovejoy, T.L. (Eds.), 1992. *Global Warming and Biological Diversity*. Yale University Press, London. Cited in Sivakumar, M. V. K., 2007, Interactions between climate and desertification. *The Contribution of Agriculture to the State of Climate*, 142(2–4), 143-155.
- Platonov, A., Wegerich, K., Kazbekov, J. and Kabilov, F., 2014, Beyond the State Order? Second Crop Production in the Ferghana Valley, Uzbekistan. *International Journal of Water Governance*, Vol. 2(2), 83–104. DOI: 10.7564/14-IJWG58.
- Polat Z.A. (2019) Evolution and future trends in global research on cadastre: a bibliometric analysis. *GeoJournal*, 84, 1121–1134. DOI: 10.1007/s10708-019-09973-5.
- Population Density Map 2020. Retrieved August 19, 2020, from https://popdensitymap.ucoz.ru/news/167_population_density_administrative_bou ndaries_map_of_uzbekistan/2020-08-19-195

- Propastin, P. A., 2008, Inter-Annual Changes in Vegetation Activities and Their Relationship to Temperature and Precipitation in CA from 1982 to 2003. *Journal of Environmental Informatics*, 12(2), 75-87.
- Propastin, P., Kappas, M. and Muratova, N. R., 2008, A Remote Sensing Based Monitoring System for Discrimination between Climate and Human-Induced Vegetation change in CA. *Management of Environmental Quality*, 19(5), 579-596.
- Pulatov, B., Umarova, Sh. and Alikhanov, B., 2020, Assessment of Land Degradation Changes in Mountain Areas in Tashkent Province. *IOP Conf. Ser.: Mater. Sci. Eng.*, Vol. 883, DOI: 10.1088/1757-899X/883/1/012087.
- Quynh Trang, N. Thi., Le Toan, Q., Huyen Ai, T. Thi., Vu Giang, N. and Viet Hoa, P., 2016, Object-Based vs. Pixel-Based Classification of Mangrove Forest Mapping in Vien An Dong Commune, Ngoc Hien District, Ca Mau Province Using VNREDSat-1 Images. *Advances in Remote Sensing*, Vol. 5, 284-295 DOI: 10.4236/ars.2016.54022.
- Roll, G., Alexeeva, N., Aladin, N., Plotnikov, I., Sokolov, V., Sarsembekov, T., Micklin, P., 2005, Aral Sea: Experience and Lessons Learned Brief. Report Lake Basin Management Initiative, Shiga, Japan, International Lake Environment Committee, 1–14.
- Rouse, J. W., Haas, R. H., Schell, J. A., & Deering, D. W. (1974). Monitoring vegetation systems in the Great Plains with ERTS. *NASA special publication*, 351(1974), 309.
- Rouse, J.W., Haas, R.H., Schell, J.A. and Deering, D.W., editor (1974) *Monitoring Vegetation Systems in the Great Plains with ERTS*.
- Saah, D., Tenneson, K., Matin, M., Uddin, K., Cutter, P., Poortinga, A., Nguyen, Q. H., Patterson, M., Johnson, G., Markert, K., Flores, A., Anderson, E., Weigel, A., Ellenberg, W. L., Bhargava, R., Aekakkararungroj, A., Bhandari, B., Khanal, N., Housman, I. W., Potapov, P., Tyukavina, A., Maus, P., Ganz, D., Clinton, N. and Chishtie, F., 2019, Land Cover Mapping in Data Scarce Environments: Challenges and Opportunities. *Front. Environ. Sci.*, Vol. 7, doi: 10.3389/fenvs.2019.00150.

- Saini R. & Ghosh S.K. (2018) CROP CLASSIFICATION ON SINGLE DATE SENTINEL-2 IMAGERY USING RANDOM FOREST AND SUPPORT VECTOR MACHINE. The International Archives of the Photogrammetry, Remote Sensing and Spatial Information Sciences, XLII-5, 683–688. DOI: 10.5194/isprs-archives-XLII-5-683-2018.
- Schmidt-Traub G. (2021) National climate and biodiversity strategies are hamstrung by a lack of maps. *Nature ecology & evolution*, 5, 1325–1327. DOI: 10.1038/s41559-021-01533-w.
- Schmidt-Traub, G. (2021). National climate and biodiversity strategies are hamstrung by a lack of maps. *Nature Ecology & Evolution*, 5(10), 1325-1327.
- Shavkat Mirziyoyev, 2020, Digital Technologies will Be Introduced in the Sphere of Cadastre. Available online at <https://president.uz/uz/lists/view/3717>.
- Shavkat Mirziyoyev, 2021, These Numbers are noting Any Statistics. I declare to answer before my conscience - President Spoke about the Situation with Serious Diseases in Karakalpakstan. Tashkent. Available online at <https://kun.uz/news/2021/09/21/bu-raqamlar-hech-qaysi-statistikada-yoq-vijdonim-oldida-javob-berish-uchun>.
- Shokparova, D. K., Issanova G. T., 2013, Degradation of Sierozem Soils in the Ile Alatau Foothills. *World Applied Sciences Journal* 26 (7), 979-986.
- Sivakumar, M. V. K., 2007, Interactions between climate and desertification. *The Contribution of Agriculture to the State of Climate*, 142(2–4), 143-155.
- Sommer, R., Glazirina, M., Yuldashev, T., Otarov, A., Ibraeva, M., Martynova, L., 2013, Impact of climate change on wheat productivity in CA. *Agriculture, Ecosystems & Environment*, 178, 78-99.
- Song X.-P., Huang W., Hansen M.C. & Potapov P. (2021) An evaluation of Landsat, Sentinel-2, Sentinel-1 and MODIS data for crop type mapping. *Science of Remote Sensing*, 3, 100018. DOI: 10.1016/j.srs.2021.100018.
- Sonobe R., Yamaya Y., Tani H., Wang X., Kobayashi N. & Mochizuki K.-i. (2018) Crop classification from Sentinel-2-derived vegetation indices using ensemble

- learning. *Journal of Applied Remote Sensing*, 12, 1. DOI: 10.1117/1.JRS.12.026019.
- Sonobe, R., Yamaya, Y., Tani, H., Wang, X., Kobayashi, N. and Mochizuki, K., 2018, Crop Classification from Sentinel-2-derived Vegetation Indices Using Ensemble Learning. *J. Appl. Rem. Sens.*, Vol. 12 (02), DOI: 10.1117/1-.JRS.12.026019.
- State Committee for Statistics, 2018, *Statistical Review - Agriculture of Uzbekistan between 2014-2018*. The State Committee for Statistics of the Republic of Uzbekistan, Tashkent.
- Stephan von Cramon-Taubadel, Shavkat Hasanov (2021): Agricultural Policy in Uzbekistan Challenges and Priorities. Berlin. Available online at https://berlin-economics.com/wp-content/uploads/2021/06/GET_UZB_PB_06_2021_en.pdf, checked on 5/25/2022.
- Stephenson P.J. (2020) Technological advances in biodiversity monitoring: applicability, opportunities and challenges. *Current Opinion in Environmental Sustainability*, 45, 36–41. DOI: 10.1016/j.cosust.2020.08.005.
- Suranjana Saha, Shrinivas Moorthi, Xingren Wu, Jiande Wang, Sudhir Nadiga, Patrick Tripp, David Behringer, Yu-Tai Hou, Hui-ya Chuang, Mark Iredell, Michael Ek, Jesse Meng, Rongqian Yang, Malaquías Peña Mendez, Huug van den Dool, Qin Zhang, Wanqiu Wang, Mingyue Chen, and Emily Becker, 2014, The NCEP Climate Forecast System Version 2. *Journal of Climate*, 27, 2185–2208.
- Tachikawa T., Hato M., Kaku M., Iwasaki A., 2011, The characteristics of ASTER GDEM version 2. *IEEE Geoscience and Remote Sensing Symposium*, 3657 – 3660.
- Thanh Noi, P., Kappas, M. (2018). Comparison of Random Forest, k-Nearest Neighbor, and Support Vector Machine Classifiers for Land Cover Classification Using Sentinel-2 Imagery. *Sensors* 2018 (1), 18, 18; doi:10.3390/s18010018
- The Central Asian Countries Initiative for Land Management (CACILM), 2006, Country Pilot Partnerships on Sustainable Land Management. CACILM Multicountry Partnership Framework. Executive Summary. Rajabov, T., Thorsson J., 2009, Ecological assessment of spatio-temporal changes of vegetation in

response to biosphere effects in semi-arid rangelands of Uzbekistan. Report: Land Restoration Training Programme, Reykjavík, Iceland.

The State Committee of the Republic of Uzbekistan on Land Resources, Geodesy, Cartography and State Cadaster (Goskomzemgeodezkadastr), 2008, National Report on State of Land Resources of the Republic of Uzbekistan. Language in Russian. Tashkent, Uzbekistan.

The State Committee of the Republic of Uzbekistan on Land Resources, Geodesy, Cartography and State Cadaster (Goskomzemgeodezkadastr), 2010, National Report on the State of Land Resources of the Republic of Uzbekistan. Language in Russian. Tashkent, Uzbekistan.

The State Committee of the Republic of Uzbekistan on Statistics. (2014). Agriculture of Uzbekistan. Tashkent, Uzbekistan.

The State of the World's Land and Water Resources for Food and Agriculture – Systems at breaking point (SOLAW 2021) (2021): FAO.

UNCCD, 1994, Elaboration of an International Convention to Combat Desertification in Countries Experiencing Serious Drought and/or Desertification, Particularly in Africa. UN, Bonn.

Unger-Shayesteh, K., Vorogushyn, S., Farinotti, D., Gafurov, A., Duethmann, D., Mandychev, A., Merz, B., 2013, What do we know about past changes in the water cycle of CA headwaters? A review. *Global and Planetary Change*, 110, 4-25.

United Nations Convention to Combat Desertification (UNCCD), 2006, CA Countries Initiative for Land Management. National Programming Framework, Uzbekistan. Retrieved 3 August, 2009, from <http://www.unccd.int/cop/reports/asia/asia.php>.

USGS (2020a) Earth Explorer. URL <https://earthexplorer.usgs.gov/> [accessed on 16 March 2020].

USGS (2020b) Landsat 8. URL https://www.usgs.gov/core-science-systems/nli/landsat/landsat-8?qt-science_support_page_related_con=0#qt-science_support_page_related_con.

- Uzbekistan Population 2022 - World Population Review. (2022). Retrieved 15 March 2022, from <https://worldpopulationreview.com/countries/uzbekistan-population>
- UzGosKomStat (2019) Agriculture of Uzbekistan, and official figures on structure of individual farms by production specialization across provinces. Tashkent, Uzbekistan.
- V.G. Prikhodko, S. NerozinA. (2005): Socio-economic and agro-economic survey of the Chirchik and Akhangaran river basins. Project RIVERTWIN.
- Vapnik V.N. (1982) Estimation of dependences based on empirical data. Springer, New York.
- Virnodkar S., Pachghare V.K., Patil V.C. & Jha S.K. (2021) Performance Evaluation of RF and SVM for Sugarcane Classification Using Sentinel-2 NDVI Time-Series. In: Progress in advanced computing and intelligent engineering (ed. by C.R. Panigrahi, B. Pati, P. Mohapatra, R. Buyya & K.-C. Li), pp. 163–174. Springer, Springer.
- Vuolo F., Neuwirth M., Immitzer M., Atzberger C. & Ng W.-T. (2018) How much does multi-temporal Sentinel-2 data improve crop type classification? *International Journal of Applied Earth Observation and Geoinformation*, 72, 122–130. DOI: 10.1016/j.jag.2018.06.007.
- Wang S., Chen J., Rao Y., Liu L., Wang W. & Dong Q. (2020) Response of winter wheat to spring frost from a remote sensing perspective: Damage estimation and influential factors. *ISPRS Journal of Photogrammetry and Remote Sensing*, 168, 221–235. DOI: 10.1016/j.isprsjprs.2020.08.014.
- Wardlow B.D. & Egbert S.L. (2010) A comparison of MODIS 250-m EVI and NDVI data for crop mapping: a case study for southwest Kansas. *International Journal of Remote Sensing*, 31, 805–830. DOI: 10.1080/01431160902897858.
- Weiss M., Jacob F. & Duveiller G. (2020) Remote sensing for agricultural applications: A meta-review. *Remote Sensing of Environment*, 236, 111402. DOI: 10.1016/j.rse.2019.111402.

- Wikipedia (2021): List of countries by irrigated land area. Available online at https://en.wikipedia.org/wiki/List_of_countries_by_irrigated_land_area, checked on 5/7/2022.
- Williamson, I. P., Grant, D., & Rajabifard, A. (2005). *Land administration and spatial data infrastructures* From Pharaos to Geoinformatics FIG Working Week 2005 and GSDI-8, Cairo.
- World Food and Agriculture – Statistical Yearbook 2021.
- WorldBank (2002). Global condition of environment. World Bank for Reconstruction and Development: Tashkent. Cited in Dubovyk, O., Menz, G., Conrad, C., Kan, E., Machwitz, M. and Khamzina, A., 2013, Spatio-Temporal Analyses of Cropland Degradation in the Irrigated Lowlands of Uzbekistan using Remote-Sensing and Logistic Regression Modeling. *Environmental Monitoring and Assessment*, 185(6), 4775-4790.
- Wulder M.A., Loveland T.R., Roy D.P., Crawford C.J., Masek J.G., Woodcock C.E., Allen R.G., Anderson M.C., Belward A.S., Cohen W.B., Dwyer J., Erb A., Gao F., Griffiths P., Helder D., Hermosilla T., Hipple J.D., Hostert P., Hughes M.J., Huntington J., Johnson D.M., Kennedy R., Kilic A., Li Z., Lyburner L., McCorkel J., Pahlevan N., Scambos T.A., Schaaf C., Schott J.R., Sheng Y., Storey J., Vermote E., Vogelmann J., White J.C., Wynne R.H. & Zhu Z. (2019) Current status of Landsat program, science, and applications. *Remote Sensing of Environment*, 225, 127–147. DOI: 10.1016/j.rse.2019.02.015.
- Wulder, M. A., Loveland, T. R., Roy, D. P., Crawford, C. J., Masek, J. G., Woodcock, C. E., Allen, R. G., Anderson, M. C., Belward, A. S., & Cohen, W. B. (2019). Current status of Landsat program, science, and applications. *Remote Sensing of Environment*, 225, 127-147.
- Xie, Z., Chen, Y., Lu, D., Li, G. and Chen, E., 2019, Classification of Land Cover, Forest, and Tree Species Classes with ZiYuan-3 Multispectral and Stereo Data. *Remote Sensing*, Vol. 11 (2), DOI: 10.3390/rs11020164.

- Yi Z., Jia L. & Chen Q. (2020) Crop Classification Using Multi-Temporal Sentinel-2 Data in the Shiyang River Basin of China. *Remote Sensing*, 12, 4052. DOI: 10.3390/rs12244052.
- Yusupov B., Lerman Z., Chertovitskiy A. S., Akbarov O. M., 2010, Livestock Production in Uzbekistan: Current State, Challenges and Prospects. Review in the Context of Agricultural Sector Development Trends. Edited by Amir Khudoyberdiyev, (Karshi: Nasaf).
- Yusupov, S. U., 2003, Interaction between livestock and the desert environment in Uzbekistan. In: Schrader F, Alibekov L, Toderich K (Ed.) Proceedings of NATO Advanced Research Workshop “Desertification problems in CA and its regional strategic development”, Samarkand, Uzbekistan, 93-96.
- Zaragozí B., Giménez-Font P., Belda-Antolí A. & Ramón-Morte A. (2019) A graph-based analysis for generating geographical context from a historical cadastre in Spain (17th and 18th centuries). *Historical Methods: A Journal of Quantitative and Interdisciplinary History*, 52, 228–243. DOI: 10.1080/01615440.2019.1590269.
- Zhang L., Liu Z., Ren T., Liu D., Ma Z., Tong L., Zhang C., Zhou T., Zhang X. & Li S. (2020) Identification of Seed Maize Fields With High Spatial Resolution and Multiple Spectral Remote Sensing Using Random Forest Classifier. *Remote Sensing*, 12, 362. DOI: 10.3390/rs12030362.
- Zhu G. & Blumberg D.G. (2002) Classification using ASTER data and SVM algorithms;. *Remote Sensing of Environment*, 80, 233–240. DOI: 10.1016/S0034-4257(01)00305-4.
- Zvi, L., 2018, Agricultural Development in Uzbekistan: The Effect of Ongoing Reforms. Available online at <http://departments.agri.huji.ac.il/economics/indexe.html>.